Role of *Fusobacterium nucleatum*-oral keratinocyte interactions in the progression of oral dysplasia and Oral Squamous Cell Carcinoma

A thesis submitted to the University of Dublin, Trinity College, in fulfilment of the requirements for the degree Doctor of Philosophy (Ph. D) by

Ajith Kumar Selvaraj

March 2023

Trinity College Dublin
Coláiste na Tríonóide, Baile Átha Cliath
The University of Dublin

DUBLIN DENTAL UNIVERSITY HOSPITAL
OSPIDÉAL DÉADACH OLLSCOILE ÁTHA CLIATH

Division of Oral Biosciences,

Dublin Dental University Hospital,

Trinity College Dublin,

Dublin 2

Declaration

I declare that this thesis has not been submitted as an exercise for a degree at this or any other university and it is entirely my own work.

I agree to deposit this thesis in the University's open access institutional repository or allow the Library to do so on my behalf, subject to Irish Copyright Legislation and Trinity College Library conditions of use and acknowledgement.

I consent to the examiner retaining a copy of the thesis beyond the examining period, should they so wish (EU GDPR May 2018).

_____

Ajith Kumar Selvaraj

Summary

Fusobacterium nucleatum is a species of bacteria commonly found in the oral cavity. It is one of the most isolated bacterial species from dental plaque and hence its strong association with gingivitis and periodontitis. Apart from causing gum disease in the oral cavity, *F. nucleatum* has been implicated in other extra-oral abnormalities such as urinary tract infections, adverse pregnancy outcomes, respiratory tract infections and most recently, its association with cancers.

The aim of this study was to characterize the pathogenicity of *F. nucleatum* isolates recovered from dysplastic oral epithelia in patients with malignant and premalignant conditions. The data obtained in our study suggests *F. nucleatum* subsp. *polymorphum* to be the most isolated *Fusobacterium* species from dysplastic oral epithelia. Loss of E-cadherins is one of the earliest signs in oral dysplasia and the concurrent epithelial to mesenchymal transition of the epithelial cells during the development of OLK and OSCC may select for a specific microbiome. By designing a novel method to assess and quantify bacterial invasion of OSCC cells using confocal microscopy, our data suggests that intracellular invasion may not necessarily be a significant requirement for induction of pro-malignant phenotypes, as seen in the invasion of epithelial cells that had lost their E-cadherins. Our data also indicate that bacterial adhesion, likely mediated by the adhesins FadA and Fap2, plays a vital role in promoting colonisation of dysplasic tissue. Adhesion to dysplasic tissue was strain dependent and may be related to copy numbers of FadA- and Fap2-like adhesins.

The overexpression of chemokines by OSCC cells when infected with *F. nucleatum* subsp *polymorphum* strains was characterised and the highest levels were observed in the most adherent clinical isolate of *F. nucleatum* subsp. *polymorphum* 43A3. We could also show that the absence of E-cadherin in OSCC cells was associated with increased cell motility, migration and invasion and these phenomena were enhanced in the presence of *F. nucleatum* subsp. *polymorphum* infection. The E-cadherin negative cells due to their EMT phenotype were far more motile and invasive when infected with *F. nucleatum* subsp. *polymorphum* strains. Also, infecting the OSCC cells with *F. nucleatum* subsp. *polymorphum*

significantly enhanced the secretion of chemokine VEGF-A and resulted in increased tube-like vessel formation in vitro.

In summary, this study shows that *F. nucleatum* subsp. *polymorphum* recovered from oral dysplasia may exhibit high levels of adherence and can promote cellular responses in E-cadherin negative cells that could promote tumour growth and metastasis.

Abstract

Dysplastic changes of the oral epithelium have a potential for malignant transformation. Several studies have identified increased abundance of *Fusobacterium* spp. on malignant and premalignant oral lesions. The potential role of *Fusobacterium* spp. in oral malignancy and its interaction with oral cells is poorly characterised. Oral malignancy is associated with the loss of epithelial biomarkers such as E-cadherin in dysplastic events and in the current study we examined the interaction of *Fusobacterium* spp. with E-cadherin positive and negative oral keratinocytes.

For these analyses, we investigated the interaction of a type strain ATCC10953/NCTC10562 and clinical isolates of *F. nucleatum* subsp. *polymorphum* with oral cells. In our hands, traditional antibiotic protection assays to measure invasion were unable to discriminate internal and external bacteria, which lead us to develop a novel confocal microscopy-based assay to measure bacterial invasion. Epithelial cells were negatively stained with fluorescein and internalised bacteria were visualised using propidium iodide staining. Cells were scanned with a Leica confocal microscope and the images were analysed using Imaris image analysis software. Using this assay, we showed that *F. nucleatum* subsp. *polymorphum type* strain ATCC10953/NCTC10562 is highly adherent and invasive to E-cadherin expressing H357 oral keratinocytes. Clinical isolates of *F. nucleatum* subsp. *polymorphum* (n=7) were generally less adherent and invasive to E-cadherin expressing H357 compared to the type strain ATCC10953. Conversely, when E-cadherin negative H376 cells were used, clinical isolates exhibited greater adherence and invasion compared to the type strain ATCC10953. These data show that clinical isolates of *F. nucleatum subsp. polymorphum* adhere to and invade oral keratinocytes using E-cadherin independent mechanisms.

Furthermore, we also demonstrate the effects of *F. nucleatum* subsp. *polymorphum* on cellular responses. OSCC cell motility, migration, invasion and the ability to form new blood vessels were increased in the presence of active *F. nucleatum* subsp. *polymorphum* infection. These mechanisms were enhanced due to the increase in secretion of essential chemokines such as MCP-1/CCL2, RANTES/CCL5, IP-10, MCS-F and extracellular matrix

proteinase such as MMP-9. The E-cadherin negative cells due to their EMT phenotype were more invasive and were far more motile and invasive when infected with *F. nucleatum* subsp. *polymorphum* strains. Infecting the OSCC cells with *F. nucleatum* subsp. *polymorphum* significantly enhanced the secretion of chemokine VEGF-A required for tube-like vessel formation in vitro. The over-expression of this chemokine in E-cadherin negative cells reflects the selective affinity of *F. nucleatum* subsp. *polymorphum* to E-cadherin negative and a possible EMT cell phenotype.

In summary, loss of E-cadherin expression in an early event in oral dysplasia, suggesting that dysplastic tissues may select microbiome constituents that adhere via E-cadherin independent mechanisms.

Table of Contents

Index of Figures

Chapter 2

Chapter 3

Index of Tables

List of Abbreviations

ADH3	Alcohol dehydrogenase type 3
Aid1	Adherence Inducing Determinant 1
AIDS	Acquired Immune Deficiency Syndrome
ATCC	American Type Culture Collection
BHI	Brain-heart infusion
$CaCl_2$	Calcium Chloride
CAF	Cancer-associated fibroblasts
CAMs	Cell adhesion molecules
CCL1	Chemokine Ligand 1
CCL2	Chemokine Ligand 2
CCL3	Chemokine Ligand 3
CCL5	Chemokine Ligand 5
CCL7	Chemokine Ligand 7
CCR1	Chemokine receptor type 1
CCR2	Chemokine receptor type 2
CCR3	Chemokine receptor type 3
CCR5	Chemokine receptor type 5
CDK	Cyclin dependent kinases
CFUs	Colony Forming Units
CI	Confidence Intervals
CIS	Carcinoma-in-situ
CM	Conditioned media
CRC	Colorectal Carcinoma
CO_2	Carbon-di-Oxide
COX	Cyclooxygenase
CXCL1	Chemokine ligand 1
DAPI	4’,6-diamidino-2-phenylindole
DCs	Dendritic cells
DMEM	Dulbecco’s Modified Eagle Medium
DNA	Deoxyribose Nucleic Acid
ECM	Extracellular matrix
ECMP	Extra cellular matrix proteins
EDTA	Ethylenediaminetetraacetic acid
EGF	Epidermal Growth Factor
ELISA	Enzyme-linked immunosorbent assay
EMT	Epithelial-mesenchymal transition
FadA	*Fusobacteria* Adhesin A
FadAc	Pre-FadA-mFadA complex
FAK	Focal adhesion kinase

Fap2	Fibroblast activation protein 2
FBS	Foetal Bovine Serum
FITC	Fluorescein isothiocyanate
FOM	Floor of mouth
Fn	*Fusobacterium nucleatum*
Gal-GalNAc	D-galactose-(1-3)-N-acetyl-D-galactosamine
GC	Gastric cancer
G	Gravity
HCl	Hydrochloric Acid
HIF-1α	Hypoxia-inducible factor-1α
HIOEC	Human immortalized oral epithelial cells
HIV	human immunodeficiency virus
HNSCC	Head and neck squamous cell carcinoma cells
HOMD	Human Oral Microbiome Database
HOXB7	Homeobox 7
HOX gene	Homeobox gene
HPV	Human Papilloma Virus
HRE	Hypoxia response element
HUVEC	Human umbilical vascular epithelial cells
IL-6	Interleukin-6
IL-8	Interleukin-8
ILK	Integrin linked kinase
KDR	Kinase Insert Domain Receptor
KGM	Keratinocyte Growth Media
KRT7-AS	Keratin7-antisense
LA	Luria Agar
LB	Luria Broth
LBM	Left buccal mucosa
LLBT	Left lateral border tongue
LPS	Lipopolysaccharides
LRM	Left retromolar pad
LVT	Left ventral tongue
MCP-1	Monocyte chemoattractant protein-1
M-CSF	Macrophage colony stimulating factor
MDSC	Myeloid derived suppressor cells
MEK 1/2	Mitogen activated protein kinase 1/2
$MgCl_2$	Magnesium Chloride
MMP9	Matrix metalloproteinase 9
MOI	Multiplicity of infection
NAOH	Sodium Hydroxide
NCBI	National Centre for Biotechnology Information

NF-κβ	Nuclear factor-κβ
NK cells	Natural Killer cells
NNK	Nitrosamines 4-(methylnitrosamino)-1-(3-pyridyl)-1-butanone
NNN	N'-nitrosonornicotine
NOD1	Nucleotide oligomerization domain 1
OD	Optical density
OHI-S	Oral hygiene index-simplified
OLK	Oral leukoplakia
OMP	Outer membrane protein
OR	Odd's Ratio
OSCC	Oral squamous cell carcinoma
OSMF	Oral Submucous Fibrosis
PAH	Polycyclic aromatic hydrocarbons
PBS	Phosphate buffered saline
PCR	Polymerised Chain Reaction
PD-L1	Programmed death ligand 1
PFA	Para formaldehyde
PI_3	Phosphoinositide-3 kinase
PI	Propidium Iodide
PKC	Phosphokinase C
PLC	Phospholipase C
pRb	Retinoblastoma protein
PRC1	Protein regulator of cytokinesis 1
RANTES	Regulated upon Activation, Normal T Cell Expressed and Presumably Secreted
rhCCL5	Recombinant human CCL5
rhVEGF-A	Recombinant human VEGF-A
RIPK2	Receptor-interacting protein kinase 2
RNA	Ribose Nucleic Acid
ROS	Reactive oxygen species
SFM	Serum free media
SNAI1	Snail Family transcription repressor 1
Spp	Species
TAM	Tumour associated macrophages
TLR-4	Toll-like receptor 4
TNF-α	Tumour necrosis factor alpha
VEGF-A	Vascular endothelial growth factor A
WISP-1	WNT1-inducible-signaling pathway protein 1

Acknowledgements

Firstly, I would like to express my deepest gratitude to my supervisor Dr. Gary Moran, without whom it would have been utterly impossible for me to be at this stage of my academic career. He has been an enormous support and guide throughout this project, bursting with ideas and encouragement every time I thought I had reached a dead end. I would like to thank him for always giving me the liberty to openly discuss any issues I encountered at work and helping me deal with them promptly. Again, an enormous thank you to Dr. Moran for giving me this opportunity to work with him and encouraging me to present my work at different conferences.

I would also like to thank Prof. David Coleman and Dr. Mary O'Donnell for looking out for me during my time in the laboratory and their constant support and words of wisdom when I needed the most. I have thoroughly enjoyed and gained a lot of general knowledge in my conversations with them. I would also like to thank them both for helping me resolve any technical issues I was challenged with whilst using the equipment in the facility. A special thanks to Prof. Derek Sullivan for giving me ideas in our weekly laboratory meetings when I needed them the most.

I would also like to thank Dr. Gavin McManus from the confocal microscopy facility in TBSI for helping me enormously with imaging and accommodating me every time I needed his advice. A special thanks to Prof. Ursual Fearon and Dr Brianne Baker from the School of Medicine at TCD for helping me with my angiogenesis work. I am also thankful to Dr. Claire Healy and Dr. Sheila Galvin for accommodating me in the dysplasia clinics with them. A special thanks to all my colleagues Peter, Emily, Brenda, Claire, Bisola, Nicole and Wen Jun Lim in the Oral Biosciences division of DDUH and all the other hospital staff I constantly engaged with for making my experience in the hospital memorable. James, thank you for helping me with the dilutions and calculations when I was stuck, the chats, the laughter and for generally being a nice guy.

Big thanks to Liam for making my duration in the lab enormously enjoyable. Your constant jokes made me laugh insanely all the time and our friendship that has strengthened over

the years is something I shall always cherish. To Leenah, thank you for becoming such a good friend and helping me with new techniques in the lab. I've always enjoyed our long walks and shopping together. And Elaine Moloney, thank you for being a good friend. I wish you all the very best for your future!

To Michael Kelly, my husband, thank you so much for sticking with me through thick and thin and making me laugh every single minute since we met. I couldn't have done this without you by my side. To my parents, who have always supported me unconditionally with every decision I've made, words cannot express my gratitude and love. To my brother Arun (anna) sister Prema (akka), May and all my extended family and friends across the globe, thank you so much for your love and support.

Lastly to Prajith (appu), Raghav, Noah, Juliette, Leo, Ricky, Tina, Jackie and Tinku, you'll always be special to me.

Chapter 1

Introduction

1.1 Historical view of cancers

Cancers of the human body have been observed and explicitly recorded in the literature since time immemorial. It is well accepted in modern medicine that the first mention of the disease predates to well over a millennium (Skuse, 2015). The description of the intervention and treatment of cancers has been mentioned in ancient texts such as the 3rd century BC scrolls of Hippocrates, texts of the Egyptian Edwin Smith Papyrus from c1600-3000 BC, and the Indian Epic Ramayana from c2000 BC (Karpozilos and Pavlidis, 2004, Suciu et al., 2014, Skuse, 2015). Therefore, cancers in the human body are not a modern phenomenon. Cancers are aberrant, uncontrolled proliferations of cells, lacking any clear cellular differentiation. An excellent literature review by W.B. Morrison in 2010 described in detail the ancient chronological histories of the origin of cancers and how various cultures and civilisations dealt with them. The term "cancer" was coined by the father of medicine, Hippocrates (ca. 460-370 BC), who theorised that an excess of black bile in the body caused cancer. This theory thus challenged and subsequently terminated the belief of the vengeance and wrath of gods being the cause of such sinister conditions which was thought to be the "retribution for sin" in adults who were victims of tumours. Hippocrates used the term "carcinos" (Greek for crabs) to describe cancers, that apparently had raised elevated margins, that projected like the claws of a crab. From his recorded literary work, it seemed he had a great knowledge of the existence of cancerous lesions as he described different types of cancers of the skin, breasts, cervix, rectum and the stomach (Morrison, 2010). This Greek term was later translated to Latin by the Roman physician Celcus and the modern word "cancer" was conceived. Also, Galen, who was a Roman physician (129-210 AD) described swellings and coined the Greek term "onkos" for "tumours", which was of great significance to medicine, to this day (Morrison, 2010, Raven, 1985).

Surprisingly, the treatment approaches for cancers remained relatively unchanged for centuries to come, until the discovery of radiation therapy in the 19th century (Abshire and Lang, 2018). However, chemotherapy was employed in the treatment of cancers as early as the 1st century AD and perhaps much earlier. Ancient surgeons and physicians used plant herbal extracts and products that possessed chemotherapeutic properties, as reported by Morrison in his review. The same compounds where developed in the mid twentieth century for cancer treatment and are actively being used to the present day.

1.2 Oral Squamous Cell Carcinoma

Squamous cell carcinoma is defined as “an invasive epithelial neoplasm, with variable degrees of squamous differentiation, with or without keratinization”(Suciu et al., 2014). Anatomically, the distribution of oral cancer includes the lips, the oral cavity including minor and major salivary glands and extends posteriorly to include the oropharynx. Oral squamous cell carcinoma (OSCC) is a pathological type of cancer and the most common malignant epithelial neoplasm of the oral cavity, accounting for over 90% of all oral cancers and 2-4% of all cancer cases worldwide (Neville and Day, 2002). The anatomic site for the development of OSCC varies largely on the geographical distribution of populations, with the lateral border of tongue, lip and floor of mouth being the most common (Markopoulos, 2012). The five years survival rate of OSCC is less than 40%, making it one of the most devastating cancers in the human body.

1.3 Aetiology of OSCC

Oral cancers often develop from certain precancerous lesions of the mouth which are known to have high malignant potential. These often present themselves as red and white patches on the oral mucosa and have the potential for malignant transformation. The most common of these is leukoplakia, defined as "a predominantly white lesion or plaque of questionable behaviour having excluded, clinically and histo-pathologically, as any other definable white disease or disorder" (Brouns et al., 2013). Oral leukoplakia (OLK) is a potentially malignant disease and the risk factors for OLK are similar to those for OSCC. Transformation rates are variable, and the only reliable predictor of malignant transformation is the degree of dysplasia, with those exhibiting severe dysplasia having the greatest risk of progression. An altered oral microbiome in patients with either precancerous lesions or OSCC has been identified. Colonisation of dysplastic lesions with *Candida* species and bacteria such as *Fusobacteria, Leptortichia, Rothia* and *Campylobacter* species have been reported (Amer et al., 2017) and the role of *Fusobacterium nucleatum* as a driver in colorectal carcinoma has been suggested (Kostic et al., 2013). However, the role of these microorganisms in the progression of oral malignancies is unknown.

The known risk factors for OSCC are the use of tobacco in various forms, alcohol, betel and areca nut chewing, narcotics and cannabis use (Bolstad et al., 1996). A summary of the known causative factors of OSCC is shown in figure 1.1. OSCC has a higher male to female predilection and is most often seen in older adult patients, generally in their fifth to sixth decade of life. However, a recent study focussing on age distribution of OSCC prevalence found an increase in incidence in patients younger than 45 years (Ye et al., 2017). Increase in age is a risk factor for OSCC, however, the major risk factors in the aetiology of OSCC are multi-factorial.

- **Tobacco use**

  Tobacco use in either smoked or non-smoked form is one of the major risk factors in the development of OSCC and oral dysplasia like oral leukoplakia. Albeit the carcinogens in smokeless tobacco are less compared to smoked tobacco, the risk of the development of cancer in either form cannot be underestimated. Strong carcinogens such as polycyclic aromatic hydrocarbons (PAH), nitrosamines and aromatic amines and weak carcinogens such as acetaldehyde have been identified in higher quantities in smoked (burned) tobacco such as cigarettes and bidi, their unburnt counterparts such as snuff, chewed tobacco and smokeless tobacco products contain high levels of tobacco specific nitrosamines 4-(methylnitrosamino)-1-(3-pyridyl)-1-butanone (NNK) and N'-nitrosonornicotine (NNN) (Hecht, 2003). The levels of polycyclic aromatic hydrocarbons in non-smoked tobacco is typically less. The constituent carcinogens in tobacco can cause various alterations in the human body, at a cellular level. Their excessive usage dramatically alters DNA repair and interferes with normal cell cycle. Souto et al. used exfoliative cytology and Feulgen's staining method to demonstrate significant increase in aneuploid nuclei in cigarette smokers as compared to cigarette non-smokers. Aneuploidy is the loss or acquisition of chromosomes in the cells (Souto et al., 2010). Whilst excessive cigarette smoking is generally associated with western countries, the smoking of tobacco in the form of bidi (rolled tobacco leaf) and chewed tobacco is a major aetiological factor for OSCC in underdeveloped and developing countries, and the countries of South-Central Asia (Moore and Moore, 1994).

- **Betel quid chewing**

  A common practice in South-Central Asian countries like Pakistan, India, Bangladesh, Taiwan, China and Papua New Guinea, chewing betel quid consists of a mixture of betel nut (areca nut), slaked lime (calcium hydroxide), catechu, sweeteners, spices (cardamom, coconut, saffron etc) and other flavouring agents rolled within the betel leaf (*Piper betel*) to form a bite size parcel. The practice of adding tobacco to the prepared betel leaf known as *paan* is exclusively seen in India, Pakistan and Bangladesh, however, the practice is also common in South Asian communities in the UK and other western countries, indicating a strong cultural association (Guha et al., 2014, Mirza et al., 2011). Chewing betel quid with or without tobacco has been classified as carcinogenic (1985, Guha et al., 2014, 2004). The betel quid combination is chewed over prolonged periods during the day (or night) and stored in the buccal vestibule as a bolus and the juice released by the chewed ingredients is slowly sucked and most often, swallowed. Betel quid mastication is highly addictive in nature. The carcinogenic components of the betel nut which include alkaloids, polyphenols and tannins, cause cellular atypia and dysplasia, which over time, can transform to OSCC (Gmur et al., 2006). Areca nut extract trigger c-jun protooncogene expression in the mucosal fibroblasts, contributing to the development of Oral Submucous Fibrosis (OSMF) (Warnakulasuriya et al., 2002, Ho et al., 2000). In addition, slaked lime usage may contribute to the production of reactive oxygen species (ROS) that lead to DNA damage in the surrounding oral epithelium, along with mucosal ulcerations that expose basal cells to mutagenesis. A study by the World Health Organisation showed that over 60% of oral cancers were attributed to the habit of chewing betel quid (Wang et al., 2018).

- **Alcohol consumption**

  Alcohol and alcoholic beverage consumption without moderation is one of the main risk factors for OSCC and pharyngeal cancers worldwide (Eren et al., 2014). Whilst there are different types of alcohol such as methyl alcohol and isopropyl alcohol employed for various industrial and domestic uses, ethyl alcohol or ethanol with a combination of glucose and water is solely used in alcoholic beverages for human consumption. Acetaldehyde production as a result of ethanol metabolism in alcoholic beverages by the enzyme alcohol dehydrogenase type 3 (ADH3) is a potent known carcinogen for OSCC and pharyngeal carcinoma. Alcoholic beverages also contain other impurities that play an important role as carcinogens. Impurities such as N-nitrosodiethylamine and polycyclic hydrocarbons in whiskeys and beers have been deemed carcinogenic (Reidy et al., 2011). Ethanol is also a solvent, and when consumed, causes cellular permeability and therefore, increases the susceptibility of exposure of oral and pharyngeal mucosal cells to various carcinogens (Lopes et al., 2012). In the oral cavity, mucosal alcohol dehydrogenase produced by the oral epithelium metabolises ethanol to acetaldehyde and the oral microflora contribute to additional acetaldehyde levels by directly metabolising alcohol (Homann et al., 1997, Pikkarainen et al., 1981). High alcohol consumption also activates cytochrome P450 2E1 to produce reactive oxygen species along with acetaldehyde during its metabolism in the liver that causes cellular DNA damage (Zygogianni et al., 2011). One study reported that chronic alcoholics with poor oral hygiene and polymorphisms of alcohol metabolizing genes ADH1B and ALDH2 accelerated OSCC progression (Tsai et al., 2014, Mathur et al., 2019)

- **Oral hygiene**

  Poor oral hygiene is a potential risk factor for the development of OSCC. Several studies have shown the correlation between poor oral hygiene and the development of OSCC. Although not an isolated entity for the cause of OSCC, poor oral hygiene has been associated with catalysing the activity of other known carcinogens in the process. In a case-control study conducted by Talamini et al, patients from Europe, India, Africa, Australia and North America were recruited for a potential link between oral cancer and Human Papilloma Virus (HPV). Details regarding tooth brushing habits revealed that cases rather than controls brushed their teeth less often and complained of bleeding gums with an overall poor oral health status (Odd's Ratio OR =1.8, 95% Confidence Intervals CI= 0.9-3.6) compared to healthy controls (Talamini et al., 2000). Critchlow et al. conducted a study of oral health of patients visiting for oral cancer treatment in the UK. 71% of patients were fully dentulous and had moderate to severe periodontal disease, with 51% having a probing depth of more than 6mm. The loss of gingival attachment was associated with a combination of systemic diseases, poor oral hygiene and irregular dental visits. 61% of patients presented with one or more carious tooth (Critchlow et al., 2014). Poor oral hygiene can increase the microbial burden in the oral cavity and alter the structure of the microbiome towards a pathogenic, Gram negative and inflammatory population. This could potentially cause a chronic inflammatory environment in the oral tissues, resulting in chronic periodontitis and associated tooth loss. A previous study showed that each millimetre of alveolar bone loss was associated with 5.23-fold increase in the incidence of squamous cell carcinoma of the tongue (Scully and Bagan, 2009, Tezal et al., 2007). The concurrent use of tobacco and alcohol compounded with poor oral hygiene has been reported to accelerate the activities of carcinogenic metabolites in the early stages of oral dysplasia (Guha et al., 2007, Pöschl and Seitz, 2004). Increased formation of nitrite and nitric acid in the mouths of tobacco users with high plaque deposits along with an increased formation of bacterial enzyme based nitrosamines has been reported by Calmels et al. (Calmels et al., 1996). Chronic fungal infections such as oral candidiasis have been suggested to alter the normal oral mucosa and lead to leukoplakia and other potential pre-malignant lesions that can progress to OSCC

(Hsiao et al., 2018). A case-control study by Alnuaimi et al. reported a significant association between oral candida colonisation and the occurrence of OSCC (OR = 3.242; 95% CI = 1.505–6.984) (Alnuaimi et al., 2015, Mathur et al., 2019). However, further research to support a direct correlation between *Candida albicans* and OSCC is required. Further to this, poor oral hygiene increases oral colonisation of *Porphyromonas gingivalis*, a chief oral pathogen in gingivitis and periodontitis. This organism assists OSCC by activating matrixmetalloprotinase-9 (MMP-9) which in turn promotes OSCC cell motility and migration (Inaba et al., 2014, Mathur et al., 2019).

- **Human Papilloma Virus (HPV)**

  HPV are a group of DNA viruses that belong to the *Papovaviridae* family, consisting of two sub-families, namely, *Papillomaviridae* and Polyomaviruses (Kim, 2016). Exposure to HPV predisposes to the development of anogenital cancers, cancers of the oropharynx, tonsils and in about 20-50% of reported cases of OSCC (Chocolatewala and Chaturvedi, 2009, Jiang and Dong, 2017). Strong evidence of the association of HPV and cancers of oropharyngeal region including the tonsils and anogenital region are available in the scientific literature, however, its association with oral cancers as one of the prime aetiologic factors is debatable (Chocolatewala and Chaturvedi, 2009). The lifecycle of HPV in the host epithelium begins as microlesions encapsulating viral capsid proteins with the infected epithelial cells as a result of virion synthesis and promoter activation. It is postulated that α6-integrin with heparin sulphate in keratin filled sacs are the HPV receptors involved (Kim, 2016). There are various classes of HPV amongst which HPV 16 and HPV 18 are the most common types to infect humans. HPV 16 is the most commonly identified virus in cervical, oral, oropharyngeal and penile carcinoma (Kim, 2016). One study by Shigeishi et al. showed that OSCCs with HPV-16 infection showed better prognosis whilst OSCCs with other types of HPV infections did not, indicating the significance in prognosis of OSCC based on the type of HPV infection. The involvement of the E6 and E7 oncoproteins of HPV have been recognised in OSCC (Eren et al., 2013, Henne et al., 2018). It is believed that these oncoproteins in the malignant form of oral tumours act through inactivation of tumour suppressor proteins such as p53 and pRB (Herrero et al., 2003, Jiang and Dong, 2017).

- **Host susceptibility and genetic predisposition to OSCC**

  A multitude of chemicals which are potentially carcinogenic are ingested by the human body, along with exposure to ionising radiation absorption and other environmental agents. Cellular and DNA damage (to chromosomes) are generally efficiently repaired in a healthy individual. Genes identified in the repair of such damaged cellular DNA include OGG1, XRCC1, ERCC1, XPC, XPD, XPF, BRCA2, and XRCC3. Polymorphism in these repair genes have been associated with various cancers including OSCC (Goode et al., 2002). Individuals with defective genes for metabolism of carcinogens and pro-carcinogenic agents or polymorphism in repair genes lead to accumulation of genetic and epigenetic changes which over time results in expression of the damage in the form of OSCC and other head and neck cancers (Kim et al., 2010). The genes that are critically altered in such events include cyclin D1, p53, signal transducer and activator of transcription 3, epidermal growth factor receptor, retinoblastoma, and vascular endothelial growth factor receiver. Repair genes such as p53 are essential for repairing damaged DNA and hypoxic conditions of the cells. They also play key roles in cell survival and cell death. Mutations in these genes have been observed in more than half of the reported OSCC cases as reported by Rivera et al. Also, overexpression of the gene homeobox 7 (HOXB7) which is one of the key genes in cell differentiation and morphogenesis in embryogenic phase of life has been identified as a strong influencer in carcinogenesis, specifically, OSCC (Rivera and Venegas, 2014). The HOXB7 gene is crucial in controlling cell proliferation and overexpression of this gene in OSCC is associated with poor prognosis of the cancer (Liao et al., 2011, Bitu et al., 2012, Rivera and Venegas, 2014). The genetic changes related to OSCC will be further discussed later in this chapter.

  A compromised immune system has also been shown to be associated with development of malignancies, including oral cancers. Conditions such as HIV that proceed to develop into AIDS have higher risk of developing malignancies such as OSCC, Kaposi's sarcoma, Hodgkin's lymphoma and Non-Hodgkin's lymphoma (Epstein et al., 2005).

- **Modern diet and lifestyle practices**

  Modern diet and lifestyle practices have changed considerably, contributing to the risk of development of OSCC. Apart from the increased consumption of alcohol and the use of tobacco in various forms, poor diet has emerged as a major concern in the recent past. Reduced consumption of green leafy vegetables, fresh fruits and vegetables, pulses, cruciferous vegetables, dietary fibres, fish and eggs contribute to deficiency of micronutrients such as vitamin C, E, zinc, beta-carotene and folate essential for reducing oxidative stresses in the body. Increased consumption of red meat, microwaved food (forms heterocyclic amines), deep fried food items and fats increase the risk of development of OSCC (Foster and Kolenbrander, 2004, Chenicheri et al., 2017). It has been reported that even with an increased alcohol consumption and smoking, one fourth of OSCC cases of the head and neck can be reduced by increased intake of dietary fruits and vegetables (Scully and Bagan, 2009, Boccia et al., 2008)

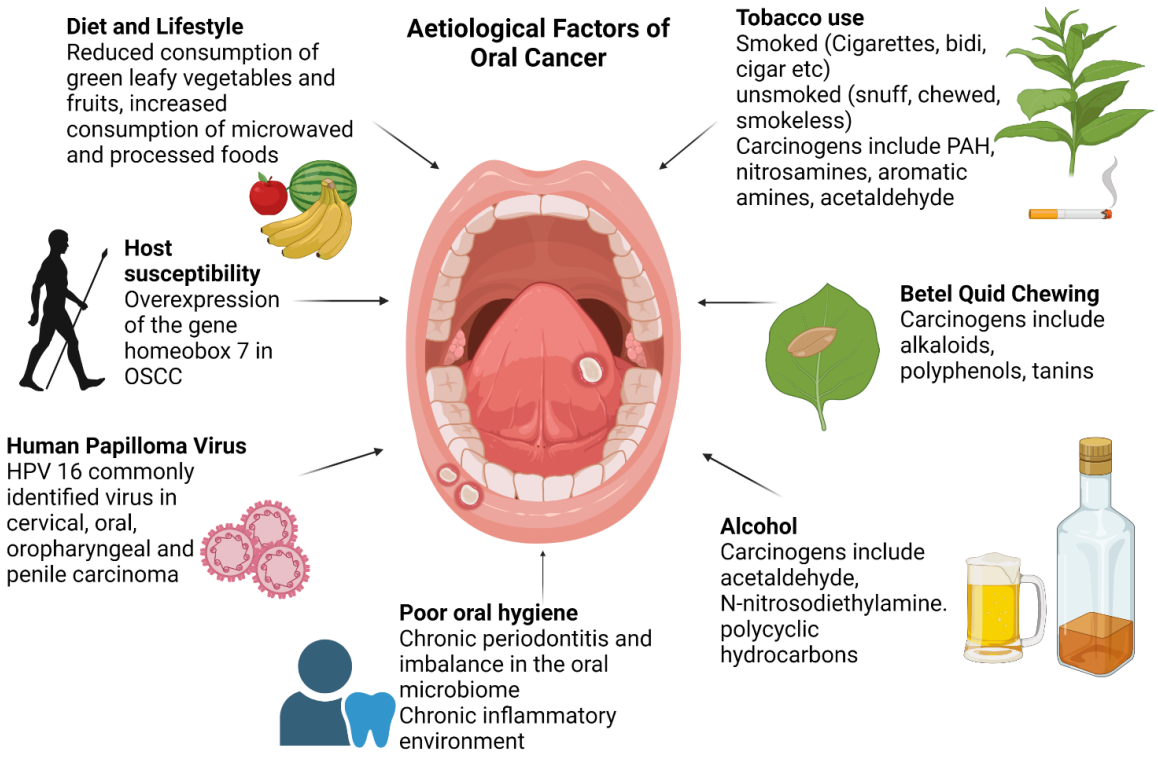

Figure 1.1 A summary of the aetiological factors of OSCC. Several known factors contribute to the development of oral cancer. The most notorious of them all is the use of tobacco and alcohol consumption without moderation. The risk of developing OSCC is increased in the concomitant use of both tobacco and alcohol. Other factors contributing to the risk of cancer development are poor oral hygiene (either due to systemic illness, physical disability or a habitual disregard), infection with the human papilloma virus, host susceptibility (either genetic predisposition or immunocompromised conditions such as HIV/AIDS) and poor diet and lifestyle habits.

1.4 Oral Dysplasia

Dysplasia of the oral epithelium is an abnormality in the stratification and maturation of the epithelial cells, displaying cellular inconsistencies or atypia (Warnakulasuriya et al., 2008). The WHO defines dysplasia of the oral epithelium as “an altered epithelium with an increased likelihood for progression to squamous cell carcinoma” (Ranganathan and Kavitha, 2019). Based on the extent of the dysplastic changes within the oral epithelium, the WHO has classified dysplasia into mild, moderate, severe and carcinoma-in-situ (Figure 1.2). Mild dysplasia is when the dysplastic changes are within the lower third of the basal lamina of the epithelium, moderate dysplasia is when dysplastic changes show up to the basal two thirds of the epithelium and severe dysplasia is when more than the basal two-thirds of the epithelium show dysplastic changes. Carcinoma-in-situ is a histopathologic diagnosis when cancer like features of the cells appear contained within the full thickness of the epithelium, without breaching the basal lamina. When the basal lamina is breached and there’s invasion of the underlying connective tissue, its classified as carcinoma (Geetha et al., 2015).

There are twelve characteristic histopathological features for the diagnosis of oral dysplasia and one of them is the reduction in cellular cohesion. Recent studies have shown that loss of cellular surface markers is an early feature noticeable in a dysplastic event. One such epithelial cell surface markers is E-cadherin, which plays a crucial role in cell-to-cell adhesion. Either a decreased expression of E-cadherin or a total loss of E-cadherin expression on epithelial cell surfaces are early occurrences in oral dysplastic events (Abdalla et al., 2017b).

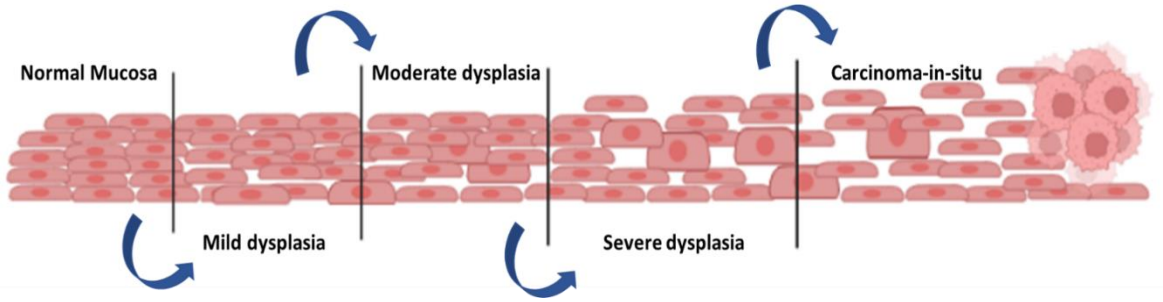

Figure 1.2 Transition of the normal oral epithelium to a dysplastic type. The normal mucosa has a definite stratification and cell type. As the tissue begins to deviate towards dysplasia, the cells lose their tight junctions owing to the loss of E-cadherins. The normal stratification of the keratinocytes is lost, and the epithelial cells show varied appearances such as larger nuclei resembling the basal cells, nuclear hyperchromatism and an increase in mitotic figures. Loss of cell-cell adhesion may lead to acantholysis (loss of attachment between keratinocytes). All these changes are restricted to the mucosal layer, with an intact basement membrane.

1.5 E-cadherin

E-cadherins are adhesive molecules, belonging to a family of genes encoding for cell surface bound glycoproteins called calcium dependent cell adhesion molecules (CAMs) (Halbleib and Nelson, 2006). There are five major subtypes identified in the cadherin family, namely, type I cadherins, type II cadherins, desmosomal cadherins, proto cadherins and cadherin like molecules. E-cadherins belong to type I cadherins (van Roy and Berx, 2008). E-cadherins facilitate specific Ca^{2+} dependent cell-cell adhesions in mammalian cells that are vital in the maintenance of a normal and healthy epithelia. A mature E-cadherin molecule has an N-terminal domain, which is essential for the homophilic calcium dependent cell-cell adhesion (figure 1.3). Intracellularly, a short cytoplasmic E-cadherin domain is linked to actin filaments via a catenin complex. Beta and/or gamma catenin bind to the c-terminus of the E-cadherin chain, whilst the alpha catenin binds the beta and/or gamma catenin to the actin cytoskeleton (Pećina-Slaus, 2003). Research has shown that E and N-cadherin are the two most important cadherins in maintaining a continuous tight cell to cell adhesion in epithelia and their role in gastrulation, neurulation and organogenesis in the early stages of human embryo development is also significant (Barth et al., 1997).

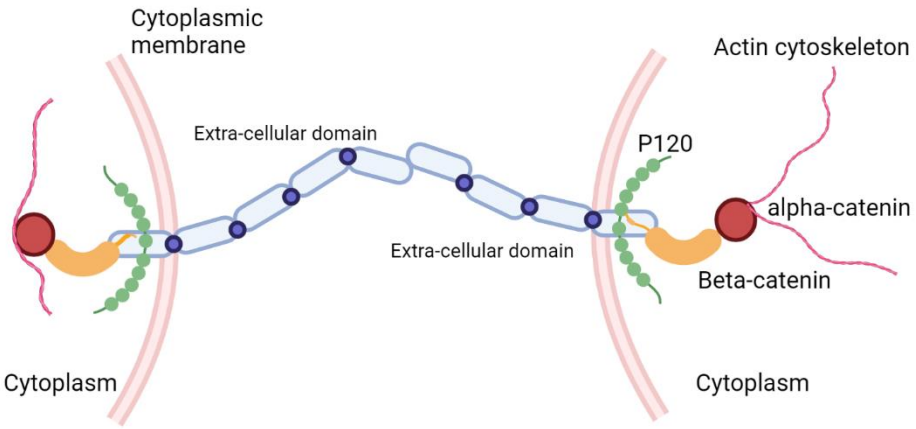

Figure 1.3. **E-cadherin in cell-cell junction**. The extracellular domain of e-cadherin forms a continuous chain with the active participation of the N-terminals. Calcium ions aid in the overlapping and interlacing of the two E-cad N-termini of adjacent cells, forming a tight cell-cell junction. The intra-cellular cytoplasmic domain of the E-cadherin molecule remains bound to the actin cytoskeleton through linker molecules such as alpha catenin (indicated in red circular-shape), beta catenin (indicated in orange bean-like shape) and P120 protein-essential in clustering and cell adhesion (indicated in green beads like shape). Adapted from Nives Pecina-Slaus, 2003.

1.6 Genetic influences in OSCC

As mentioned earlier, genetic and epigenetic changes are the prime drivers in cancer biology. In relation to OSCC, there are several genes that need exploration; however, a few genes have been well known to be associated with cancer induction, progression and metastasis. One such gene is the p53 tumour suppressor gene that plays a key role in tumour growth suppression (Liu et al., 2009). It does so by arresting cell cycle, repairing damaged DNA and inducing programmed cell death (apoptosis). The p53 gene is activated by DNA damage, cellular hypoxia, and exposure to oncogenic toxins (Vousden, 2002, Liu et al., 2009). Frequent mutations in the transcription factor for p53 gene known as *TP53* occur in cancers, wherein, a single nucleotide is replaced by another (Rivlin et al., 2011). This results in the synthesis of a full protein chain with a single amino acid substitution which fails to bind DNA in a sequence specific manner required for p53 related tumour suppression activity. Cho et al. reported that the DNA binding domain encoded by the exons 4-9 of the *TP53* gene, exhibits six hotspots residues (residues R175, G245, R248, R249, R273, and R282) that are unmistakably omnipresent in all cancer types (Cho et al., 1994, Rivlin et al., 2011). The overall effect of the mutation results in facilitation of tumour cell survival and resistance to multiple stress conditions (intrinsic and extrinsic) and defect accumulation in cells due to positive loop feedback (stress adaptive processes due to mutant p53 triggers further mutations)(Del Sal, Mantovani and Collavin, 2019).

Another gene implicated in cancers and OSCC is the homeobox gene (HOX gene). These genes are a family of 39 transcription factors that are cardinal to the tissue patterning and cell fate along the cranio-caudal axis of the developing animals and humans alike (Procino and Cillo, 2013, De Souza Setubal Destro et al., 2010). In relation to cancer pathogenesis, HOX genes play a dual role as both transcriptional activators and transcriptional repressors (Bhatlekar et al., 2014). The HOX transcriptional factors are divided into four clusters (A-D) and HOXB cluster is implicated in cancers of the mouth. De Souza Setubal Destro et al. reported a significantly high expression of HOXB7 in OSCC compared to the normal controls through RT-PCR analysis. Further immunohistochemical analysis revealed a significantly high HOXB7 labelling index in HOXB7 positive OSCC cases (De Souza Setubal Destro et al., 2010). These results were corroborated by Xiang Wu et al. in their study, who knocked down HOXB7 gene and demonstrated *in-vitro* experimental impairment in cell migration

and invasion in head and neck squamous cell carcinoma cells (HNSCC) and an impairment in tumour growth in an *in-vivo* mouse study model (Wu et al., 2021).

The cell cycle is governed by a plethora of proteins, however, a few proteins such as the retinoblastoma protein (pRb) and cyclin-dependent kinases (CDK) are key in organising orderly fashioned events within the cell such as chromosomal repair, duplication and separation. pRb plays an important role in the transition of G1 to S phase of the cell cycle, therefore, a mutation in this gene can alter and disrupt the process. Altered pRb and overexpression of mutated cyclin D1 gene have been reported in oral and head and neck cancers (Schoelch et al., 1999). Protein regulator of cytokinesis 1 (PRC1) is a microtubule associated protein and is required for the transition from G2 to M phase of the cell cycle through p53. Overexpression of PRC1 in OSCC has been reported, interfering with cell-cycle by supressing G2/M phase, thereby inducing increased cellular proliferation and transition as seen in OSCC (Wu et al., 2018).

1.7 The tumour microenvironment

The immune system of the human body plays a critical role in counteracting a plethora of antigens and pathogens; therefore, it's not surprising the immune cells also check countless potential cancer cells daily. This phenomenon of identifying and destroying cancer cells by the immune system is known as immune surveillance (Swann and Smyth, 2007). Activation of the immune response in the host by the advancing front of tumour tissues is the expected physiological outcome in an individual. However, tumours engineer mechanisms that successfully evade the immune surveillance and proceed to developing into a separate, fully functional pathologic entity. The microenvironment that supports such a fully functional tumour involves genetic and epigenetic instability of the cancer cells themselves that trigger factors such as the Cancer-associated fibroblasts (CAF), T and B lymphocytes of the immune system, myeloid derived suppressor cells (MDSC), tumour associated macrophages (TAM), extra cellular matrix proteins (ECMP), growth factors and cytokines (Khowal, Mughees and Sengupta, 2021, Wajid). Studies have shown that infiltration of tumours with TAMs expressing CD68 and CD163 is associated with poor prognosis (Huang et al., 2019). On the other hand, infiltration of tumours with other immune cells such as Natural Killer cells (NK cells) and memory T-cells, both characterized by CD57 and CD45RO respectively, show better survival and good prognosis. This could be associated with the active immune surveillance and killing of tumour cells by NK and memory T-cells.

The importance of cancer-related fibroblasts (CAFs) in the tumour microenvironment, specifically to OSCC was described elaborately in a review article published by Pena-Oyarzun et al. in 2020. The CAFs reportedly generate exosomes that contain microRNA-382-5p (miR-382-5p) which is believed to reduce the expression of tumour suppressor genes in OSCC (Peña-Oyarzún et al., 2020). Studies based on other cancers such as breast cancer and hepatic cancer have shown the suppressive effect of CAFs on genes such as MDX1 (in breast cancer) and DLC-1 (in liver cancer) which are essential in combating and controlling the proliferation of these cancer cells. Active OSCC cells promote the secretion of several chemokines from CAFs that alter the behaviour of the cancer itself. Chemokines such as CCL3, CCL5 and CCL7, all of which activate and promote OSCC cell migration were

reportedly increased significantly, as shown in figure 1.4 (Jung et al., 2010, Peña-Oyarzún et al., 2020).

Several cellular pathways have been investigated in the pathogenesis of oral cancers that contribute to an overall immunosuppressive and pro-inflammatory microenvironment. Hirai et al. suggest that the highly immunosuppressive nature of OSCC is associated with a programmed death ligand-1 (PD-L1) pathway through PD-L1 receptor. The group suggest that successful inhibition of this pathway and its receptor could perhaps supress tumour growth and an increase in an overall survival of patients (Hirai et al., 2017). Through their *in-vitro* studies performed on invasive OSCC cell lines (TSU) and cancer tissues samples, Hirai et al. showed high expression of PD-L1 on macrophages and dendritic cells in the stroma, the expression of which was successfully downregulated by treatment with TLR-4 inhibitory peptides. The upregulation of PD-L1 is believed to be associated with an epithelial-mesenchymal transition (EMT) taking place in the stromal cells, and when the stromal cells were co-cultured with TSU, PD-L1 expression was noted in macrophages and DCs and not in TSU cell line. This suggested the possibility of the involvement of an EMT-induced tumour antigen yet to be identified that perhaps induced the expression of PD-L1 on macrophages and DCs associated with tumours.

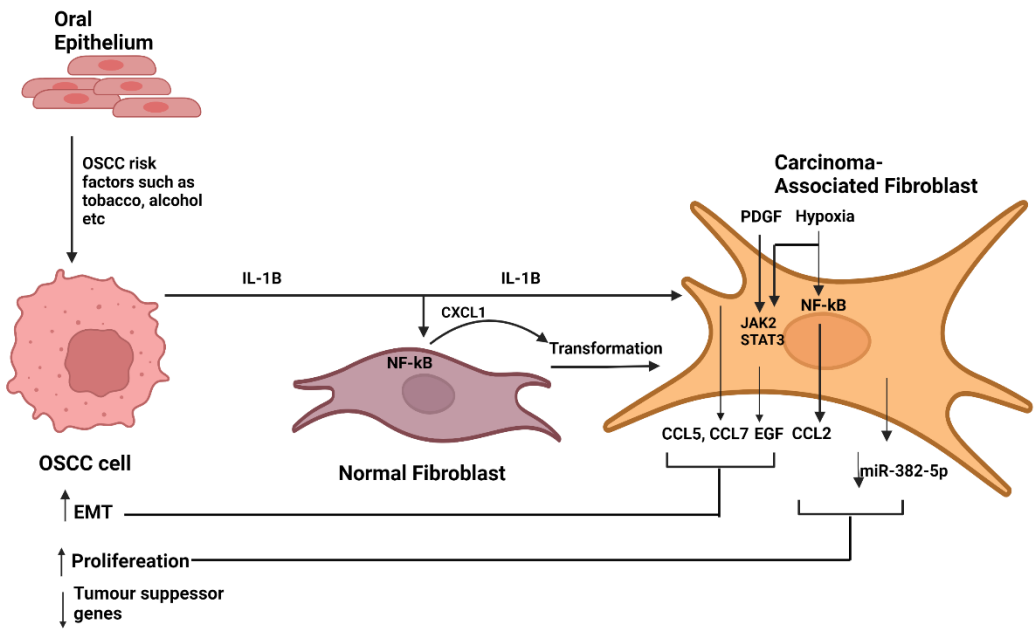

Figure 1.4. OSCC tumour microenvironment. Carcinoma associated fibroblasts play a key role in contributing to the tumour microenvironment in OSCC. The IL-1β secreted by active OSCC cells stimulate the expression of chemokine ligand CXCL1 via nuclear factor κβ (NFκβ) mechanism in fibroblasts, which transform into CAFs. The CAFs are responsible for causing an upregulation of epithelial-mesenchymal transition (EMT) and OSCC cell proliferation by overexpression of chemokines such as CCL5, CCL7, EGF and CCL2. Environmental factors such as hypoxia also trigger CCL2 expression via NFκβ mechanism (Peña-Oyarzún et al., 2020).

1.8 *Fusobacterium nucleatum*

Fusobacterium species are considered as normal commensals of the oral cavity, upper respiratory tract and the gut microbiota, and yet, have remained an enigma in their specific roles in pathologies associated with these complex body systems. Several researchers have implicated *F. nucleatum* in a plethora of disease conditions, ranging from pulpitis in a tooth to malignant cancers elsewhere in the body (Brennan and Garrett, 2019) (figure 1.5). The contribution of *F. nucleatum* in the progression of colorectal carcinoma has been studied by several researchers and some believe it to be a driver in this event (Healy and Moran, 2019, Han, 2015) .

Fusobacterium species are Gram-negative, fusiform, obligate anaerobes belonging to the phylum Fusobacteria. They are non-sporulating, non-motile and weak sugar fermenters. *Fusobacterium spp.* are occasionally encapsulated with a variable degree of mucopolysaccharide and this could potentially enhance *F. nucleatum* virulence and pathogenicity (Brook and Walker, 1986, Bolstad et al., 1996). The outer membrane of *F. nucleatum* has a variable degree of lipopolysaccharides, which perhaps plays an important role in its pathogenicity and ultimately, evasion of immune responses of the host (Ganesan et al., 2019). It is a secondary colonizer of dental plaque, mainly found on transparent gingiva and the gingival groove, and is a component of the normal oral flora (Healy and Moran, 2019). *F. nucleatum* has a high rate of detection in destructive periodontal disease and infectious dental pulp, as it assists other pathogens in establishing oral infectious diseases (Han, 2015).

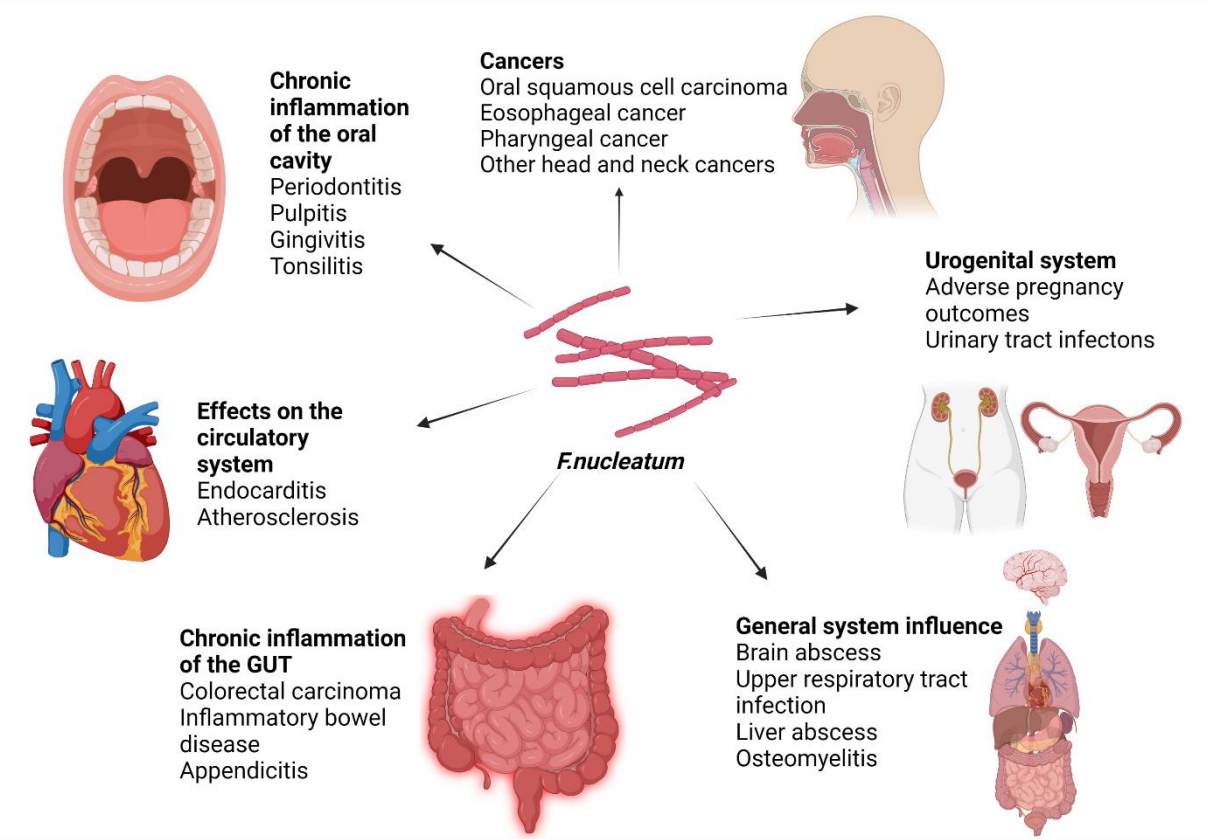

Figure 1.5. *F. nucleatum* in human diseases. Though a normal commensal in the oral cavity, *F. nucleatum* is implicated in a plethora of diseases in the human body, including a combination of bodily systems. Its role in the gastrointestinal tract (GIT) as a potential causative factor in CRC has been studied in detail and described. In the oral cavity, *F. nucleatum* is considered as a pathogen in periodontal diseases such as periodontitis and gingivitis and is a commonly isolated organism from periapical lesions and dental pulp. Modified from Brennan and Garrett, 2019.

1.9 Taxonomy

Fusobaterium nucleatum previously belonged to the family *Bacteroidaceae.* However, recent taxonomic investigations based on 16S rRNA analysis have re-classified them to their exclusive phylum Fusobacteria and family *Fusobacteriaceae* (Gupta and Sethi, 2014). Currently there are five recognised subspecies of *F. nucleatum*, namely, subspecies *nucleatum, polymorphum, animalis, vincentii* and *fusiforme*. There have been recent developments in this categorisation of the sub-species and proposals to re-classify subspecies *fusiforme* and *vincentii* as one have been proposed based on the similarity of the RNA polymerase beta subunit gene, zinc protease gene and 16S rRNA gene sequences (Henne et al., 2018, Kim et al., 2010). All the five subspecies are common inhabitants of the mouth, respiratory tract and the gut microbiota, however, some researchers believe subspecies *vincentii, nucleatum* and *polymorphum* to be predominant in the oral cavity (Gmur et al., 2006, Moore and Moore, 1994, Strauss et al., 2008). Oral microbiome studies have investigated the distribution of *F. nucleatum* and the closely related *F. periodonticum* in the various sites within the oral cavity. Eren and colleagues studied the oral microbiome using a high-resolution 'oligotyping' method that evaluated individual nucleotide positions to define oligotypes from 16S RNA gene data (Eren et al., 2013). This technology of oligotyping has enabled in the identification of several commensals and potentially pathogenic species of *F. nucleatum* that are widespread across the oral cavity (Eren et al., 2014). The distribution of *F. nucleatum* in the oral cavity is variable (Eren et al., 2014, Eren et al., 2013) and there is an indication of variation in distribution based on sex (Henne et al., 2018) (figure 1.6). Through oligotyping analysis, Eren et al. showed abundant oligotypes of *F. nucleatum* and their habitat differentiation in the oral cavity. Of the five different sub-species, *F. nucleatum* ssp *polymorphum* was the most common in supragingival plaque, whereas *F. periodonticum* dominated the mucosal surfaces of the oral cavity including the hard palate, throat, palatine tonsils, dorsum of tongue and saliva (Eren et al., 2014).

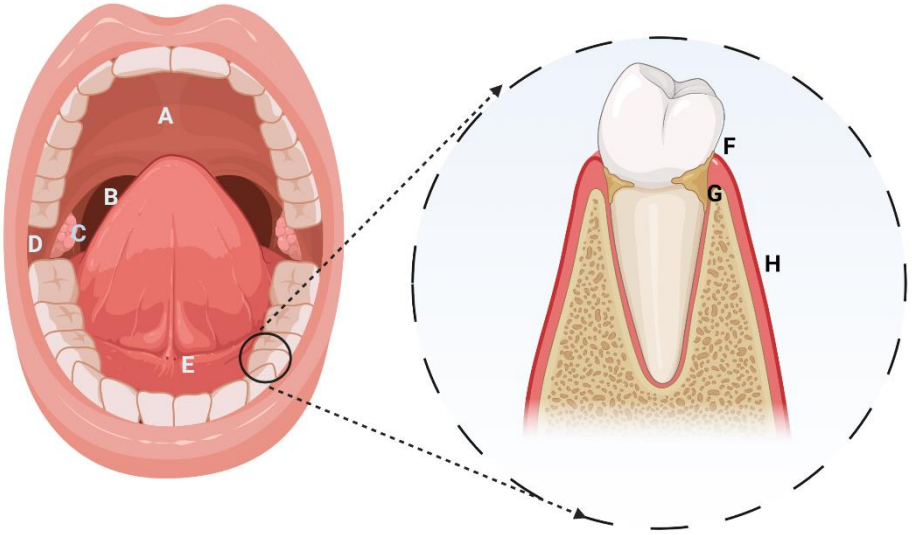

Figure 1.6. Distribution of *F. nucleatum* in the oral cavity. *F. nucleatum* is distributed throughout the oral cavity including (A) hard palate, (B) throat, (C) palatine tonsils, (D) buccal mucosa, (E) salivary pool, (F) supragingival plaque, (G) sub-gingival plaque and (H) keratinized gingiva. Modified from Eren et al, 2014.

1.10 Virulence factors of *F. nucleatum*

F. nucleatum is an intermediary colonizer and co-aggregates with other organisms, forming biofilms in the oral cavity and the gut mucosa. It is also an adherent bacterium, therefore, adherence to and invasion of host cells are essential mechanisms for its colonization, dissemination, evasion of host cell defence and induction of host response. Once internalised into host cells through active invasion, *F. nucleatum* can induce cytoskeletal rearrangements through actin filaments (Gursoy et al., 2008). It encodes several adhesins belonging to the type V autotransporter secretion system for the purpose of adhering to host cells, namely, Fap2, RadD, and Aid1. An additional adhesin, FadA is believed to bind to host cells and is the best known virulence factor for *F. nucleatum* in CRC *(Han, 2015).* Most studies on adhesion to date have focused on subspecies *nucleatum,* however orthologues of most of these adhesins are found in the other subspecies.

Most Gram-negative bacteria such as *F. nucleatum* are encapsulated by an outer membrane layer, which requires specialised secretion systems for exchange of essential solutes and polypeptides. To overcome this hurdle, they have evolved to develop secretory systems that essentially "inject" substances into their surroundings. The type V secretory system is one such mechanism by which the Gram-negative bacteria achieve this successfully. The type V secretory system is comparatively smaller to the other eight classes of secretory systems, and its size is limited to the thickness of the bacterial outer membrane (Meuskens et al., 2019). This secretory system is composed mainly of classical autotransporters (type Va), two-partner secretory system (type Vb) and type Vc autotransporters (Henderson et al., 2004). Recent research on type V autotransporter has led to identifying sub-classes, namely, type Va, type Vb, type Vc, type Vd, type Ve and most recently, type Vf autotransporters (Grijpstra et al., 2013, Meuskens et al., 2019). These Type V autotransporter protein secretion systems have been known to contribute to virulence properties including ability to adhere and invade the host cell, toxicity, coaggregation with other pathogenic strains and biofilm formation (Coppenhagen-Glazer et al., 2015).

The structure of a typical autotransporter consists of three functional regions- an N-terminal signal peptide, a secreted passenger domain (also referred to as α-domain) and a β-barrel domain (translocator or β-domain). The N-terminal targets the protein to the Sec

translocon for translocation across the inner membrane, the α-domain is the actual secreted moiety or passenger and the C-terminal β-domain or translocator facilitates the transportation of the passenger from the periplasm to the exterior through the outer membrane. Both the α and the β domain are found within a single polypeptide chain (Pohlner et al., 1995, Meuskens et al., 2019, Henderson et al., 2004) as shown in figure 1.7.

Research work by Doron et al identified a serine protease actively involved in the functionality and survival of *F. nucleatum* and termed it "fusolisin". Fusolisin is a serine protease with a molecular weight of 61-65 kDa belonging to the Type Va autotransporter secretory system (Doron et al., 2014). The serine protease is derived from a precursor peptide (approx. 115kDa) that is removed when it crosses the cytoplasmic membrane. A β-barrel pore structure is formed on the outer membrane by the C-terminal domain. The N-terminal serine endopeptidase domain is transported across the cell membrane to the exterior of the cell via the autotransporter mechanism. Apart from providing nutritional support to the bacteria, fusolisin has also been demonstrated to help the bacteria evade host immune responses by inactivating immune responses by the host (Doron et al., 2014). *F. nucleatum* achieves this by secreting as fusolisin in the extracellular spaces and inactivating chemokines and host ligands. Once released by the vesicles that contain them, fusolisin degrades extracellular matrix causing damage to the host tissues such as periodontal ligaments, and hydrolyse IgA antibody essentially providing first defence of the immune system against bacterial pathogens (Bachrach et al., 2004). Further investigation on the extracellular activity of fusolisin by Bachrach et al. revealed that the protease targeted fibrinogen and fibronectin and matrix collagens I and collagen IV. Degradation of these proteins were observed at a body temperature of 37^{o}C *in vitro* (Bachrach et al., 2004).

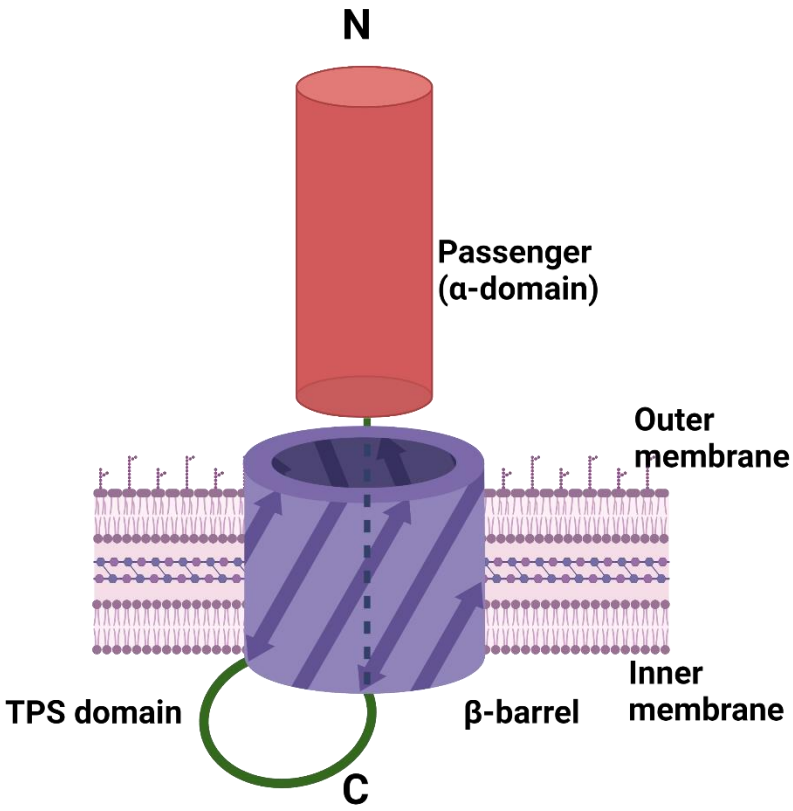

Figure 1.7. A simple schematic representation of a typical type Va autotransporter. The β-barrel is represented in blue and the α-domain (passenger) is shown in red. The N and C terminals are indicated at their respective positions. The β-barrel extends from the inner cell membrane to the outer cell membrane, facilitating the transportation of the secreted passenger into the exterior of the bacterial cell.

Fap2

Fibroblast activation protein 2 (Fap2), is an outer membrane protein (OMP) exclusive to *F. nucleatum* adhesins that is a galactose sensitive haemagglutinin protein. It binds to host epithelial cells via D-galactose-(1-3)-N-acetyl-D-galactosamine (Gal-GalNAc) binding receptor sites and thus, contributes to both adhesion and invasion of the host cell (Ganesan et al., 2019). The Fap2 protein is the largest protein encoded in *F. nucleatum* and belongs to the Type Va autotransporter family. This adhesin has been shown to play crucial roles in coaggregation with other species in the oral cavity such as *Candida* species and *P. gingivalis* (Coppenhagen-Glazer et al., 2015).

In a recent study by Gur et al., the Fap2 adhesin was shown to inhibit the antitumor activity of lymphocytes by binding to TIGIT receptor expressed by T cells and NK cells and CEACAM1 receptor also expressed by T cells and NK cells, ultimately inhibiting immune cells activity in CRC, promoting cancer growth and survival (Gur et al., 2019b). Along with other OMPs such as RadD, Fap2 induces cell death in human lymphocytes as a mechanism of virulence attributed to pathogenic bacteria (Kaplan et al., 2010). Studies involving *F. nucleatum* mutants, which were defective of the D-galactose sensitive adhesins (*Δ fap2*) showed reduced or complete loss of coaggregation with *P. gingivalis* in the oral cavity and defective or loss of adhesion to mammalian cells *in-vitro* and placental colonisation *in-vivo* (Coppenhagen-Glazer et al., 2015).

RadD

RadD is an outer membrane protein (OMP) and arginine-inhibitable adhesin found associated with other adhesins of *F. nucleatum* such as Fap2. Early genome analysis of these proteins showed that RadD belonged to the autotransporter type Va class of secretory proteins. Further gene sequencing revealed that these proteins had a characteristic C-terminal autotransporter domain (Kaplan et al., 2009). The RadD molecule helps in the formation of biofilms in the human body, and has been shown to play a key role in the bridging of early and late colonizers that usually do not interact with each other, thus, co-aggregating many different species in the oral biofilm (Kaplan et al., 2009). Further investigation of RadD and its relationship with blood cells implied that it induced cell death

of human lymphocytes not by secreting effector proteins, but rather by a contact-based mechanism (Kaplan et al., 2010).

Aid1

Adherence Inducing Determinant 1 (Aid1) is a small membrane associated adhesive protein, that plays a key role in aiding RadD to interact with other Gram positive species in the oral cavity (Kaplan et al., 2014). It was shown that the activity of Aid1 was dependent on the presence of RadD, and in the absence of RadD, overexpressed Aid1 failed to produce co-aggregation between bacterial species (Kaplan et al., 2014).

FadA

Fusobacteria Adhesin A (FadA) is an adhesin, composed of a small α-helical peptide, that plays a very important role in the adhesion and invasion of host epithelial cells by *F. nucleatum* in CRC. It is composed of 129 amino acid residues, with an 18 amino acid signal peptide. It is present as a pre-secreted form pre-FadA and a post-secreted mature form, mFadA (Ikegami et al., 2009). The FadA adhesin is unique in the sense that both forms of it combine to form a pre-FadA-mFadA complex (FadAc) that's anchored in the inner cellular membrane with the complex protruding out, that participates in the adhesion and invasion of host cells (Xu et al., 2007). The FadAc has been demonstrated to be the functional unit of the FadA adhesin to specifically bind to receptors of the cadherin family. In the endothelium, FadA was shown to mediate adhesion via the VE-cadherin receptor, causing alterations in the endothelial cell architecture, ultimately causing increased vascular permeability to *F. nucleatum* as a result of reduced cell-cell junction (Fardini et al., 2011). In a similar fashion, in CRC cells, the FadA adhesion attaches to the E-cadherin on epithelial cells, activating various intracellular changes such as β-catenin/wnt signalling pathways and E-cadherin/β-catenin pathways, overexpressing oncogenic genes. A recent study identified region 3 of the EC5 receptor responsible for the FadA binding (Rubinstein et al., 2013).

1.11 Pellicle and dental plaque formation

F. nucleatum is an opportunistic commensal of the oral cavity that belongs to the orange-complex. It is an intermediary coloniser, actively participating in coaggregation with other bacterial species in this rich, aqueous ecosystem that is the oral cavity. Biofilm formation on the mucosal surfaces and teeth surfaces as a result of the complex interactions between various microbial species ultimately contribute to the sequences leading to the formation of dental plaque. Primary colonizers such as *Streptococcus oralis, Streptococcus sanguis, Streptococcus mutans, Streptococcus gordonii* and *Lactobacillus acidophillus* adhere to salivary derived pellicles on teeth surfaces and thus, the initial planktonic inoculum facilitates the adherence of other co-aggregators such as *F. nucleatum* (Foster and Kolenbrander, 2004, Chenicheri et al., 2017). *F. nucleatum* subsp. *polymorphum* has been demonstrated to adhere to salivary α-amylase in early stages of biofilm formation, thereby, playing an intermediary role in interactions between early and late colonizers (Zulfiqar et al., 2013). The coaggregation between *F. nucleatum* and *Streptococcus* spp., particularly *S. sanguis* is described as "corncob" in dental plaque (Lancy et al., 1983). Such bacterial coaggregations have been described much earlier in time, dating back to as early as 1890 by Vincentini and by the end of the 19th century, Williams in 1899 reported similar findings in a collection of dental plaque samples. Nearly a century later, Jones in 1972 used a scanning electron microscope and reported observing similar co-aggregations between filamentous and coccoidal bacteria and described them as corncob like structures (Jones, 1972). However, the role of such intimate relationships between different bacterial species were poorly understood and a concrete explanation was lacking. A year later, in 1973, Listgarten and colleagues continued the investigation using a transmission electron microscope and explained the exact nature of the participants in such complex microscopic structures (Listgarten et al., 1973). The attachment was observed to be between a coccoidal species and a filamentous species and the coccoidal bacteria provided the attachment apparatus from its outer capsular layer, forming tufts of fimbriae (Lancy et al., 1983, Listgarten et al., 1973). The corncob formation between the two species has been now indicated as a bridging link between aerobic supragingival plaque bacteria and their anaerobic subgingival counterparts. The distribution of bacterial species in dental plaque biofilm is variable, depending on the anatomical locations such as supragingival and subgingival plaque and also on oxygen availability (Marsh, 2006, Chenicheri et al., 2017).

1.12 Periodontal health and disease

A healthy periodontium is one with no gingival inflammation or loss of epithelial attachment, characterized by absence of gingival bleeding and shallow gingival pocket depth on examination (Li et al., 2020). Gingivitis is the earliest sign of periodontal disease caused by accumulation of dental plaque on tooth surfaces. With prolonged exposure to dental plaque, there is loss of epithelial attachment and a consequent deepening of the periodontal pocket. A deepened pocket is a nidus for the growth of proteolytic Gram negative anaerobes, eliciting host response leading to further destruction of the periodontium (Edwards et al., 2006, Signat et al., 2011). As mentioned earlier, the role of *F. nucleatum* is quite indirect in periodontal disease. It seems to aid periodontitis by helping the coaggregation between early plaque colonizers such as *Streptococcus* spp. and periodontal pathogens such as *P. gingivalis*, *Tannerella forsythia*, and *Treponema denticola*, which are late colonizers. Due to its coaggregation and high invasion properties, studies have shown that *F. nucleatum* is able to transport non-invasive organisms into epithelial cells (Edwards et al., 2006, Signat et al., 2011, Han et al., 2000). The overall effect is a chronic inflammatory state of the gingival epithelium, stimulating the infiltration of immune cells and production of pro-inflammatory cytokines such as IL-8 and matrix metalloprotease 13 that further support periodontal tissue destruction and progression of the disease.

1.13 *F. nucleatum* and human cancers

As part of the commensal microflora, *F. nucleatum* forms an integral part of various microbial niches in the human body. All major microbiomes, from the oral cavity to the rectum, are inclusive of this bacterium and many pathologies in the GI tract have been associated with this bacterium. The most significant association with *F. nucleatum* that has gathered much attention is cancer. Several studies have emerged in the medical literature recently that implicate the involvement of *F. nucleatum* in carcinogenesis. Biopsies of cancers of the lower abdomen such as colorectal carcinoma have shown excessive bioburden with *F. nucleatum* and there is evidence that this bacterium could be more than a mere bystander in tumorigenesis (Brennan and Garrett, 2019). In 2012, the first studies to associate *F. nucleatum* and CRC were reported in back-to-back papers published in Genome Research (Kostic et al., 2012, Castellarin et al., 2012). Since then, newer evidence suggesting the involvement of *F. nucleatum* in other cancers such as breast, oesophageal and gastric cancer have also emerged. Parhi et al. investigated fifty formalin-fixed paraffin embedded biopsy samples of breast cancer obtained from patients visiting Sheba Medical Center and the Maccabi Health Care Services, Israel. The results showed that cancer tissues were heavily colonized by *F. nucleatum* and the concurrent expression of the Fap2 receptor N-acetyl-D-Galactosamine (Gal-GalNAc) was increased markedly in the cancer cells. Through in-vivo mouse study models the group demonstrated that the bacterium used a haematogenous route to colonize tumour tissues using Fap2 adhesin (Parhi and Alon-Maimon, 2020). The events following this attachment of the bacteria to breast cancer tissues is unclear, however, researchers postulate the involvement of immunosuppression in the host by activation of toll like receptors 4 (TLR4) pathway, amongst many other potential pathways yet to be discovered (Van der Merwe et al., 2021). In oesophageal cancer, inoculation of cancer cells *in-vivo* and *in-vitro* with *F. nucleatum* was reported to activate the NF-κβ pathway that directed the tumour progression (Nomoto et al., 2022). Activation of the NF-κβ pathway by *F. nucleatum* infection is believed to be mediated by nucleotide oligomerization domain 1 (NOD1) and receptor-interacting protein kinase 2 (RIPK2). *In-vivo* studies of nude mice inoculated with *F. nucleatum* subcutaneously showed an accelerated oesophageal tumour growth and increased tumour mass as compared to control mice that were inoculated with PBS and *S. mutans* (Nomoto et al., 2022). The activation of the NF-κβ pathway has also been implicated in colorectal carcinoma. Chen et

al. showed that infecting HTC-116 CRC cell line *in-vitro* with *F. nucleatum* significantly upregulated the expression of the long non-coding RNA Keratin7-antisense (KRT7-AS) and Keratin 7 (KRT7), both of which are responsible of CRC cell migration (Chen et al., 2020). The prognosis of cancers colonized by *F. nucleatum* have been reported to be poor (Hsieh et al., 2021, Han et al., 2000, Nomoto et al., 2022). Increased abundance of *F. nucleatum* in gastric cancers seem to affect the long-term prognosis and clinical outcome. As in colorectal carcinoma, Bohem et al. suggest that colonisation of the bacteria in gastric cancer (GC) and gastric preneoplastic conditions resulted in extremely poor outcomes (Boehm et al., 2020). They compared the *F. nucleatum* loads in both CRC and GC and in non-CRC and non-GC samples. The bacterial loads were much higher in non-tumour sites in both cases, however, the tumour sites seemed to accommodate significantly higher levels of *F. nucleatum* as well. Further to this, they demonstrated higher levels of Gal-GalNAc expression in CRC and GC cells and this corroborated with other studies that suggested the role of Gal-GalNAc in attracting the Fap2 adhesin of *F. nucleatum* in cancerous lesions (Boehm et al., 2020, Abed et al., 2016). Overall, the evidences in the literature seem to point in the direction of the involvement of hematogenous spread of *F. nucleatum* as the route of cancer infection. The increased bacterial load in cancerous lesions seem to be the result of either overexpression of the polysaccharide receptor Gal-GalNAc on cell surfaces attracting Fap2 adhesin or the direct involvement of the FadA adhesin of *F. nucleatum* with epithelial cadherins.

The role of *F. nucleatum* in OSCC is much less investigated and the evidence of the relationship of the bacteria in OSCC tumorigenesis is less well developed. Studies such as Amer et al (2017) focussing on the relationship of the oral microbiome and oral dysplastic events have shown an enrichment of *Fusobacteria* and other species in pre-malignant and malignant conditions of the oral cavity such as OLK and OSCC (Amer et al., 2017). Studies examining the tumour microbiome of OSCC have consistently shown that *F. nucleatum* is the most overrepresented microbe at these sites (Schmidt et al., 2014, Perera et al., Perera and Al-Hebshi, 2018).

Although these studies only show an association, mechanistic studies also support a role for *F. nucleatum* in oral carcinogenesis. Zhang et al. investigated the role of *F. nucleatum* in epithelial-mesenchymal-transition (EMT) associated in the initiation of OSCC. *In-vitro*

experiments were conducted on non-cancerous human immortalized oral epithelial cells (HIOEC) and oral cancerous cells lines SCC-9 and HSC-4. The results revealed that *F. nucleatum* infection upregulated mesenchymal markers expression such as vimentin, N-cadherin and Snail Family transcription repressor 1 (SNAI1) whilst E-cadherin expression was downregulated and translocated intracellularly. MMP9 expression was significantly increased, promoting cell migration. Regulation of EMT was investigated by quantifying the expression of a novel MIR4435-2HG gene through RT-qPCR, which was significantly increased. Knockdown of this gene significantly reduced the expression of SNAI1 required for initiating EMT. Knockdown of MIR4435-2HG also significantly increased the expression of miR-296-5p, that promotes EMT. Another protein called Akt2 belonging to AKT family of proteins was upregulated in *F. nucleatum* infection of both cancerous and non-cancerous cell lines, which is required in the upregulation of SNAI1 in EMT (Zhang et al., 2020). More direct evidence for the involvement of *F. nucleatum* in the development of OSCC was provided by Gallimindi et al (Binder Gallimidi et al., 2015) who used a chemically-induced (4-nitroquinoline-1-oxide) murine oral dysplasia model to investigate the impact of *F. nucleatum* infection on oral carcinogenesis. Chronic bacterial infection was found to promote OSCC in this model and this was associated with augmented signalling along the IL-6-STAT3 axis. These data represent the most direct evidence for the role of *F. nucleatum* in promoting carcinogenesis.

1.14 Proposed mechanisms of *F. nucleatum* pathogenesis in Colorectal Carcinoma (CRC)

The most intensely studied malignancy for the involvement of *F. nucleatum* is colorectal carcinoma (CRC). CRC is a lethal malignancy, being the third most common cancer type worldwide, with a five years survival rate of 65% (Shang and Liu, 2018, Zhang et al., 2018). The aetiology of CRC was thought to be solely due to genetic and environmental factors, until recent studies showed an increased evidence of the role of the gut microbiota as a potential aetiological factor. *F. nucleatum* in particular has largely been isolated at high abundance from colorectal carcinoma lesions compared to the adjacent unaffected sites, suggesting its involvement in tumorigenesis (Kostic et al., 2013).

In CRC, *F. nucleatum* modulates cellular properties, influencing cellular survival, growth and proliferation. The contribution of the bacterial adhesins in tumorigenesis has been extensively researched in recent years. Through the FadA adhesin, *F. nucleatum* binds to E-cadherin expressing cancerous colonic cells, activating a cascade of intracellular reactions responsible for cellular proliferation, including an upregulation of β-catenin signalling which increases the transcription factors for oncogene expression. This also activates pro-inflammatory cytokines such as IL-6 and IL-8, creating an exaggerated inflammatory microenvironment within the cellular compartment, promoting tumorigenesis. An intracellularly invaded *F. nucleatum* also activates p38, responsible for the expression of matrix metalloproteinases MMP-9 and MMP-13, both of which have an important role in tumour invasion and progression. Uitto et al. further demonstrated the significance of increased collagenase 3 (MMP-13) and gelatinase B (MMP-9) expression in infected cell migration and survival (Uitto et al., 2005). Inhibition of the p38 MAP kinase by SB 203580 (p38 specific inhibitor) could reduce collagenase 3 mRNA expression and cellular migration in infected cells. Figure 1.8 shows the proposed mechanism of *F. nucleatum* pathogenesis in CRC.

Infection of CRC tissue by *F. nucleatum* has also been proposed to modulate anti-tumour immunity. A study by Ye et al. showed that carcinoma lesions in CRC were heavily colonised by *F. nucleatum* subsp*. animalis* and the chronic infection and subsequent inflammation with these bacteria resulted in a marked increase in the tumour levels of cytokines, specifically, IL-17A and TNF-α and induced monocyte/macrophage migration, ultimately contributing to a pro-inflammatory micro environment further promoting a malignant

transformation of the tumour (Ye et al., 2017). As mentioned earlier, Gur et al. have also implicated the Fap2 adhesin as an inhibitor of T cells and NK cells activity, which may promote cancer growth and survival (Gur et al., 2019b). Several studies have shown the importance of Gal-GalNAc receptors and Fap2 adhesin in colorectal carcinoma progression (Yang and Shamsuddin, 1996, Gur et al., 2019a, Abed et al., 2016). Gal-GalNAc, also known as Thomson-Friedenreich Antigen or T-antigen is a tumour associated disaccharide moiety, clinically used as a tumour bio-marker which is most often overexpressed on neoplastic cells of the colon and on rare occasions identified on distant non-cancerous mucosa (Said et al., 1999). Several studies have reported not identifying Gal-GalNAc on normal colonic mucosa in healthy individuals. Experiments conducted by Abed et al. showed that *F. nucleatum* mutants that were devoid of Fap2 adhesin showed reduced adhesion to colonic tumour cells that expressed Gal-GalNAc in mice models (Abed et al., 2016). To demonstrate the haematogenous mode of transportation of *F. nucleatum* from the native oral cavity to distant neoplasms such as the colon, Abed et al. injected *F. nucleatum* ATCC 23726 via the tail vein of BALB/cJ wild-type mice that were previously inoculated with cancerous cells for tumour formation. 24 hours post inoculation, tumour samples were harvested that showed an abundance of *F. nucleatum* in tumour site compared to adjacent normal site.

The interaction of *F. nucleatum* with the host cell via the Fap2 adhesin triggers various cellular responses as discussed earlier, and these cellular responses play a significant role in modifying and in some instances, altering the tumour behaviour. According to a recently study, an increased cellular secretion of IL-8 and C-X-C motif chemokine ligand 1 (CXCL1) creates a favourable proinflammatory microenvironment for the tumour cells to thrive and proliferate at a rapid rate and contribute in an increased recruitment of tumour associated fibroblasts and macrophages. *In-vivo* demonstration of immune cell recruitment in mouse study models showed an increased secretion of CCL3, CXCL2, CCL5 and TNF-α. CCL3 has been shown to recruit lymphocytes in metastatic CRC, CXCL2 induces angiogenesis in tumour tissues and CCL5 induces CRC cell migration and invasion (Aldinucci and Colombatti, 2014, Chuang et al., 2009, Casasanta and Yoo, 2020). *In-vitro* experiments investigating these effects revealed an enhanced cellular migration of HCT116 CRC cell line

and CRC progression (Casasanta and Yoo, 2020). Clinically, an increased CXCL1 has been associated with poor prognosis in CRC patients as indicated by Casasanta et al.

Apart from the potential for inducing tumour growth and malignant transformation, recent studies have also focused on the effects of *F. nucleatum* on long-term prognosis and response to treatments in CRC. A study by Bullman et al. showed that distal metastases of colorectal carcinoma were heavily inoculated predominantly with *F. nucleatum* followed by other associated bacteria from their microbiome such as *Bacteroides* and *Provetella sp*. When these bacteria were treated with antibiotics, namely, metronidazole, the bacterial load of *Fusobacterium* reduced drastically in mice models, ultimately reducing the proliferation of cancerous cells and overall reduction in tumour growth (Bullman et al., 2017). The presence of a heavy load of *F. nucleatum* in tumorous tissues has been consistent with poor prognosis as these bacteria have been shown to supress T-cell mediated immune responses towards tumours as discussed earlier. However, some researchers believe that the presence of the bacterial DNA can be exploited as a prognostic biomarker in colorectal carcinoma. Mima et al. in a retrospective analysis of 1069 colon and rectal cancers showed that the level of *F. nucleatum* DNA was significantly associated with patient survival times (Mima et al., 2016).

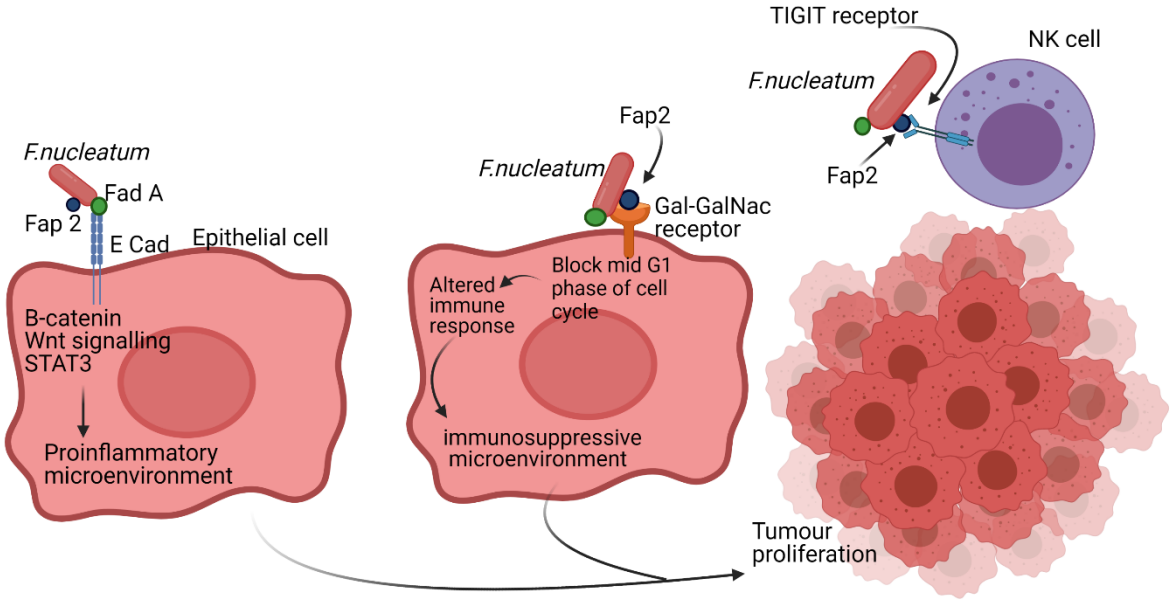

Figure 1.8. Interactions between *F. nucleatum* and epithelial cells in CRC that could produce an oncogenic phenotype. Binding of FadA adhesin to E-cadherin receptor on colon tumour cells activates expression of β-catenin, which is responsible for the production of various transcription factors for cellular growth and proliferation. An upregulation in β-catenin production takes a sinister route toward tumorigenesis. *F. nucleatum* also activates p38, increasing the expression of MMP-9 and MMP-13 responsible for tumour invasion and progression. Fap2 adhesin binding to N-acetyl-D-galactosamine (Gal-GalNAc) and galactose receptors of epithelial cells interfere with the G1 phase of the cell cycle, and TIGIT receptors of NK cells lead to an altered immune response, resulting in upregulation of tumour proliferation.

1.15 Rationale for this study

As outlined earlier in this chapter, *F. nucleatum* is a normal commensal of the oral cavity, however, its association with oral and extra-oral abnormalities and increasing evidences of its role as a driver in the progression of CRC is concerning (Boehm et al., 2020, Brennan and Garrett, 2019, Brook and Walker, 1986). Although recent works by Eren et al (2014) and Amer et al (2017) have shown the abundance in distribution of bacterial species in the oral cavity in health and in oral diseases such as OLK, the evidence of the role of *F. nucleatum* in OLK and OSCC is lacking. In this study we focus on the role of *F. nucleatum* in events such as OLK and OSCC where E-cadherins have been downregulated as a consequence of dysplasia.

A further section of this study also focuses on developing a novel method to assess the bacterial invasion of oral keratinocytes using confocal microscopy that enables quick and rapid imaging and quantification of bacterial invasion of oral keratinocytes. The study also explores the effects of *F. nucleatum* induced secretion of chemokines on dysplastic oral keratinocytes essential for cancer progression and metastasis.

Specific aims of the project include:

- To investigate the role of E-cadherin in dysplastic epithelia and the subsequent effects of FadA and Fap2 adhesins of *F. nucleatum* on oral dysplasia and OSCC
- The effect of *F. nucleatum* subsp. *polymorphum* strains on adhesion and invasion and the influence of epithelial cell receptors on the same
- The influence of *F. nucleatum* adhesin genes on their interactions with dysplastic epithelia
- The effects of *F. nucleatum* subsp. *polymorphum* on cellular induction of cytokine and chemokine secretion
- The overall influence of induced cytokine and chemokines on the OSCC cell motility, migration, invasion and angiogenesis essential for OSCC progression and metastasis

Chapter 2

General Materials and Methods

2.1 General microbiological Methods

2.1.1 Bacterial strains

The bacterial type strain *Fusobacterium nucleatum* subsp*. polymorphum* ATCC 10953/NCTC10562 used in this study was obtained from the Dublin Dental University Hospital microbiological strain collection, Division of Oral Biosciences. All clinical isolates of *F. nucleatum* subsp*. polymorphum* used in this study were obtained by swabbing diseased oral mucosa of patients referred to the dysplasia clinic in the Oral Maxillofacial, Oral Medicine and Oral pathology department, Dublin Dental University Hospital, Dublin, Ireland, following written informed patient consent.

Escherichia coli type strain DH-5α was also obtained from the Dublin Dental University Hospital microbiological strain collection, Division of Oral Biosciences.

2.1.2 Patient selection criteria and swabbing

Information regarding the biopsy results of lesions (degree of dysplasia, Carcinoma-In-Situ or Oral Squamous Cell Carcinoma), history of habits (smoking and alcohol consumption), patient dental history for oral hygiene (tooth brushing frequency, use of mouthwashes, oral hygiene index-simplified), loss of tooth (due to periodontitis, trauma, dental caries or any other relevant cause) and denture history (partial or complete dentures, acrylic or metal, dental implants) were recorded. Exclusion criteria for obtaining samples from patients included any form of diabetes, Crohn's disease or Ulcerative Colitis; a history of gastric or bowel cancer, recent or current history of cold or flu or any other viral infections, antibiotics regimen in the last two months, use of systemic, inhaled or locally administered steroids over the last two months, and a history of dry mouth. In this current study a total of seven patient samples and one standard type strain sample were considered (n=8). A summary of the patient samples details is listed in table 2.1.

Table.2.1. Sample collection and criteria. A total of seven patient samples (n=7) were considered for this study.

Sample	Lesion site	Diagnosis	Control swab	Smoking h/o	Alcohol h/o	OHI-S
40A2	WP LVT	Moderate Dysplasia	LLBT	Former smoker, stopped >12 months	40 units/week	0.6
41A	WP LLBT	Severe Dysplasia/CIS	LBM	Current smoker	40 units/week	N/A
41B2	Normal BM	NA	LBM			
43A2	WP R&L FOM	Moderate Dysplasia	Dorsum Tongue	Current smoker	6 units/week	N/A
43A3	Erythroplakia RFOM	Moderate Dysplasia	RLBT	Current smoker	6 units/week	N/A
43B1	Normal RLBT	NA	RLBT	Current smoker	6 units/week	N/A
60A2	WP LRM pad Sublingual Keratosis	Moderate Dysplasia	RLBT	Current smoker	0 units/week	0.4

* LVT: Left ventral tongue; LLBT: Left lateral border tongue; LBM: left buccal mucosa; FOM: Floor of mouth; LRM: left retromolar pad, OHI-S: oral hygiene index-simplified

2.1.3 Microbial bacterial culture method

Mucosal swabs of patients presenting with leukoplakia, erythroplakia, carcinoma-in-situ and squamous cell carcinoma of the oral cavity and mucosa of the normal contralateral side if present were collected using catch-all collection swabs (Epicentre, Madison, WI, United States of America). The swabs were plated and sub-cultured in the laboratory within 24 hours using brain-heart infusion agar (BHI; Sigma-Aldrich, St. Louis, USA) supplemented with 5% defibrinated horse blood (Thermo Scientific, Hampshire, UK), 7.5 µg/ml vancomycin and 20 µg/ml streptomycin to isolate fusobacterial strains. The identity of suspected *F. nucleatum* was confirmed by Sanger sequencing (section 2.1.6). The *F. nucleatum* strains were collected and stored in microbank microbial storage vials (Pro-Lab Diagnostics, Canada) at -80^{o}C. Bacterial cultures were thereafter, regularly maintained in BHI agar plates, supplemented with 5% defibrinated horse blood for 5-7 days and cultured in BHI broth (Sigma-Aldrich, St. Louis, USA) supplemented with 2.5 g yeast extract (Sigma-Aldrich, St. Louis, USA), 0.3 g L-Cysteine (Sigma-Aldrich, St. Louis, USA), 5 µg/ml Haemin and 1 µg/ml Menadione for 48 hours before using broth cultures for experiments. Both culture plates and broth cultures were maintained in anaerobic jars supplemented with AnaeroGen™ 3.5L sachets (Thermo scientific, UK) in 37^{o}C incubators. Overnight broth cultures of *Fusobacterium nucleatum* subsp*. polymorphum* were grown to exponential phase, centrifuged (4000 rpm for 5 minutes) and washed three times with sterile phosphate buffered saline before standardising the bacterial suspension at OD_{600} of 0.7. Bacterial staining by Rue's method and phase contrast microscopy was used to check the purity.

Escherichia coli type strain DH5α was used as a positive control for serum assay and enzyme-linked immunosorbent assay and multiplex assay for the detection of relevant cytokines and chemokines. *E. coli* was sub-cultured on L-agar regularly and grown to exponential phase in L-broth overnight at 37^{o}C shaking incubator revolving at 200 rpm for experimental purposes.

2.1.4 Buffers and solutions

Formulations of specific buffers and solutions used are described in relevant experimental protocols when used. Solutions were sterilised by either filtration or autoclaving as described later in this section. All solutions were made up to a final volume with ultra-pure, sterile water (Milli-Q) processed using a Milli-Q Biocel system (Merck-Millipore, MA, USA).

Solutions that required to be a specific pH was adjusted using a Thermo Scientific Orion 3-star bench top pH meter (Thermo-Fischer Scientific, Ballycoolin, Dublin 15, Ireland). The pH was adjusted to higher pH using 5M Sodium Hydroxide (NAOH) supplied by Sigma-Aldrich, Germany, or lower pH using 37% (by volume) Hydrochloric Acid (HCl), also supplied by Sigma-Aldrich.

2.1.5 Chemicals, enzymes, reagents and antibiotics

All chemicals, enzymes, reagents and antibiotics used in this study were of molecular biology grade and suppliers for specific chemicals, enzymes, reagents and antibiotics are given in the relevant sections of this study.

2.1.6 Identifying *F. nucleatum* strains

The *F. nucleatum* strains stored at -80^{o}C were reactivated by plating on BHI-agar supplemented with 5% defibrinated horse blood. Colonies were picked for overnight broth culture. 1 ml of overnight culture was spun down at 12000-13000 rpm for 2-3 mins and pellet re-suspended in 200 µl breaking buffer. The above suspension was transferred into screw-cap tube with 0.3 g of glass beads. 200 µl phenol:chloroform:isoamyl alcohol at a ratio of (24:24:1) was added and cells lysed in a bead breaker for 30 sec. The lysate was centrifuged for 10mins at maximum speed (15000 rpm). The aqueous phase was removed and put into a fresh tube (100 µl) with equal amount of chloroform:isoamylalcohol (24:1). The mixture was centrifuged for 2 mins at maximum speed (15000 rpm). The aqueous phase was removed into a new tube. 1µl of the supernatant was used in the PCR as the template DNA.

To carry out the PCR, GoTaq PCR Core System (Promega) was used. The recipe that was used for the PCR included 5 µL 5x Green Taq Buffer, 15.5 µL nuclease-free water, 2.5 µL $MgCl_2$ (25 mM), 0.5 µL dNTPs (10 mM), 0.5 µL of each oligonucleotide (10 µM) (27F

Forward; 5'-AGAGTTTGATCMTGGCTCAG-3', 1592R Reverse 5'-ACCTTGTTACGACTT-3'), 0.5 µl Taq polymerase and 1 µL DNA template as described earlier.

The PCR cycle was set with an initial denaturation at 90°C for 3 minutes followed by denaturation at 95°C for 30 seconds, annealing at 55°C for 30 seconds, extension at 72°C for 59 seconds, returning to the denaturing step for 30 cycles and a post cycling extension step at 72°C for 5 minutes.

PCR products were purified with GenElute PCR Clean-Up Kit (Sigma) as per the manufacturer's instructions. DNA concentrations were quantified using a Nanodrop 2000 (ThermoFisher Scienfiic). Products were sent to Source Bioscience Limited (Dublin City University, Glasnevin, Dublin, Ireland) for Sanger sequencing of the 16s rRNA gene. Isolates were speciated by comparing the sequence to entries in the Human Oral Microbiome Database (HOMD) and the National Centre for Biotechnology Information (NCBI).

2.2 Mammalian Cell culture

2.2.1 Cell lines

H357 (E-cadherin expressing, Oral Squamous Cell Carcinoma, human tongue), H376 (E-cadherin non-expressing, Oral Squamous Cell Carcinoma, human floor of mouth), OFK6/TERT-1 (telomerase immortalized, human floor of mouth, normal keratinocytes) and HUVEC (Human Umbilical Vascular Endothelial Cells) mammalian cell lines were used for assays to demonstrate epithelial cell to bacterial adhesion, epithelial cell invasion by bacteria, inflammatory cellular responses, cell migration and endothelial tube formation.

2.2.1.1 H357 (ECACC 06092004) cell line

H357 cell line was kindly provided by Tissue Cell Culture Collection, department of Oral Biosciences, Dublin Dental University Hospital, Trinity College Dublin. The cell line was established from oral squamous cell carcinoma of tongue of a seventy-four years old male patient. The OSCC lesion measured 20 mm in diameter and the histopathology staging of the cancer was Stage I without any lymph node involvement. The H357 cells are polygonal in shape and adhere to tissue culture treated flasks. These cells have a mutant p53 gene.

2.2.1.2 H376 (ECACC 06092005) cell line

H376 cell line was kindly provided by Tissue Cell Culture Collection, department of Oral Biosciences, Dublin Dental University Hospital, Trinity College Dublin. These malignant cells were established from OSCC of the floor of the mouth of a forty-year-old female patient. The OSCC lesion measured 20mm to 40mm in diameter and the histopathology grading of the lesion was stage III, well differentiated with lymph node metastasis. Like H357 cell line, these cells are also polygonal in shape and adhere to tissue culture treated flasks. They also have a mutant p53 gene.

The E-cadherin positive H357 cells and E-cadherin negative H376 cells were grown and maintained in 75cm^2 tissue culture flasks with vent caps (Corning® incorporated, NY, USA) in Keratinocyte Growth Media (KGM) prepared by the addition of 50 ml foetal bovine serum (Thermo Scientific, Hampshire, UK), 1.3 g F-12 Ham nutrient mixture (Sigma-Aldrich, UK), 0.5 µg/ml hydrocortisone, 10 ng/ml cholera toxin, 5 µg/ml insulin, 10 ng/ml epidermal growth factor, 25 ng/ml adenine, 200 IU/ml penicillin and 200 µg/ml streptomycin to 450 ml Dulbecco's Modified Eagle Medium (DMEM) 1X supplemented with glutamine (Gibco,

Thermo Scientific, UK). Old media was replaced by fresh media every third day and cells were harvested every 5-6 days after reaching 100% confluence and sub-cultured in fresh sterile tissue culture flasks.

2.2.1.3 TERT-1/OKF6 telomerase immortalized cell line

TERT-1/OKF6 telomerase immortalized cells were generously donated by Dr Antonio L Amelio, Department of Oral and Craniofacial health Science, University of North Carolina at Chapel Hill, US. The cells were grown and maintained in 75cm^2 tissue culture flasks as mentioned above, however, serum free media for keratinocytes (SFM) obtained from Gibco, Thermo Scientific, USA was used to culture these primary cells. 500 ml SFM was supplemented with 2.5 µg epidermal growth factor, 25 mg Bovine Pituitary Extract, 200 IU/ml penicillin, 200 µg/ml streptomycin to reduce bacterial contamination and 0.3 mM $CaCl_2$ to facilitate adhesion of epithelial cells to the base of the flask. Old media was replaced by fresh media every third day and cells were harvested at no more than 8 days irrespective of degree of confluence achieved and sub-cultured in fresh tissue culture flasks.

2.2.1.4 HUVEC cell line

HUVEC cell line was kindly provided by Dr. Ursula Fearon, Department of Molecular Rheumatology, Trinity Biomedical Sciences Institute, Trinity College Dublin, Ireland. The cells were cultured in MCDB media obtained from Thermo Fischer Scientific, supplemented with 20 ml L-glutamine 100x obtained from Thermo Fischer Scientific, 1 mg/ml Hydrocortisone (600 µl) purchased from Biosciences, 10 µg/ml EGF (600µl) purchased from R&D Systems, 6ml of 100% Penstrep, a combination drug consisting of 5000 units per ml of penicillin G that acts as an active base and 5000 ug of streptomycin suspended in 0.85% saline was purchased from Sigma-Aldrich, 6ml of 100% Amphotericin B purchased from Sigma-Aldrich and 75 ml of heat inactivated foetal calf serum purchased from Thermo Scientific. The cells were continuously grown in 75cm^2 cell culture flasks purchased from Corning® incorporated, NY, USA and maintained at a temperature of 37^{o}C and circulating 5% CO_2.

2.2.2 Sub-culturing Cell lines

2.2.2.1 H-357 and H-376 cell lines

Cells were regularly checked for possible contamination and the degree of confluence. Once the cells reached about 100% confluence (at this stage, there is a uniform carpet of mono-layered epithelial cells at the base of the 75cm^2 flask). Maintaining a sterile environment using aseptic technique in a Class II cabinet, the media from the flask was carefully removed without disturbing the monolayer of epithelial cells and carefully discarded without causing spills. The cells were then washed with sterile phosphate buffered saline (PBS, Oxoid limited, Basingstoke, Hampshire, England) to remove all remnants of culture media and 2-4 ml of 0.05% trypsin-EDTA (Gibco, Life Technologies Corporation, NY, USA) was added to each flask to detach the epithelial cells from the flask surface. The cells were incubated for 8 minutes (H-376) and 12 minutes (H-357) respectively at 37^{o}C and 5% CO_2 for this purpose. The trypsinisation process was neutralised by the addition of 10 ml fresh KGM media to the flasks and the trypsinised cells were transferred to a sterile 50 ml falcon tube (Greiner Bio-One, Germany) and centrifuged at 3000 rpm for 5 minutes. The supernatant was discarded, and cells re-suspended in 10 ml of fresh KGM media. 200 µl of the H-357 cells and 180 µl of H-376 were suspended in 13 ml of KGM and cultured in respective labelled 75cm^2 flasks with vent caps at 37^{o}C and 5% CO_2 for 5-7 days until the next splitting.

2.2.2.2 TERT-1/OKF6 cell line

Cells were regularly checked for possible contamination and harvested every eighth day (at this stage, there well-formed large islands of epithelial cells at the base of the 75cm^2 flask) under a sterile environment and using aseptic technique, the media from the flask was carefully removed without disturbing the epithelial cells and discarded. The cells were washed with sterile phosphate buffered saline (PBS, Oxoid limited, Basingstoke, Hampshire, England) and 2 ml of 0.05% trypsin-EDTA (Gibco, Life Technologies Corporation, NY, USA) was added to the flask to detach the epithelial cells from the flask surface. The cells were incubated for 12 minutes at 37^{o}C and 5% CO_2 for this purpose. The action of trypsin was neutralised by the addition of 10ml fresh DMEM media containing 5% FBS to the flasks and the trypsinised cells were transferred to a sterile 50ml conical falcon tube (Greiner Bio-One, Germany) and centrifuged at 400 xg (1800 rpm) for 5 minutes. The

supernatant was discarded, and cells re-suspended in 10ml SFM. 1ml of the cell suspension was added to 13 ml of SFM and cultured in labelled 75cm^2 flasks with vent caps at 37^{o}C and 5% CO_2 for 8-10 days until the next splitting.

2.2.2.3 HUVEC line

Cells were regularly checked for possible contamination and the degree of confluence. Once the cells reached about 100% confluence (at this stage, there is a uniform carpet of mono-layered endothelial cells at the base of the 75cm^2 flask). Maintaining a sterile environment using aseptic technique in a Class II cabinet, the media from the flask was carefully removed without disturbing the monolayer of endothelial cells and carefully discarded without causing spills. The cells were then washed with sterile phosphate buffered saline (PBS, Oxoid limited, Basingstoke, Hampshire, England) to remove all remnants of culture media and 2-4 ml of 0.05% trypsin-EDTA (Gibco, Life Technologies Corporation, NY, USA) was added to each flask to detach the epithelial cells from the flask surface. The cells were incubated for 5 minutes at 37^{o}C and 5% CO_2 for this purpose. The trypsinisation process was neutralised by the addition of 10 ml fresh MCDB media to the flasks and the trypsinised cells were transferred to a sterile 50 ml falcon tube (Greiner Bio-One, Germany) and centrifuged at 1400 rpm for 5 minutes. The supernatant was discarded, and cells re-suspended in 2 ml of fresh MCDB media. 1ml of the endothelial cells were suspended in 13 ml of MCDB media and cultured in 75cm^2 flasks with vent caps at 37^{o}C and 5% CO_2 for 5-7 days, with changing media every two days until the next splitting.

2.2.3 Counting of cells for seeding

For experimental purposes, cells were counted regularly before seeding in µ-slide 8-wells (Ibidi, Germany), 6-wells, or 24-wells plates (Cellstar, Greiner Bio-One, Germany). A 10 µl volume of trypan blue purchased from Sigma-Aldrich was added to 90 µl volume of cell suspension in a sterile Eppendorf tube to obtain a dilution factor of 10. 10 µl of this suspension was used to count the total cell count using a Neubauer's Haemocytometer purchased from Marienfeld Glassware, Germany. A glass square coverslip (0.13 mm – 0.17 mm width) purchased from Thermo-Fischer Scientific was used to cover the cell suspension on the haemocytometer. The cells were then counted by mounting the apparatus on a light microscope (Nikon instruments, c/o Aquilant Scientific Dublin) at 40x magnification. Five separate and non-adjacent 0.20 mm x 0.20 mm squares of the haemocytometer were

counted. An estimation of the total cell count per ml of cell suspension was calculated by using the formula as below:

$$\textit{Total cell count/ml} = \frac{\textit{Total cells counted x dilution factor x 10,000 cells/ml}}{\textit{5}}$$

Cells were then seeded on to multi-well plates at a concentration of $5x10^5$ cells/ml for H357 and H376 cell lines and at $5x10^6$ cells/ml for OKF6/TERT-1 cells. A cell count of $1x10^6$ cells/ml was used with HUVEC cells for experimental purposes.

2.3 Adhesion Assay

6-well plates purchased from Greiner CellStar, Sigma-Aldrich were seeded with 500µl of $5x10^5$ cells/ml of epithelial cells for H357 and H376 cells and 500 µl of $5x10^6$ cells/ml epithelial cells for OKF6/TERT-1 cells. The cells were incubated at 37°C and 5% CO_2 in an incubator for three to four days until the cells reached a confluence up to 60-70% (~$1x10^6$ cells/well). *F. nucelatum* subsp. *polymorphum* strains were grown to exponential phase overnight in BHI broth as described above anaerobically. The bacterial cultures were spun down at 4000 rpm for five minutes and washed with sterile PBS three times. The optical density (OD) of the broth culture was adjusted to OD_{600} of 0.7 and the bacterial suspension was diluted to 1:25 to yield a bacterial suspension of $1x10^7$ bacteria. 1ml of this bacterial dilution was added in each well of the 6-wells plate to obtain a multiplicity of infection (MOI) of 10 (ten bacteria per epithelial cell). The plate was spun at 800 xg (2600 rpm) for five minutes and incubated for two hours at 37°C and 5% CO_2 incubator. The wells were then washed three times with sterile phosphate buffered saline to remove any unattached bacteria and the epithelial cells were lysed to release adherent bacteria using sterile molecular grade water (Millipore Corporation©, Billerica, MA 01821, USA) and incubating at 37°C for 20mins. The lysed epithelial cells were serially diluted and plated on blood agar plates and incubated anaerobically at 37°C as described previously for 4-5 days. The plates were then examined for colonies and the colonies enumerated for estimating the percentage of adhesion. The adhesion assay is summarised in figure 2.1.

To observe the effect of need of spinning the infected plates prior to incubation, plates were directly placed in the incubator without spinning. The plates were incubated for two hours in a 37°C, 5% CO_2 incubator before washing the cells and collecting the lysates for serial dilution.

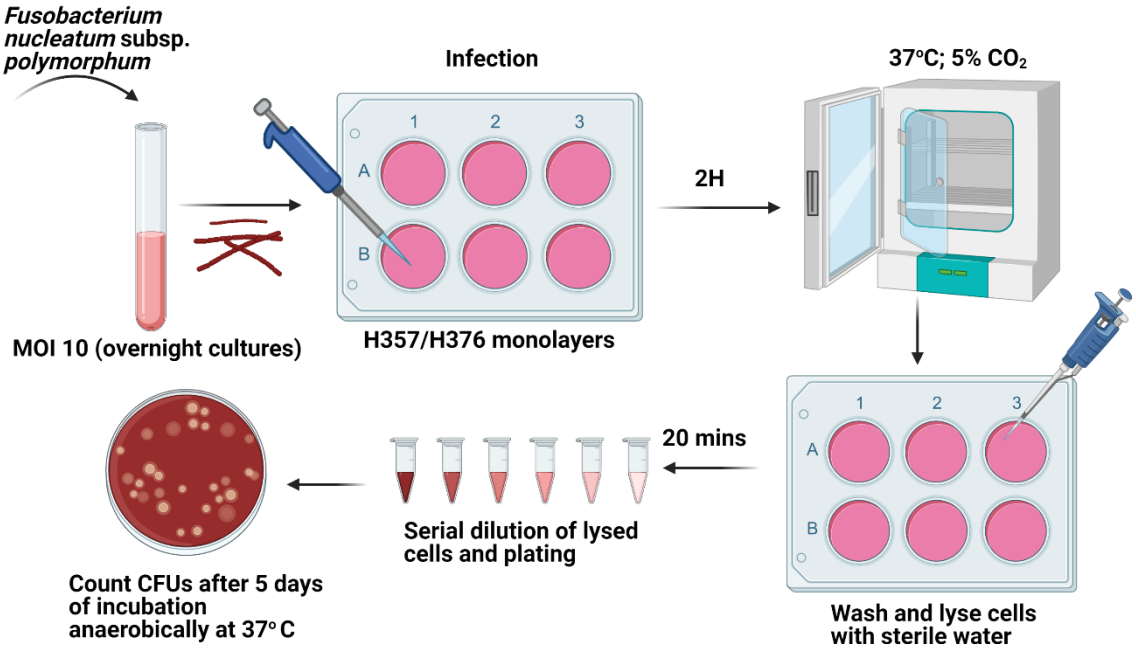

Figure 2.1. Adhesion assay of E-cadherin positive H357 and negative H376 cell lines. Epithelial cells were grown in monolayers to a confluence of 60-70% in 6-well plates and infected with *F. nucelatum* subsp. *polymorphum* strains for two hours in an incubator with controlled temperature and circulating CO_2. The cells were then washed with PBS and lysed with sterile water to release the adhered bacteria. The lysate was serially diluted and plated on BHI agar supplemented with defibrinated horse blood and incubated anaerobically for about 5 days before calculating the CFUs for adhesion estimate.

2.4 Invasion Assay

Several techniques were employed in order to estimate the invasion of *F. nucleatum* subsp. *polymorphum* before arriving at the most appropriate assay technique for the estimation of invasion of the epithelial cells by the bacteria. Some of these techniques included:

2.4.1 Antibiotic protection assay

In this method, the overnight broth cultures of bacteria at exponential phase were adjusted to $O.D_{600}$ 0.7 and a bacterial suspension was prepared at a dilution of 1:25 to yield $1x10^7$ bacteria. 1ml of this diluted bacterial suspension was added to each well of a 6-wells plate consisting of a monolayer of $1x10^6$ epithelial cells (~70-80% confluence). The plate was spun at 800 xg (2600 rpm) for five minutes and incubated at 37°C and 5% CO_2 for two hours. The wells were then washed three times with phosphate buffer saline and the bacteria outside the epithelial cells were terminated by adding 1 ml of DMEM consisting a suspension of 200 µg/ml metronidazole and 300 µg/ml gentamycin and incubating for 1 hour at 37°C. The antibiotic treated cells were again washed three times with PBS and lysed with sterile molecular grade water and incubated at 37°C and 5% CO_2 for twenty minutes to release the internalised bacteria. The suspension consisting of lysed epithelial cells and bacteria was serially diluted and plated on blood agar plates and incubated anaerobically in anaerobic jars at 37°C and 5% CO_2 for 4-5 days. The plates were then examined for colonies and the colonies enumerated for estimating the percentage of invasion.

2.4.2 Novel confocal microscopic technique

A novel technique to estimate the invasion of epithelial cells by *F. nucleatum* subsp. *polymorphum* through confocal microscopy was designed in this study. 100µl of epithelial cells at a concentration of $5x10^5$/ml were seeded on to an 8-well µ-slide (ibidi, Am Kopferspitz, Martinaried, Germany) and incubated at 37°C and 5% CO_2 to obtain a confluence of up to 60-70%. At this stage, an overnight bacterial culture of *F. nucleatum* subsp. *polymorphum* at exponential phase was adjusted to OD_{600} 0.7 and the bacterial suspension diluted to 1:25 dilution. The epithelial cells were infected with the bacteria and incubated for 4 hours at 37°C and 5% CO_2. The wells were then stained with 5µl of 1mg/ml Propidium Iodide (Sigma-Aldrich, St.Louis, USA) to stain the bacteria intracellular and extracellular to the epithelial cells and 1µl of Fluorescein Sodium Salt (Sigma Life Science, Germany) at a concentration of 1 mg/ml to negatively stain the extracellular space, just

before viewing under the confocal microscope. The prepared 8-well µ-slide was then examined using a Leica SP8 Scanning Confocal microscope for bacterial invasion of infected epithelial cells.

2.5 Serum resistance assay

An overnight broth culture of *F. nucleatum* subsp*. polymorphum* at exponential phase was adjusted to an OD_{600} of 0.7. This standardised bacterial suspension was then diluted to 1:100 dilution in assay media (consisting DMEM and 5% foetal calf serum) for the assay. A microfuge tube containing 90 µl human serum (Sigma-Aldrich, USA) was treated with 10 µl of bacterial suspension. Another microfuge tube consisting 90µl of human serum was heat inactivated at 55^{o}C for 30 minutes to destroy the complement system of the sera and treated with 10 µl of bacterial suspension as negative control. Both samples were incubated at 37^{o}C for 3 hours with samples plated on horse blood BHI agar at 0, 1, 2 and 3 hours for comparing results of *F. nucleatum* subsp*. polymorphum* resistance to human serum.

2.6 Conditioned media collection

Supernatants collected from epithelial cells that were infected with *F. nucleatum* subsp. *polymorphum* strains over 24 hours was called "conditioned media (CM)" and were used for performing several assays.

Epithelial cells were harvested from cell culture flasks and counted to obtain a cell density of $5x10^5$ cells/ml. The cells were then seeded in 24-wells plates and incubated at 37^{o}C with circulating 5% CO_2 until full confluence of cells was obtained.

The epithelial cells were then infected with overnight bacterial cultures that were standardised to OD_{600} of 0.7 and resuspended in DMEM to obtain a dilution of 1:25. This produced a multiplicity of infection of 10 when infecting the cells.

The infection was carried out for 24 hours and supernatants were collected, centrifuged at 4000 rpm for 5 minutes and stored at -20^{o}C for future use.

2.7 Human CCL2/MCP-1 ELISA protocol

Quantikine ELISA kit for CCL2/MCP-1 was purchased from R&D systems, USA.

All reagents, working standards and samples for the assay were prepared as directed by the manufacturer's direction. Wash buffer was prepared by adding 20 ml of the wash buffer concentrate to 480 ml of deionized distilled water to prepare a total of 500 ml of wash buffer. Substrate solution was prepared just before use by adding equal amounts of colouring agents A and B supplied in the kit. A calibrator diluent RD5L (dilution 1:5) was prepared by adding 20 ml of the concentrate provided in the kit to 80 ml of deionized distilled water to make up a total of 100 ml. Human MCP-1 standard concentrate was prepared by reconstituting the powder in 5ml of calibrator diluent. The stock solution (2000 pg/ml) was then serially diluted to get the following concentrations of the standard stock solution: 1000 pg/ml, 500 pg/ml, 250 pg/ml, 125 pg/ml, 62.5 pg/ml and 31.3 pg/ml. The calibrator diluent was used as zero standard.

200µl of standards, samples and controls were added to each well and covered with adhesive strip. The plate was then incubated at room temperature for 2 hours. The wells were then washed three times with wash buffer, ensuring not to scratch the base of the wells. 200 µl of Human MCP-1 conjugate was added to each well, covered with adhesive strip and incubated for 1 hour. The wells were then washed with wash buffer three times, ensuring not to scratch the base of the well. 200 µl of substrate solution was added to each well and incubated in darkness for a further 30 minutes at room temperature. The reaction was stopped by adding 50 µl of stop solution to each well. The optical density of each well was determined using a microplate reader set to 450 nm.

2.8 Human CCL5/RANTES ELISA protocol

Quantikine ELISA kit for CCL5/RANTES was purchased from R&D systems, USA.

All reagents, working standards and samples for the assay were prepared as directed by the manufacturer's direction. Wash buffer was prepared by adding 20 ml of the wash buffer concentrate to 480 ml of deionized distilled water to prepare a total of 500 ml of wash buffer. Substrate solution was prepared just before use by adding equal amounts of colouring agents A and B supplied in the kit. A calibrator diluent RD6-11 (dilution 1:5) was prepared by adding 20 ml of the concentrate provided in the kit to 80ml of deionized distilled water to make up a total of 100 ml. Human RANTES standard concentrate was prepared by reconstituting the powder in 5ml of calibrator diluent. The stock solution (2000 pg/ml) was then serially diluted to get the following concentrations of the standard stock solution: 1000 pg/ml, 500 pg/ml, 250 pg/ml, 125 pg/ml, 62.5 pg/ml and 31.3 pg/ml. The calibrator diluent was used as zero standard.

100 µl of assay diluent RD1W was added to all wells. 100 µl of standards, samples and controls were added to each well and covered with adhesive strip. The plate was then incubated at room temperature for 2 hours. The wells were then washed three times with 400 µl of wash buffer in each well, ensuring not to scratch the base of the wells. 200 µl of Human RANTES conjugate was added to each well, covered with adhesive strip and incubated for 1 hour. The wells were then washed with wash buffer three times, ensuring not to scratch the base of the well. 200 µl of substrate solution was added to each well and incubated in darkness for a further 20 minutes at room temperature. The reaction was stopped by adding 50 µl of stop solution to each well. The optical density of each well was determined using a microplate reader set to 450 nm.

2.9 Human Cytokine/Chemokine panel profiling

In this assay, a panel of 71 human cytokines and chemokines were detected using a multiplex assay developed by Eve Technologies Corporation, Calgary, Canada.

Conditioned media was collected from E-cadherin positive (H357) and E-cadherin negative (H376) cell lines as described above and stored at -20^{o}C. 25 µl of each sample was collected in sterile PCR tubes and packaged in dry ice before shipping to Canada for the cytokine and chemokine detection.

The panel of cytokines and chemokines detected by this assay is shown in table 2.2

Table 2.2. Multiplex assay panel for human cytokines and chemokines

Name	Symbol	Type
6Ckine	CCL21	Chemokine
B cell-attracting chemokine	BCA-1/CXCL13	Chemokine
Cutaneous T-cell-attracting chemokine	CTACK/CCL27	Chemokine
Epidermal Growth Factor	EGF	Cytokine
Epithelial neutrophil activating peptide-78	ENA-78/CXCL5	Cytokine
Eotaxin-1	CCL11	Chemokine
Eotaxin-2	CCL24	Chemokine
Eotaxin-3	CCL26	Chemokine
Fibroblast Growth Factor-2	FGF-2	Cytokine
FMS-like tyrosine kinase 3 Ligand	Flt3L	Cytokine
Fractalkine	CX3CL1	Chemokine
Granulocyte-Colony Stimulating Factor	G-CSF	Cytokine
Granulocyte Macrophage-Colony Stimulating Factor	GM-CSF	Cytokine
Growth-regulated alpha protein	GROα/CXCL1	Chemokine
Inducible cytokine i-309	i-309/CCL1	Chemokine
Interferon alpha 2	IFNα2	Cytokine
Interferon gamma	IFNγ	Cytokine
Interleukin 1-α	IL-1α	Cytokine
Interleukin 1-β	IL-1β	Cytokine
Interleukin 1 receptor antagonist	IL-1ra	Cytokine
Interleukin 2	IL-2	Cytokine
Interleukin 3	IL-3	Cytokine
Interleukin 4	IL-4	Cytokine
Interleukin 5	IL-5	Cytokine
Interleukin 6	IL-6	Cytokine
Interleukin 7	IL-7	Cytokine
Interleukin 8	IL-8	Cytokine
Interleukin 9	IL-9	Cytokine
Interleukin 10	IL-10	Cytokine
Interleukin 12 subunit p40	IL-12p40	Cytokine

Interleukin 12 subunit p70	IL-12p70	Cytokine
Interleukin 13	IL-13	Cytokine
Interleukin 15	IL-15	Cytokine
Interleukin 16	IL-16	Cytokine
Interleukin 17A	IL-17A	Cytokine
Interleukin 17E/Interleukin 25	IL-17E/IL-25	Cytokine
Interleukin 17F	IL-17F	Cytokine
Interleukin 18	IL-18	Cytokine
Interleukin 20	IL-20	Cytokine
Interleukin 21	IL-21	Cytokine
Interleukin 22	IL-22	Cytokine
Interleukin 23	IL-23	Cytokine
Interleukin 27	IL-27	Cytokine
Interleukin 28	IL-28	Cytokine
Interleukin 33	IL-33	Cytokine
Interferon γ induced protein 10	IP-10/CXCL10	Cytokine
Leukaemia Inhibitory Factor	LIF	Cytokine
Monocyte Chemoattractant Protein-1	MCP-1/CCL2	Chemokine
Monocyte Chemoattractant Protein-2	MCP-2/CCL8	Chemokine
Monocyte Chemoattractant Protein-3	MCP-3/CCL7	Chemokine
Monocyte Chemoattractant Protein-4	MCP-4/CCL13	Chemokine
Macrophage-Colony Stimulating Factor	M-CSF	Cytokine
Macrophage Derived Chemokine	MDC	Chemokine
Monokine induced by gamma interferon	MIG/CXCL9	Chemokine
Macrophage inflammatory protein-1 alpha	MIP-1α/CCL3	Chemokine
Macrophage inflammatory protein-1 beta	MIP-1β/CCL4	Chemokine
Macrophage inflammatory protein-1 delta	MIP-1δ/CCL15	Chemokine

Platelet Derived Growth Factor-AA	PDGF-AA	Cytokine
Platelet Derived Growth Factor-AB/BB	PDGF-AB/BB	Cytokine
Regulated upon Activation, Normal T-cell Expressed and Presumably Secreted	RANTES/CCL5	Chemokine
Soluble CD40 Ligand	sCD40L	Cytokine
Stem Cell Factor	SCF	Cytokine
Stromal Cell Derived Factor 1 α+β	SDF-1α+β/CXCL12	Cytokine
Thymus and Activation Regulated Chemokine	TARC/CCL17	Chemokine
Transforming Growth Factor alpha	TGF-α	Cytokine
Tumour Necrosis Factor alpha	TNF-α	Cytokine
Tumour Necrosis Factor beta	TNF-β	Cytokine
Thrombopoietin	TPO	Cytokine
TNF-Related Apoptosis-Inducing Ligand	TRAIL	Cytokine
Thymic Stromal Lymphopoietin	TSLP	Cytokine
Vascular Endothelial Growth Factor	VEGF-A	Cytokine

2.10 Cell migration/trans-well assay

Epithelial cells were cultured and grown on T-75 flasks (Corning® incorporated, NY, USA), regularly maintained at 37^{o}C and 5% CO_2. When the cells reached full confluence (100%), they were harvested, and counted as described earlier. A total cell volume of 5x10^5 cell/ml was prepared in serum free DMEM and stored resting on ice for the assay.

ECM gel obtained from Sigma-Aldrich was diluted in ice-cold, serum free DMEM to a final concentration of 1 mg/ml and stored at -20^{o}C. The gel was thawed overnight at 4^{o}C and kept on ice for the assay. 24-wells plate obtained from Greiner CellStar, Sigma-Aldrich and Millicell cell culture inserts (8.0 µm pore, 12 mm well diameter) purchased from Millipore, Sigma-Aldrich were chilled at 4^{o}C and kept on ice. The trans-well inserts were placed in 24-wells plate and 40 µl of ECM gel was added into the upper compartment of the trans-well inserts. The set-up was immediately placed in a 37^{o}C incubator with circulating 5% CO_2 for 2-3 hours for the ECM gel to set.To the wells of the plate, 400 µl of conditioned media (supernatants) obtained from 24-hour infection of epithelial cells with *F. nucleatum* subsp. *polymorphum* strains of interest were added as attractant. The inserts were positioned in the 24 wells ensuring the bottom of the inserts were submerged in the conditioned medium.

200 µl of the epithelial cell suspension was gently added to the upper compartment of the inserts and incubated at 37^{o}C with 5% CO_2 for 48 hours. After the incubation period, the inserts were taken out carefully and the migrated cells on the lower side of the insert membrane were fixed with 3.7% formalin for 10 minutes, followed by staining with 1% crystal violet in 2% ethanol for 20 minutes. The cells were washed thoroughly to remove excess stain and successfully migrated cells were counted using a light microscope. The summary of the assay is shown in figure 2.2.

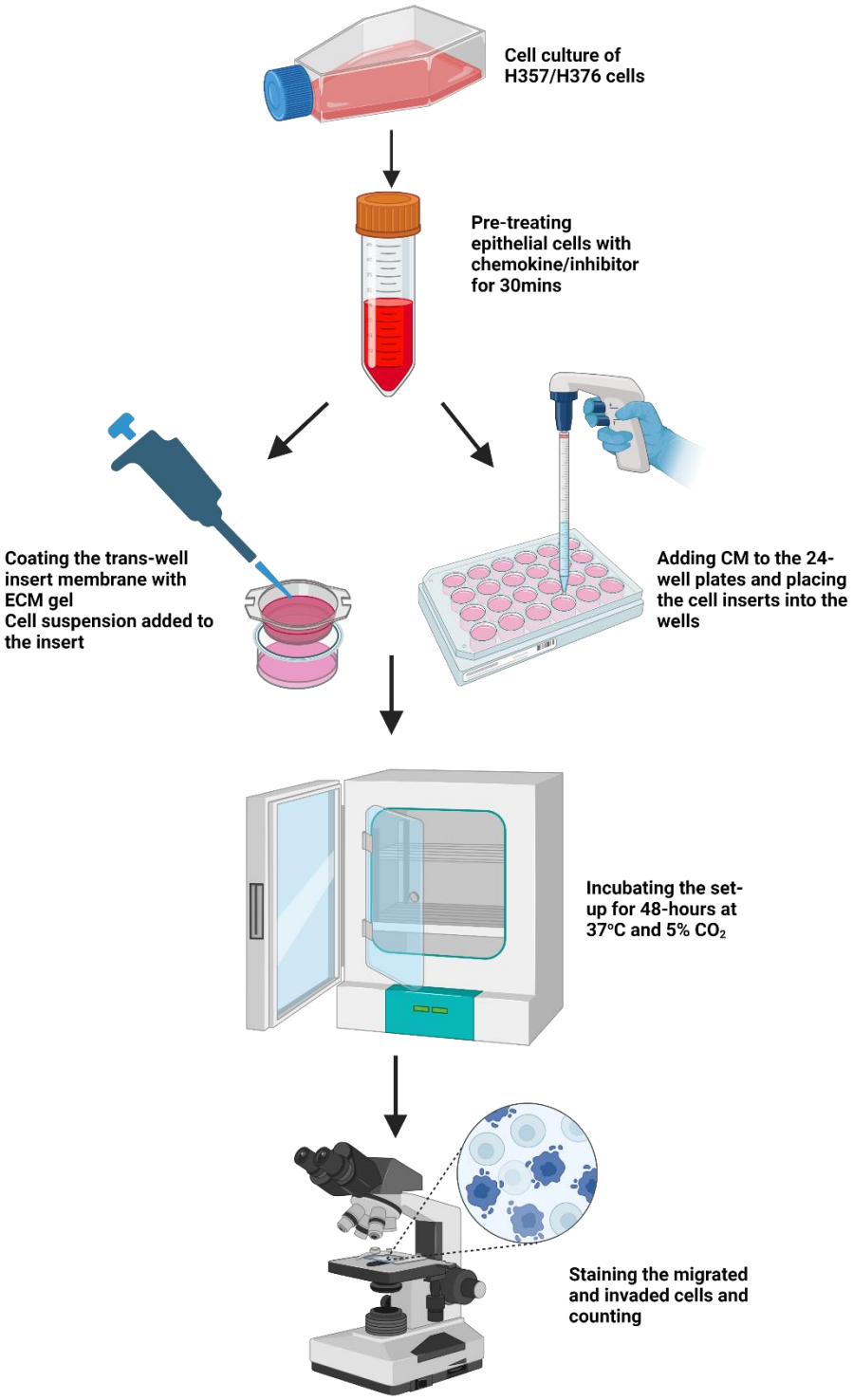

Figure 2.2. Schematic representation of the steps involved in trans-well migration/invasion assay. The E-cadherin positive H357 and negative H376 cells were sub-cultured and pre-treated with the appropriate chemokine/inhibitor for thirty minutes before adding to the trans-well inserts consisting ECM gel. After incubating the set-up for forty-eight hours, the cells on the underside of the membrane were stained using crystal violet and counted using a light microscope.

2.11 Scratch wound assay

Epithelial cells were cultured in T-75 flasks and harvested as described earlier. 500 µl of cell suspension from a suspension of $5x10^5$cells/ml were seeded in 6-well plates purchased from Greiner CellStar, Sigma-Aldrich and allowed to grow to a full confluence of 100%.

A clear linear scratch in the middle of the well with a full confluence of epithelial cells was produced using a sterile 1000 µl pipette tip purchased from Corning® incorporated, NY, USA. The cells were then treated with conditioned media obtained from 24-hour infections of *F. nucleatum* subsp*. polymorphum* strains as described earlier. Cells with the scratch wound were incubated in a 37^{o}C incubator supplied with circulating 5% CO_2 for 24 hours. The wound healing was calculated by first obtaining the images of the samples and then measuring the width of the wound at 0-hours and 24-hours using a standard graduated ruler and converting to the corresponding scale bar from the image obtained.

Chapter 3

Characterisation of adhesion and invasion of E-cadherin positive and negative OSCC cell lines by clinical isolates of *Fusobacterium nucelatum* subsp. *polymorphum*

3.1 Introduction

Bacterial adhesion to host epithelial cells is a crucial virulence mechanism that enables organisms such as *F. nucleatum* to colonise the host tissues and cause diseases, when pathogenic. As discussed earlier, *F. nucleatum* does so by using various surface adhesins that induce inflammatory responses in the host cell, facilitating tumour growth and progression. The FadA and Fap2 adhesins of *F. nucleatum* have been shown to play important roles on cancerous epithelial cells that possess E-cadherins and on cells devoid of E-cadherins. The FadA gene is highly conserved and requires the presence of the intact pre-FadA (consisting of 129 amino acid residues) and mFadA (consisting of 111 amino acid residues) to form a FadAc complex that binds successfully to E-cadherins for its actions (Rubinstein et al., 2013). Fap2 is a galactose inhibitable autotransporter, that is an essential adhesin and invasin for the virulence of *F. nucleatum* (Bachrach et al., 2004).

E-cadherin is a surface adhesive molecule expressed on epithelial cell surfaces, at the region of intercellular junctions (Pećina-Slaus, 2003). They facilitate specific Ca^{2+} dependent cell to cell adhesions in mammalian cells that are extremely important in maintaining a healthy epithelium without any breach in the epithelial network. It has been previously established that of the various other surface proteins, E and N-cadherin are the two most important cadherins in not just maintaining a continuous tight cell to cell adhesion in epithelia, but also in gastrulation, neurulation and organogenesis in the early stages of embryogenesis of the human embryo (Barth et al., 1997). An early sign of epithelial disease, specifically in tumorigenesis is a downregulation of E-cadherin expression that often leads to intercellular detachment. In this chapter, we explore the roles of the *F. nucleatum* adhesins, namely, FadA and Fap2 in events of bacterial to epithelial cell adhesion and invasion. Clinical isolates with variable copy numbers of the FadA and Fap2 adhesins are analysed for their ability to adhere to and invade two malignant oral keratinocyte cell lines which differ in their expression of E-cadherin. H357 cells have been reported to express E-cadherin, whereas H376 cells are E-cadherin negative. We also attempt to use potential inhibitors to block these adhesins and examine the effect of these inhibitors on adhesion and invasion.

3.2 Materials and methods

Bacterial cultures and cell cultures were grown and maintained to the required standards for experimental use as described previously in the general materials and methods section.

3.2.1 Determining the effects of centrifugation on adhesion of bacteria to epithelial cells

The assay was performed as described in the materials and methods chapter section 2.4.

3.2.2 Immunocytochemistry for E-cadherin staining (Paraformaldehyde fixation method)

Paraformaldehyde fixation and immunostaining of epithelial cells was used to demonstrate the expression or absence of E-cadherins in human oral epithelial cells.

E-cadherin positive H357 cells, E-cadherin negative H376 cells and TERT-1/OKF-6 telomerase immortalized primary cells were used for this experiment. Cells were cultured as described in the general materials and methods section. Epithelial cells were seeded on round glass cover slips obtained from Thermo-Fischer Scientific, Germany. 500 µl of $5x10^5$ cells/ml were seeded in each well and cells allowed to grow on the cover slips. When the cells reached about 40-50% confluence on the glass cover slips, epithelial cells were fixed with 3.7% para formaldehyde (PFA) obtained from Sigma Aldrich, Germany, by adding 500 µl of the solution directly on the epithelial cells for twenty minutes at room temperature (PFA acts as a cross linking agent for amino groups of proteins and lipids and causes immobilization, however, PFA fixation can distort proteins) for 20 minutes.

A 30 mM glycine buffer required for this technique was prepared by first preparing a 1 mM concentration stock of glycine (purchased from Sigma Aldrich, Germany) in 50 ml PBS and then adding 1.5 ml of the stock solution to 48.5 ml of PBS to obtain a final 50 ml buffer of 30 mM concentration glycine. The fixed coverslips were then quenched in 1ml of 30 mM glycine at pH 7.5 for 5 minutes. The quenched coverslips were then washed three times in 1 ml PBS for 3 minutes. To make up 0.1% triton X permeabilization buffer, 5 ml of triton X purchased from Sigma Aldrich, Germany, was added to 45 ml of PBS to obtain a 10% stock solution from which 1 ml was added to 100 ml PBS to obtain a final 0.1% triton X buffer. The cells were then permeabilized in 1 ml 0.1% triton X buffer for 5 minutes. They were subsequently washed three times in 1 ml PBS for 3 minutes to rid the buffers. The prepared coverslips were then incubated with 40 µl of primary polyclonal goat Ig antibodies

purchased from R&D systems on a clean flat surface, with the cells facing the antibody for sixty minutes in darkness. This was followed by three thorough washes in 1 ml PBS for 3 minutes. The cells were then incubated with 40 µl of secondary donkey anti-goat Ig antibody purchased from R&D systems for thirty minutes. The cells on the coverslips were washed three times thoroughly for 3 minutes in 1 ml PBS and then incubated for 10 minutes in DAPI (1:5000) to stain the nuclei.

The coverslips were again washed three times in 1 ml PBS for 3 minutes and mounted on glass slides using Mowiol purchased from Sigma-Aldrich Co, USA. Mowiol is an anti-fading and mounting agent used for mounting cells on glass slides for the detection of cell surface antigens by immunofluorescence.

3.2.3 Lectin labelling for Gal-GalNAc expression

E-cadherin positive H357 cells, E-cadherin negative H376 cells and TERT-1/OKF-6 telomerase immortalized primary cells were used for this experiment. Cells were cultured as described in the general materials and methods section. Epithelial cells were seeded on round glass cover slips obtained from Thermo-Fischer Scientific, Germany. 500 µl of $5x10^5$ cells/ml were seeded in each well and cells allowed to grow on the cover slips. When the cells reached about 40-50% confluence on the glass cover slips, the cells were washed three times in PBS and cells fixed using 3.7% paraformaldehyde for five minutes. The cells were washed with PBS and incubated with 50 µl of FITC-lectin (R&D systems) at a concentration of 100 µg protein/ml. The prepared slides were viewed in a fluorescence microscope and images obtained.

3.2.4 Distribution of *F. nucleatum* and its adhesins using whole genome sequencing - Illumina Technologies and Oxford Nanopore Technologies

Whole genome sequencing of *F. nucleatum* strains was carried out by Ms. Claire Crowley. The copy number of Type Va adhesins and FadA adhesins was determined from whole genome sequence data. Genomes were annotated using Prokka and gene families were identified by analysis of the pangenome using Roary. Gene families corresponding to FadA and type Va autotransporters (which include the adhesin Fap2), were identified using HMMSearch to predict protein structures. The gene families were then viewed as similarity networks in Cytoscape, which generated a list of proteins present in each network and the

number of different genes and their homologues in individual isolates of interest could be determined.

3.3 Results

3.3.1 Identification and Recovery of *F. nucleatum* in the oral cavity

Mucosal swabs of patients presenting with leukoplakia, erythroplakia, carcinoma-in-situ or squamous cell carcinoma (OSCC) of the oral cavity were swabbed for the presence of *Fusobacterium* spp. at the diseased lesion and a healthy contralateral normal mucosal site using catch-all collection swabs. The swabs were resuspended in TSE buffer and plated on BHI agar plates supplemented with 5% defibrinated horse blood, 7.5µg/ml vancomycin and 20µg/ml streptomycin to isolate fusobacterial strains. The bacterial colonies thus formed were checked for rod-shaped fusiform cell morphology using light microscopy and their 16S rRNA region amplified and sequenced. The resultant sequencing data were compared online on NCBI and HOMD database to identify the bacterial species isolated from patients. Overall, 71 fusobacterial isolates were identified of which, the most common subspecies to be identified was *F. nucleatum* subsp. *polymorphum* (n=54; 28 isolates obtained from the pathologic sites and 26 isolates obtained from the contralateral normal control sites). The second most common species was *F. periodonticum* (n=9; 4 isolates obtained from pathologic sites and 5 isolates from their contralateral control sites) and *F. nucleatum* subsp. *animalis* (n=8; 3 isolates from pathologic sites and 5 isolates from their contralateral normal sites) as shown in figure 3.1. The NCBI and HOMD database results of the clinical isolates that were identified and used in this study are shown in table 3.1.

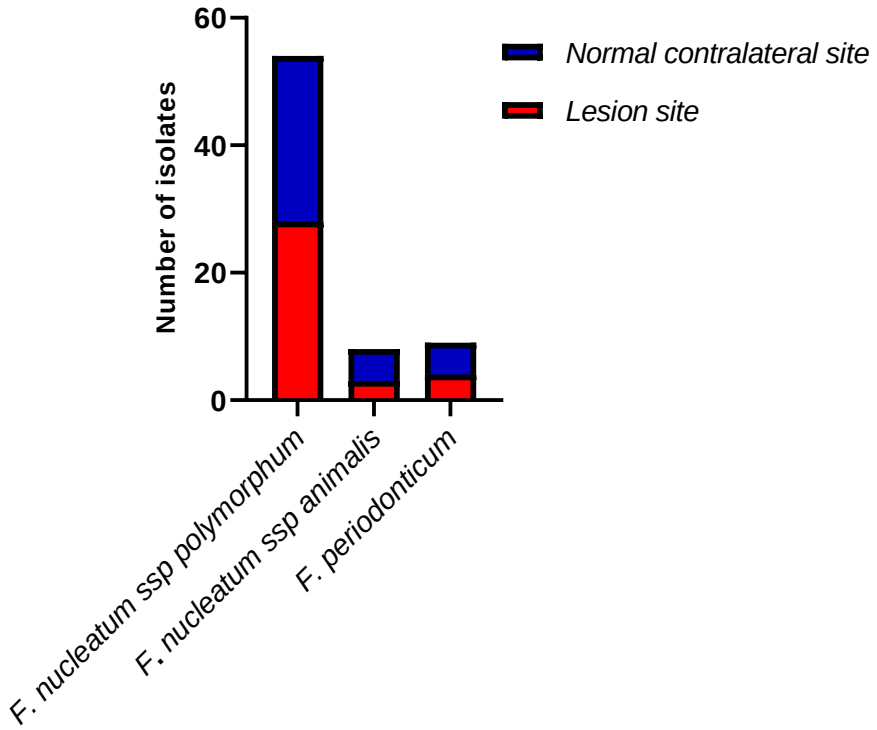

Figure 3.1. Distribution of *Fusobacterium* species in the oral cavity. Swabbing of patients for the identification the oral microbiota, specifically *F. nucleatum* revealed that *F. nucleatum* subsp. *polymorphum* was the most abundant in the mouth (79%), both in normal healthy mucosa and in the diseased mucosa. On the other hand, *F. periodonticum* was the second most abundant *Fusobacterium* species followed by *F. nucleatum* subsp. *animalis*.

Table 3.1. The Human Oral Microbiome Database (HOMD) results of the 16s RNA gene sequencing of the clinical isolates obtained from oral swabs of patients used in this study

Query sequence/Clinical isolate	Query length	HOMD clone name	Body Site	Identities	Mismatch
40A2	365	*Fusobacterium nucleatum* subsp. *polymorphum*	Oral	100	0/365
41A	630	*Fusobacterium nucleatum* subsp. *polymorphum*	Oral	100	0/630
41B2	246	*Fusobacterium nucleatum* subsp. *polymorphum*	Oral	100	0/246
43A2	317	*Fusobacterium nucleatum* subsp. *polymorphum*	Oral	99.7	1/317
43A3	330	*Fusobacterium nucleatum* subsp. *polymorphum*	Oral	99.7	1/330
43B1	480	*Fusobacterium nucleatum* subsp. *polymorphum*	Oral	100	0/330
60A2	1095	*Fusobacterium nucleatum* subsp. *polymorphum*	Oral	98	22/1095

3.3.2 Optimisation of bacterial growth and culture conditions

In order to maintain consistency in bacterial growth and culture conditions of *F. nucleatum* subsp. *polymorphum* for all experiments, the bacteria were cultured overnight in BHI broth supplemented with menadione as described earlier, and the optical density of the culture adjusted to 0.7 at an absorbance of 600. Bacterial isolates were cultured for 72 to 96 hours (3-4 days) to estimate the growth characteristics and the growth phase optimal to carry out experiments. We found that all our experimental isolates which include the type strain of *F.* nucleatum subsp. *polymorphum* ATCC10953/NCTC10562 and clinical isolates 40A2, 41A, 41B2 and 43A3 attained exponential phase within 24 hours and stationary phase was reached after 30 hours when the growth began to plateau off as shown in the figure 3.2. A bacterial count of $1x10^7$ CFU/ml was obtained at a dilution of 1:25 when the OD_{600} was standardised to 0.7 as shown in the figure 3.3.

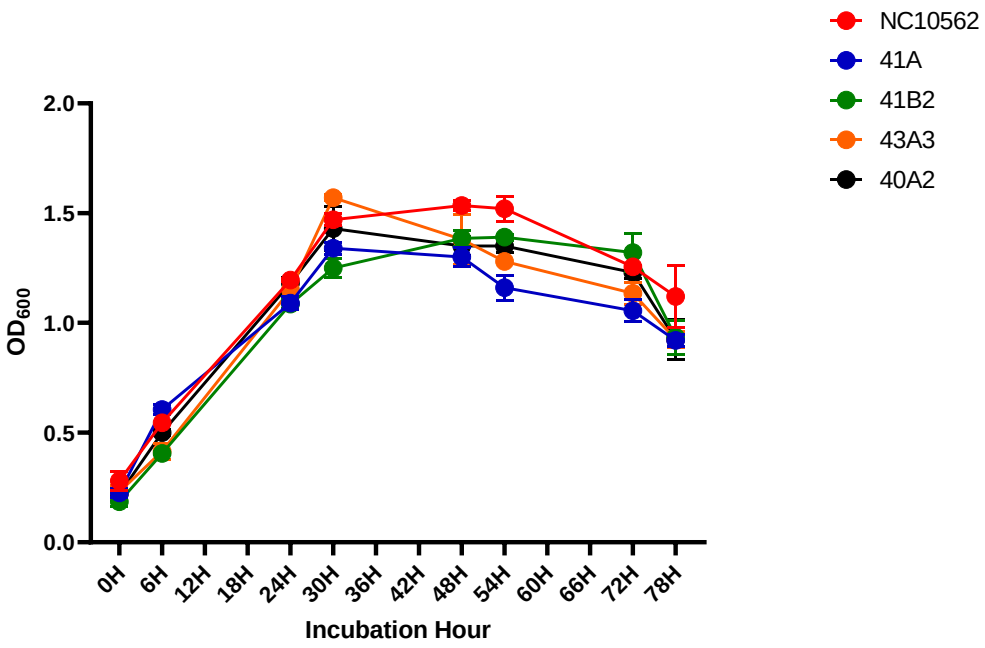

Figure 3.2. Growth and survival of *F. nucleatum* subsp. *polymorphum*. Broth cultures containing type strain ATCC10953/NC10562 and isolates obtained from clinical samples 41A, 41B2 and 43A3 were cultured separately at 37°C under strict anaerobic conditions. The absorbance of the cultures was measured twice daily (six hours and twenty-four hours) for three days and the OD_{600} values were plotted against time to obtain the growth curve. Exponential phase was achieved by 24-hours and stationary phase was reached after the first 24 hours and survival gradually declined after three days (error bars indicate standard deviation of two experimental replicates for each sample).

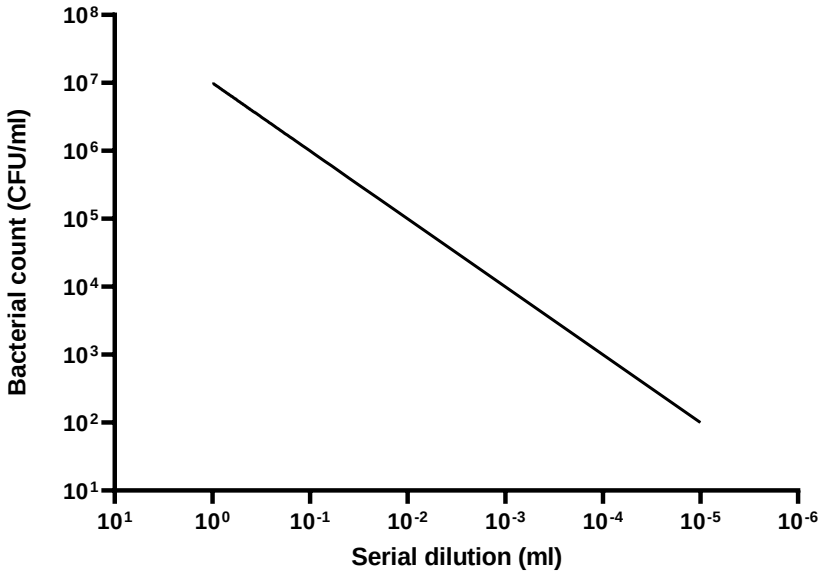

Figure 3.3. Standard curve of serially diluted *F. nucleatum* subsp. *polymorphum* ATCC10953/NC10562. Overnight bacterial broth cultures were adjusted to 0.7 at OD_{600}. A 1:25 dilution of this solution was prepared and serially diluted. The dilutions were plated on BHI agar plates supplemented with horse blood and incubated anaerobically at 37^{o}C for 4-5 days. The colonies were then counted and the colony forming units calculated thereafter. The serial dilution yielded about $1x10^7$ CFU/ml.

3.3.3 Investigating the effect of human serum on *F. nucleatum* subsp. *polymorphum*

To explore the tolerance of *F. nucleatum* subsp. *polymorphum* to human serum, all experimental samples (type strain ATCC10953/NCTC10562 and clinical isolates of *F. nucleatum* subsp. *polymorphum* (n=7)) were treated with human serum for three hours and plated on BHI agar plates supplemented with horse blood. All samples showed various degrees of resistance to human serum when treated up to three hours. Whilst clinical isolates 40A2 and 41A (both obtained from swabbing diseased mucosal sites) showed mild to moderate resistance, the remaining clinical isolates (swabs from both diseased mucosal sites and contralateral normal mucosal sites) were highly resistant to the bactericidal activity of the human serum. On the other hand, the type strain of the bacteria ATCC10953 (NCTC10562) was highly sensitive to the bactericidal activity of human serum as shown in the figure 3.4 below.

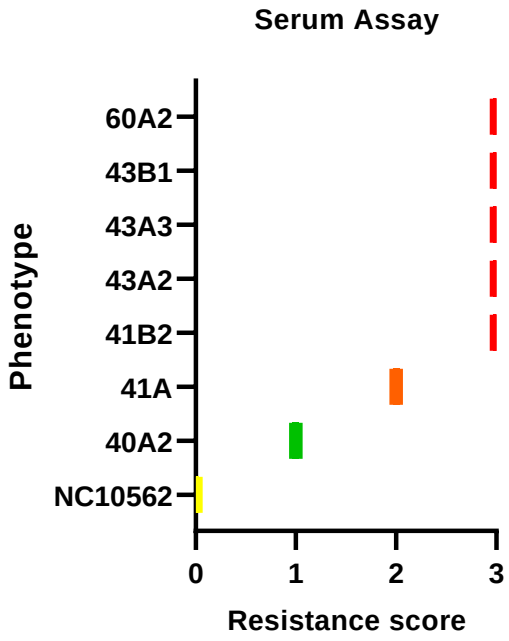

Figure 3.4. Serum resistance assay to demonstrate the effect of the complement system of human serum on *F. nucleatum* subsp. *polymorphum*. The bacterial samples were incubated with human serum for up to three hours and then plated on BHI blood agar plate to recover surviving bacteria. No bacterial colonies of the type strain ATCC10953/NCTC10562 were formed on the agar plate and was scored 0, demonstrating the highly sensitive nature of the strain to the complement system of the serum. Other clinical isolates however displayed a range of resistance, scored 1 for mild resistance, 2 for moderate resistance and 3 for high resistance. Clinical isolate 40A2 showed mild resistance to human serum with a score 1, isolate 41A showed moderate resistance with a score of 2 and all other isolates were highly resistant with score 3.

3.3.4 Characterisation of E-cadherin and Gal-GalNAc expression on OSCC cell lines

In order to characterise adhesion of *F. nucleatum* subsp. *polymorphum* to epithelial cells, we characterised two OSCC cell lines for the presence of E-cadherin and Gal-GalNAc. Both E-cadherin and Gal-GalNAc have been reported to act as receptors for *F. nucelatum* adhesion. We characterised expression of these molecules on OSCC and normal immortalised keratinocytes to be used in adhesion and invasion assays. Paraformaldehyde fixation and immunostaining of epithelial cells was used to demonstrate the expression or absence of E-cadherins in human oral epithelial cells. We used both immortalized cancerous and non-cancerous (control) cell lines for this purpose. Coverslips coated with epithelial cells were first fixed with formaldehyde as described previously and then permeabilised using TX-100 in PBS. The cells were then treated with a primary antibody (polyclonal goat Ig), followed by a secondary antibody (donkey anti-goat Ig). The cells were then treated with DAPI to stain the nuclei and images captured in confocal microscope. We found that the cell line H357 was positive for the expression of E-cadherins, whilst the cell line H376 did not express any E-cadherins. The proteins for E-cadherin were distributed on the epithelial cell surface and formed a tight network of cell-cell junction intercellularly. This pattern of E-cadherin staining was also seen in the non-cancerous, immortalised primary cell line OKF-6 cells that were used as a normal control.

Similarly, we demonstrated the presence of Gal-GalNAc protein on the OSCC cell line that had lost the E-cadherins from its cell surface. Epithelial cells were seeded on glass coverslips as previously described and were treated with FITC-lectin and image captured in a fluorescent microscope. We found that the E-cadherin positive H357 cells did not express any fluorescence for the Gal-GalNAc lectin stain, whilst the E-cadherin negative H376 cells displayed a vibrant green fluorescently stained Gal-GalNAc proteins on their cellular surfaces. As a control, we used the telomerase immortalised primary oral keratinocyte OKF-6/TERT-1 cells which also showed negative fluorescence for the Gal-GalNAc protein as did E-cadherin positive H357 cells as shown in the figure 3.5.

Although the loss of E-cadherins is a pathologic process as dysplastic tissue progresses towards forming a malignant tissue, some cancer forms tend to retain the E-cadherins as seen here in H357 cell lines. However, the cell line H376 showed a total loss of E-cadherins as expected in the true event of malignancies. Similarly, the expression of Gal-GalNAc is

upregulated in cancerous events, however, some cancer forms tend to downregulate its expression as demonstrated here in the E-cadherin positive H357 cell line. A non-cancerous cell line such as the OKF-6/TERT-1 would not exhibit Gal-GalNAc expression.

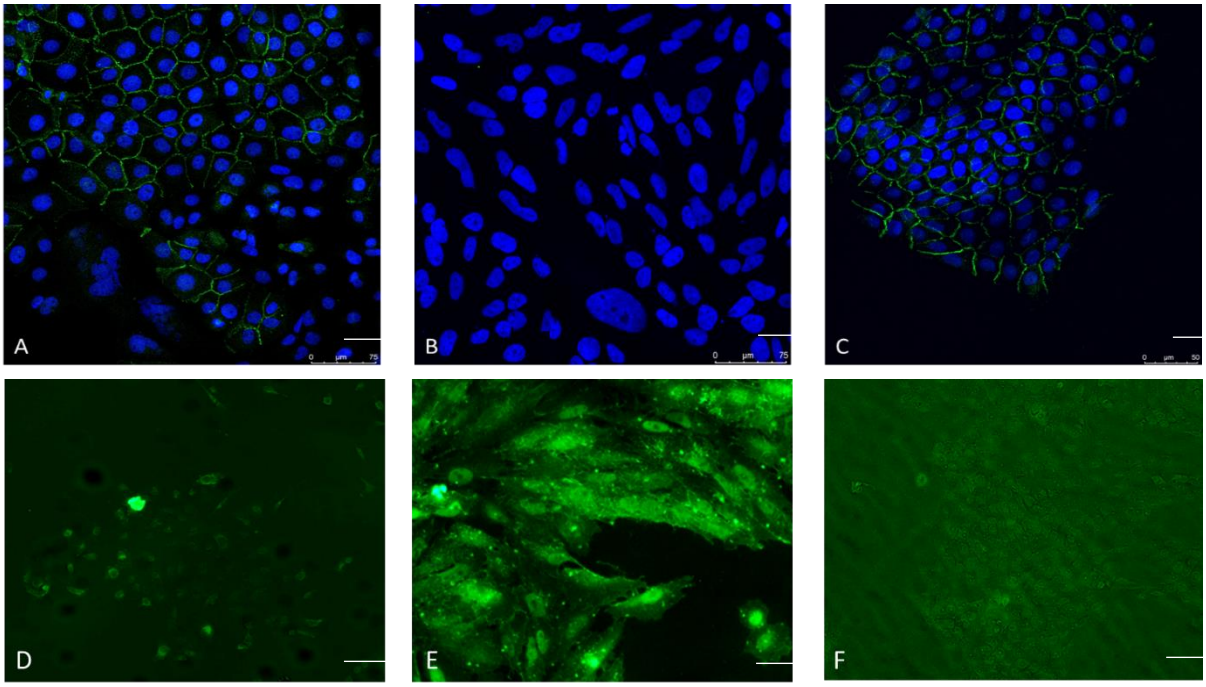

Figure 3.5. Immunostaining of epithelial cells. E-cadherins were demonstrated on epithelial cells using PFA fixation and immunostaining method. PFA fixed epithelial cells were treated with polyclonal goat primary antibody for sixty minutes and then donkey anti-goat secondary antibody for thirty minutes. Cells were then treated with DAPI at a concentration of 1:5000 for ten minutes to stain the nuclei. The H357 cell line reacted positively for the immunostaining, expressing E-cadherins as bright green proteins on the cell surfaces and interface (A), whilst H376 cell line was negative for E-cadherin expression (B). As a positive control, a telomerase immortalized TERT-1/OKF-6 cell line was used to demonstrate the expression of E-cadherins (C). Similarly, the three cell lines were treated with lectin and images captured in fluorescent microscope. E-cadherin positive H357 cells did not show any fluorescence (D), E-cadherin negative H376 cells showed fluorescence for Gal-GalNAc protein (E) and TERT-1/OKF-6 cell line didn't show any fluorescence for Gal-GalNAc proteins (F) (The scale bar represents 75 µm in length).

3.3.5 Exploring the effects of centrifugation on bacterial adhesion to OSCC cell lines and identifying the optimal incubation time and bacterial viability for adhesion assay

Prior to performing the adhesion assay on clinical isolates, we carried out experiments to determine the optimal incubation time to give maximum adhesion of bacteria to the OSCC cells. In addition, we investigated whether bringing the bacteria into contact with the OSCC cells using low speed centrifugation influenced adhesion. As some strains of *F. nucleatum* co-aggregate and sediment rapidly, we investigated centrifugation as a method to remove this variable from the assay. For this purpose, we used the type strain of *F.* nucleatum subsp. *polymorphum* to infect E-cadherin positive H357 epithelial cells. Adhesion of the bacteria to the E-cadherin positive epithelial cells was facilitated with spinning the bacterial-epithelial co-cultures and comparing the results. We found that when plates were spun at a low speed (800 xg or 2600 rpm) for 5 minutes, the bacteria adhered better to epithelial cells as compared to cells that were incubated in the incubator directly without subjecting to low speed centrifugation (Figure 3.3A and 3.3B). Concurrently, the optimal incubation time for adhesion was also determined. Bacterial infection of E-cadherin positive cells was carried out for 1 h, 2 h and 3 h respectively. The lysates of the infected cells were serially diluted after each incubation time and plated on BHI agar supplemented with defibrinated horse blood. We found that optimal bacterial adhesion to epithelial cells, corresponding to 30% of input cells took place when the plates were spun at 800 xg (2600 rpm) and infection carried out for two hours, after which there was a gradual decline in adhesion (Figure 3.7).

On the other hand, when the 6-well plates containing infected epithelial cells were incubated at 37˚C without prior spinning of the plates at 800 xg (2600 rpm), we found that the percentage adhesion of the bacteria to epithelial cells was relatively low about 10% after two hours. The percentage adhesion dropped further after three hours of incubation.

The viability of *F. nucleatum* subsp. *polymorphum* type strain ATCC10953/NCTC10562 was also evaluated over a period of seventy-two hours. For this purpose, we prepared a bacterial broth and standardized it to OD 0.7 as described in the general materials and methods section. A 1:25 dilution of the bacterial culture was prepared in DMEM medium producing a MOI of 10 and incubated aerobically in a 37^{o}C incubator with circulating 5% $CO_{2.}$ Samples were collected every 24 hours and serially diluted and plated to obtain the CFUs thus formed as described in the general materials and methods chapter. We found that after twenty-four hours of aerobic exposure of the bacteria, the bacterial survival dropped quite dramatically. There was a drop from $1x10^{7}$ cfu/ml at time interval 0-hours to $1.7x10^{4}$ CFU/ml at 24-hours. There was a complete cessation of bacterial survival to 0 CFU/ml at 48-hours and 72-hours as shown in figure 3.7.

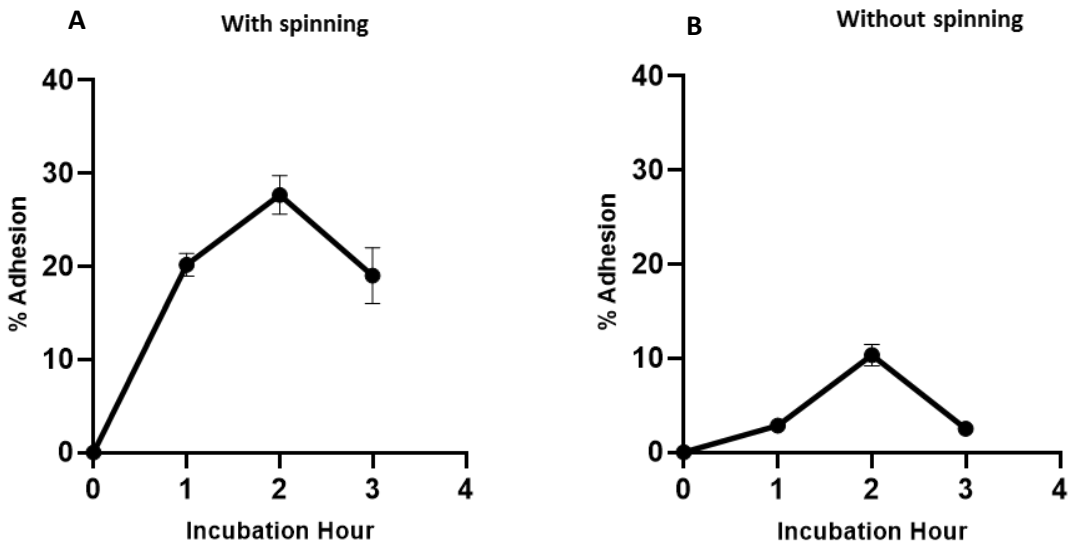

Figure 3.6. Effects of centrifugation on bacterial adhesion to E-cadherin positive OSCC cell line and bacterial survival. When plates were spun at 800 xg (2600 rpm) for 5 minutes, up to 30% bacterial adhesion to epithelial cells was achieved (A) and the adhesion dropped by 20% without spinning (B). Also, optimal adhesion of bacteria to epithelial cells was achieved at 2 hours of incubation, after which there was a drop in the adhesion.

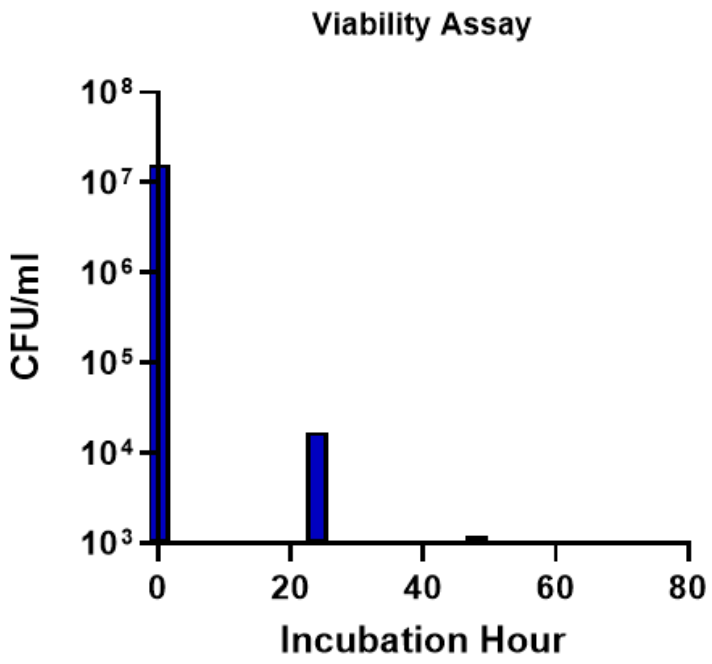

Figure 3.7. Viability assay of *F. nucleatum* subsp. *polymprphum*. A bacterial suspension with a MOI of 10 was prepared and incubated aerobically at 37^{o}C. Samples were collected every 24 hours and serially diluted and plated to obtain the CFUs thus formed. After twenty-four hours of aerobic exposure of the bacteria, the bacterial survival dropped quite dramatically. There was a drop from 1x10^{7} cfu/ml at time interval 0-hours to 1.7x10^{4} CFU/ml at 24-hours. There was a complete cessation of bacterial survival to 0 CFU/ml at 48-hours and 72-hours. The experiment was performed and repeated three times (n=3) to obtain the results shown.

3.3.6 Investigating the adhesion of *F. nucleatum* subsp. *polymorphum* with E-cadherin positive and E-cadherin negative cell lines and a non-cancerous telomerase immortalised oral keratinocyte control.

The adhesion of the type strain ATCC10953/NCTC10562 to the two experimental cell lines (E- cadherin positive H357 and negative H376) and a control cell line (non-cancerous telomerase immortalised TERT-1/OKF-6) was performed before testing the adhesion of the clinical isolates of *F. nucleatum* subsp. *polymorphum* with the E-cadherin positive and negative cell lines. The adhesiveness of the cell lines to the type strain ATCC10953/NCTC10562 and to the clinical isolates (n=7) of *F. nucleatum* subsp. *polymorphum* were compared. Adhesion effect was enhanced by centrifuging the experimental set-up (six well plates) at 800 xg (2600 rpm) for five minutes. This was done to simulate the normal physiology in the oral cavity during the acts of speech, mastication and swallowing and to remove the impacts of co-aggregation on adhesion. The six well plates were then incubated for two hours before serially diluting the lysates obtained from the epithelial cell-bacterial adhesion complex as detailed in the methods section. The CFUs thus formed were counted and the percentage adhesion calculated. We found that the type strain was the most adhesive to the E-cadherin positive cell line H357, exhibiting approximately 25% adhesion compared to the E-cadherin negative H376 cell line of approximately 11% and the least adhesion to the non-cancerous cell line of approximately 8.5% (Figure 3.8A).

The clinical isolates generally exhibited lower adhesion to the E-cadherin expressing cells, isolate 43B1 exhibiting the greatest adhesion (~15%) and 40A2 the least adhesion (~5%).

Conversely, the clinical isolates of *F. nucleatum* subsp. *polymorphum* were generally as adhesive or more adhesive than the type strain (~15%) when infecting the E-cadherin negative H-376 cell line. The clinical isolate 43A3 exhibited a significantly high adhesion of up to ~50%. Again, isolate 40A2 exhibited the least adhesion of ~5% (Figure 3.8B).

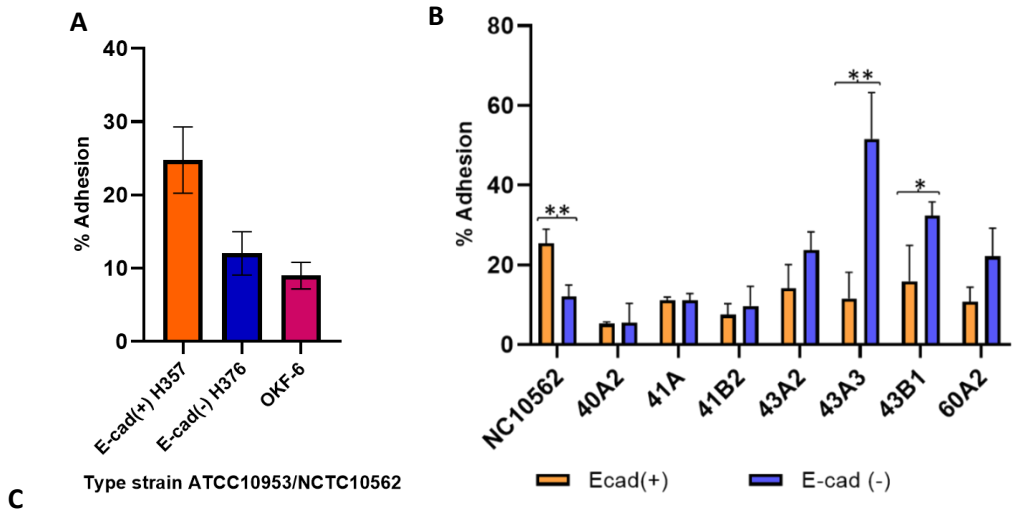

C

Ecad(+)H357	40A2	41A	41B2	43A2	43A3	43B1	60A2
Mean adhesion	5.2	11.1	7.5	14.1	11.5	15.9	10.7
Significantly different from NC10562	Yes	No	Yes	No	No	No	Yes
P-value	0.0010	0.1189	0.0042	0.1840	0.0688	0.2038	0.0495

Ecad(-)H376	40A2	41A	41B2	43A2	43A3	43B1	60A2
Mean adhesion	5.4	11.1	9.7	23.7	51.6	32.3	22.1
Significantly different from NC10562	No	No	No	No	Yes	Yes	No
P-value	0.4189	0.8174	0.8174	0.2040	0.0111	0.0496	0.2040

Figure 3.8. A comparison of adhesion of *F. nucleatum* subsp. *polymorphum* with cancerous and non-cancerous oral keratinocytes. A direct comparison of the percentage adhesion of *Fn* subsp. *polymorphum* strains with E-cad positive, E-cad negative and non—cancerous telomerase immortalised TERT-1/OKF-6 cell lines showed that the type strain ATCC10953/NCTC10562 was up to 25% adhesive with E-cadherin positive H-357 cell line, about 11% adhesive with E-cadherin negative H376 cell line and the least adhesive to TERT-1/OKF-6 cell line with approximately 8.5 % (A). However, several clinical isolates showed a significantly higher adhesion to E-cadherin negative H376 cells compared to the E-cadherin positive H357 strain with clinical isolate 43A3 showing up to ~50% adhesion with E-cadherin negative H376 cell line (B) (statistical analysis: *indicate t-test p-value < 0.05, ** indicate t-test p-value <0.001, error bars represent standard deviation of three experimental replicates). Kruskal-Wallis test compared the type strain to individual clinical isolates in both cell lines as shown in the tables (C).

3.3.7 Correlation of *F. nucleatum* adhesin copy number and adhesion

Whole genome sequencing of isolates was performed by Claire Crowley using Illumina MiSeq as previously described. Using the type strain of *F. nucleatum* subsp. *polymorphum* ATCC10953/NC10562 as the reference genome, the whole genome analysis was carried out and Roary software was used to analyse and compare pangenome to identify different genes of interest.

We found that the copy numbers of FadA genes and Type Va adhesin genes varied between most isolates. Clinical isolate 60A2 had the highest copy numbers of FadA genes with five copies, followed by the type strain ATCC10953/NCTC10562 with four FadA gene copies. Clinical isolates 40A2 and 43A3 had the least FadA gene copy numbers with one each. Clinical isolates 41A and 41B2 both had three FadA gene copies each (figure 3.9A).

On the other hand, all clinical isolates showed multiple copies for the type Va adhesin gene, except clinical isolate 40A2 which had only one copy for the Fap2 gene. The type Va autotransporter group include orthologues of known fusobacterial adhesins such as Fap2, CmpA, RadD, Aim1 and an unnamed adhesin. Clinical isolate 60A2 had two copies of the gene, followed by clinical isolate 41A with three copies, 41B2 and 43B1 with four copies each and both clinical isolate 43A3 and the type strain ATCC10953/NCTC10562 had five copies each (figure 3.9B). The clinical isolate 43A2 had the highest copy numbers (six) for type Va autotransporters (figure 3.9B). There was also an indication of a correlation between the adhesin copy numbers and the ability of *F. nucleatum* subsp. *polymorphum* adhesion characteristics as summarised in the figure 3.9C and figure 3.9D.

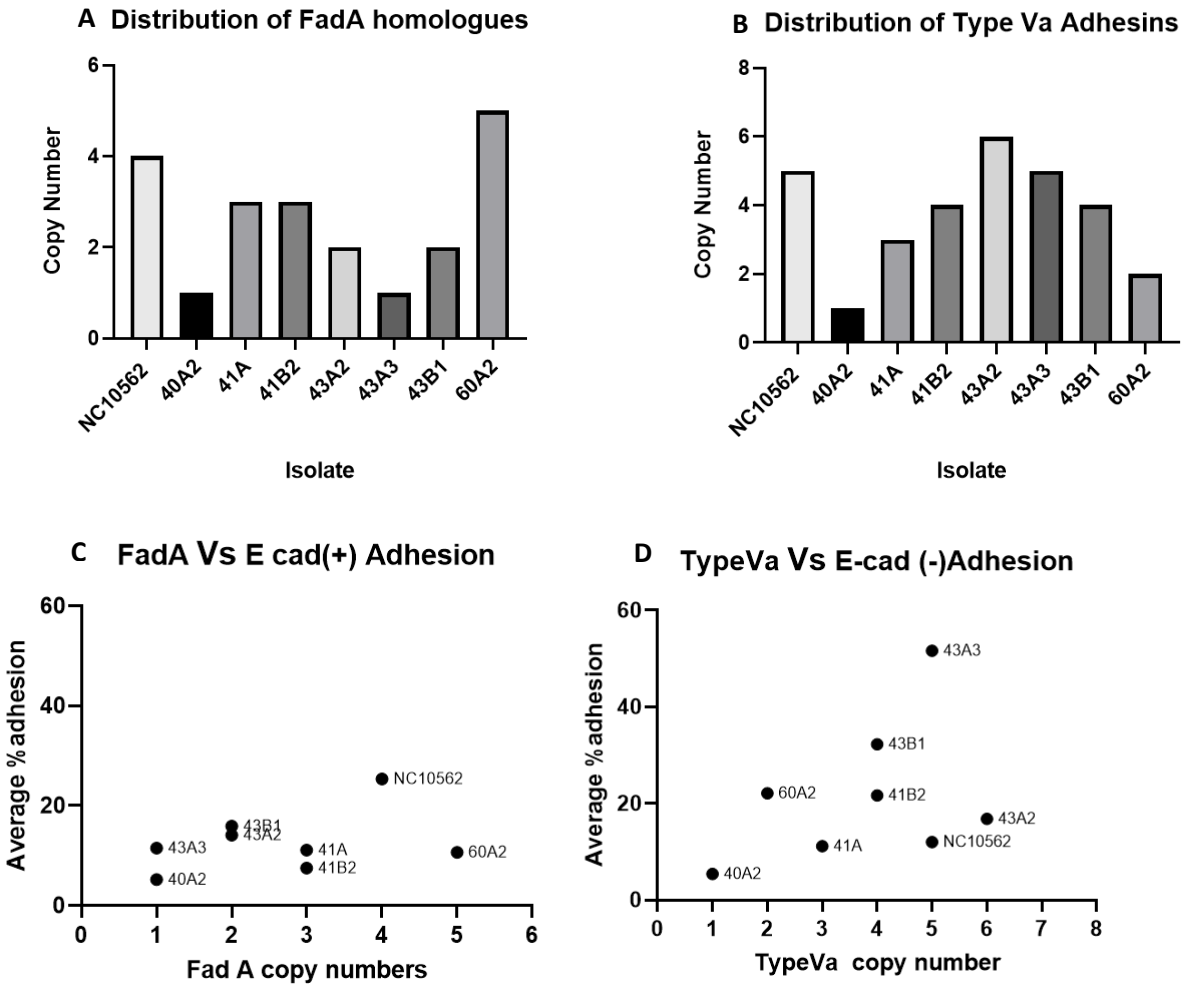

Figure 3.9. Correlation of adhesin copy numbers to adhesion of *F. nucleatum* to E-cadherin positive and negative cell lines. All samples showed a varied distribution of both FadA and type Va adhesin genes. Clinical isolate 60A2 had the highest FadA gene copies (6 copies) whilst isolates 40A2 and 43A3 had the least FadA gene copies with one copy each. When comparing the copy numbers of typeVa adhesin, clinical isolate 43A2 had the highest number of copies (six copies) and isolate 60A2 had only two copies. Interestingly, clinical isolate 40A2 had only one copy of both FadA and type Va gene (A and B). Higher copy numbers of type Va autotransporters correlated to higher average percentage adhesion in E-cadherin negative cell line in majority of the clinical isolate population (D) as compared to Fad A adhesin copy numbers to E-cadherin positive cell line (C).

3.3.8 Antibiotic protection assay does not discriminate between extracellular and intracellular *Fusobacteria*

Antibiotic treatment of infected cell monolayers is an established method to enumerate intracellular bacteria by killing extracellular adherent bacteria. To estimate the invasiveness of *F. nucleatum* subsp*. polymorphum* in OSCC cell lines, we used metronidazole and gentamycin combination drug treatment which is a potent drug regime against Gram-negative anaerobic bacterial infections.

In this assay, we first infected the epithelial cells with the type strain of *F*. *nucleatum* subsp. *polymorphum* for two hours as described in the general methods chapter. An antibiotic drug combination (200 µg/ml metronidazole and 300 µg/ml gentamycin) was then used to treat the infected cells for an additional one hour. After the drug treatment, the cells were washed and lysed to use the cell lysate for serial dilution and plating on BHI agar supplemented with defibrinated horse blood. The CFUs were counted to get an estimate of the antibiotic drug treatment and invasion. As a control, we used bacterial suspension without any epithelial cells to estimate the drug effectiveness.

We found that the combination antibiotic treatment failed to kill bacterial cells in the control sample that did not contain any epithelial cells. An average of $2.5x10^6$ CFUs/ml were recovered from the invasion assay samples. However, the control sample that contained only bacteria yielded ~$1.5x10^6$ CFUs/ml. When the bacterial recovery from both groups was expressed as percentage recovery, there was approximately 64% bacterial recovery from the epithelial cell invasion group and approximately 36% bacterial recovery from the control sample group that did not contain any epithelial cells as shown in the figure 3.10.

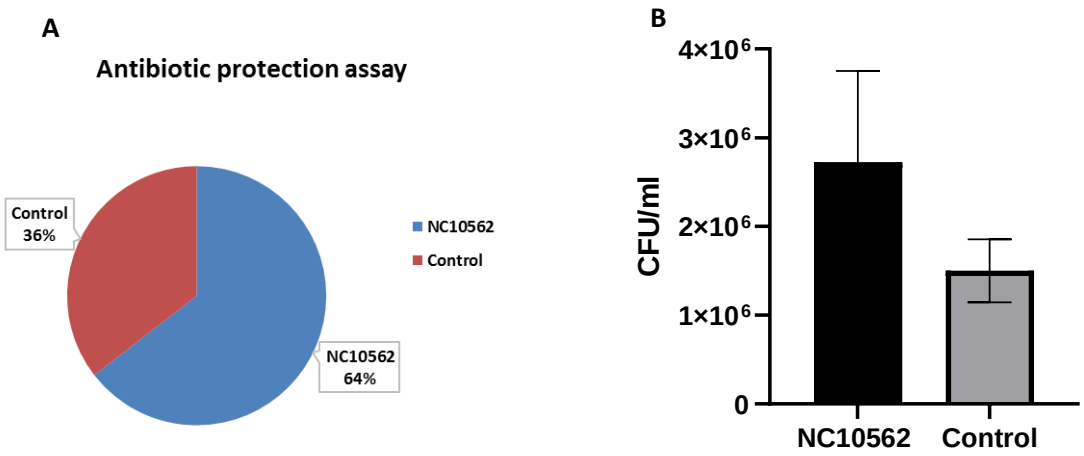

Figure 3.10. Antibiotic Protection Assay of *F. nucleatum* subsp. *polymorphum*. E-cadherin positive H357 epithelial cells were infected with the type strain of *F. nucleatum* subsp. *polymorphum* ATCC10953/NCTC10562 for two hours and then treated with 200µg/ml metronidazole and 300µg/ml gentamycin combination for an additional one hour. $1.5x10^6$ CFU/ml bacteria were recovered from controls (only bacteria and no epithelial cells) despite the antibiotic treatment (B, histogram on right). A pie chart showing the percentage of bacterial recovery after antibiotic treatment of both sample and control (A). The error bars represent standard deviation of two replicates (n=2).

3.3.9 Investigating the invasiveness of *F. nucleatum* subsp *polymorphum* using confocal microscopy

We investigated whether confocal microscopy could be used to investigate intracellular localisation of *F. nucleatum.* Visualisation of *F. nucleatum* subsp. *polymorphum* was achieved by staining with propidium iodide which resulted in red fluorescent staining of the bacteria. In order to visualise these stained bacteria within cells, we used a negative staining approach where the cell culture media was stained with fluorescein.

A 3D sagittal-section of E-cadherin positive H357 epithelial cells infected with the type strain of *F. nucleatum* subsp. *polymorphum* revealed the presence of internalised bacteria (Figure 3.11, arrows, top A). The scan also showed the presence of bacteria on the surface of the epithelial cells (stained green) by *F. nucleatum* subsp. *polymorphum* stained red with Propidium Iodide (Figure 3.11, arrow, bottom B).

Cells were scanned with Leica confocal microscope and images obtained depicted the cytoplasm as a dark shadow, allowing internalised bacteria to be viewed inside. Nuclei could also be visualised with Hoescht (Figure 3.12).

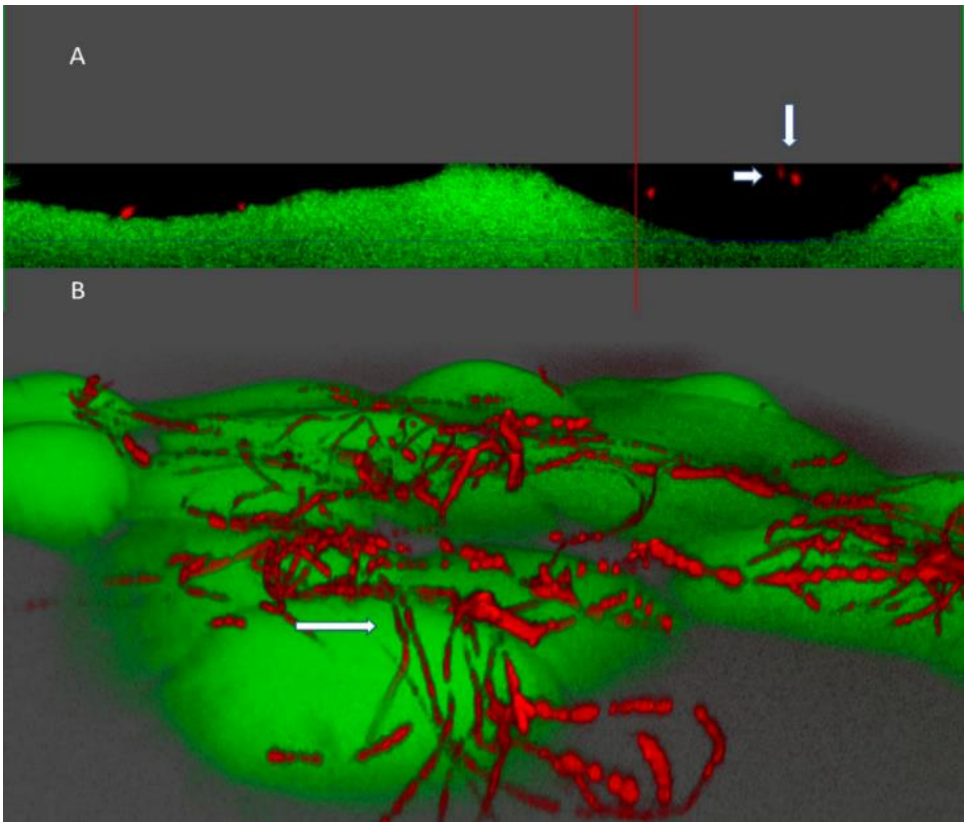

Figure 3.11. Epithelial invasion by *F. nucleatum*. 3D sagittal-section of E-cadherin positive H357 epithelial cells reveals internalised bacteria NC10562 within epithelial cells (arrows, top A) and the surface penetration of epithelial cells (stained green) by *F. nucleatum ss polymorphum* stained red with PI (arrow, bottom B).

A

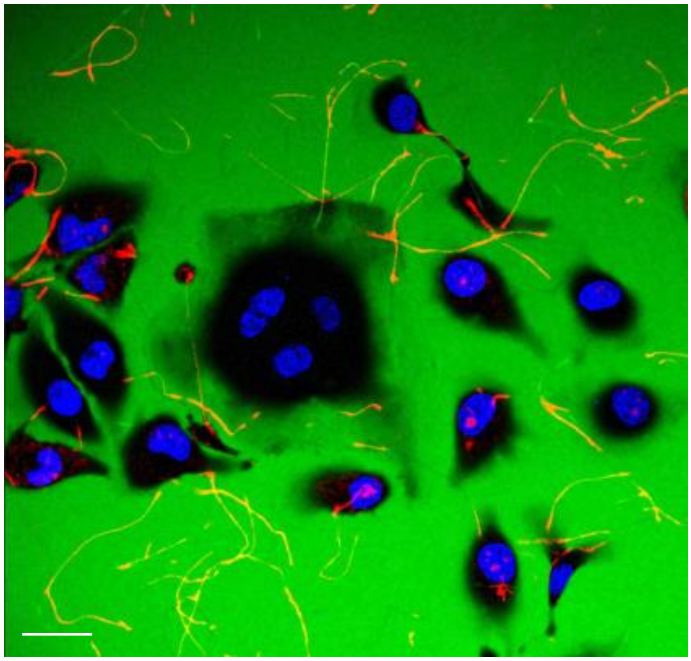

B

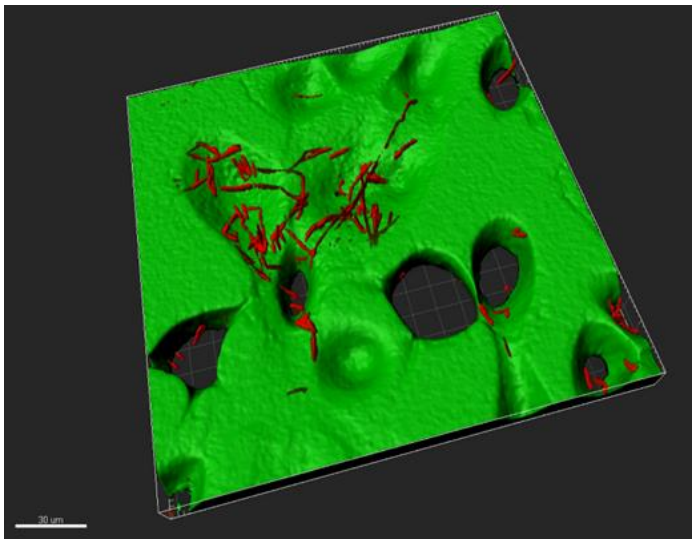

Figure 3.12. Confocal image of the invasion of E-cadherin positive H357 cells by the type strain ATCC10953/NCTC10562. The dark areas indicate the intracellular space and the blue stained areas are the nuclei. For imaging purposes, the background was stained green with fluorescein and the bacteria were stained red with propidium iodide. Internalised bacteria appear dark red and extracellular bacteria appear lighter orange in the image (A). The 3-D processed image using Imaris shows epithelial cells as grooves and hollows and internalised/invaded bacteria appear red rod-like structures stained with propidium iodide (B) (Scale bar=35µm).

3.3.10 Quantification of invasion of *F. nucleatum* subsp. *polymorphum* using a novel confocal microscopic technique

Images of infected epithelial cells were analysed using the Imaris image analysis software which allowed quantification of fluorescent signals. Data were normalised to cell surface area, as E-cadherin positive cells generally exhibited greater surface area than E-cadherin negative cells. Using this novel technique, we quantified the level of intracellular bacteria in at least three independent infection experiments for each strain in E-cadherin positive and negative cells. In general, it was determined that all isolates, including the type strain ATCC10953/NCTC10562 and clinical isolates of *F. nucleatum* subsp. *polymorphum* (n=7) were more invasive to the E-cadherin positive H357 cell line (Figure 3.13). However, the type strain ATCC10953/NCTC10562 had a significantly higher invasiveness to E-cadherin positive H357 oral keratinocytes compared to the clinical isolates of *F. nucleatum* subsp. *polymorphum*, with exceptions of clinical isolates 41A and 41B2 (more invasive than ATCC10953; Figure 3.13).

Conversely, when E-cadherin negative H376 cells were used, clinical isolates of *F. nucleatum* subsp. *polymorphum* (n=7) were more similar in terms of invasion compared to the type strain ATCC10953/NCTC10562, as shown in table 3.2.

Direct comparison between invasiveness of the two cell lines and the bacterial strains showed that the bacteria were more invasive to E-cadherin positive H357 cells than E-cadherin negative cells as shown in figure 3.13.

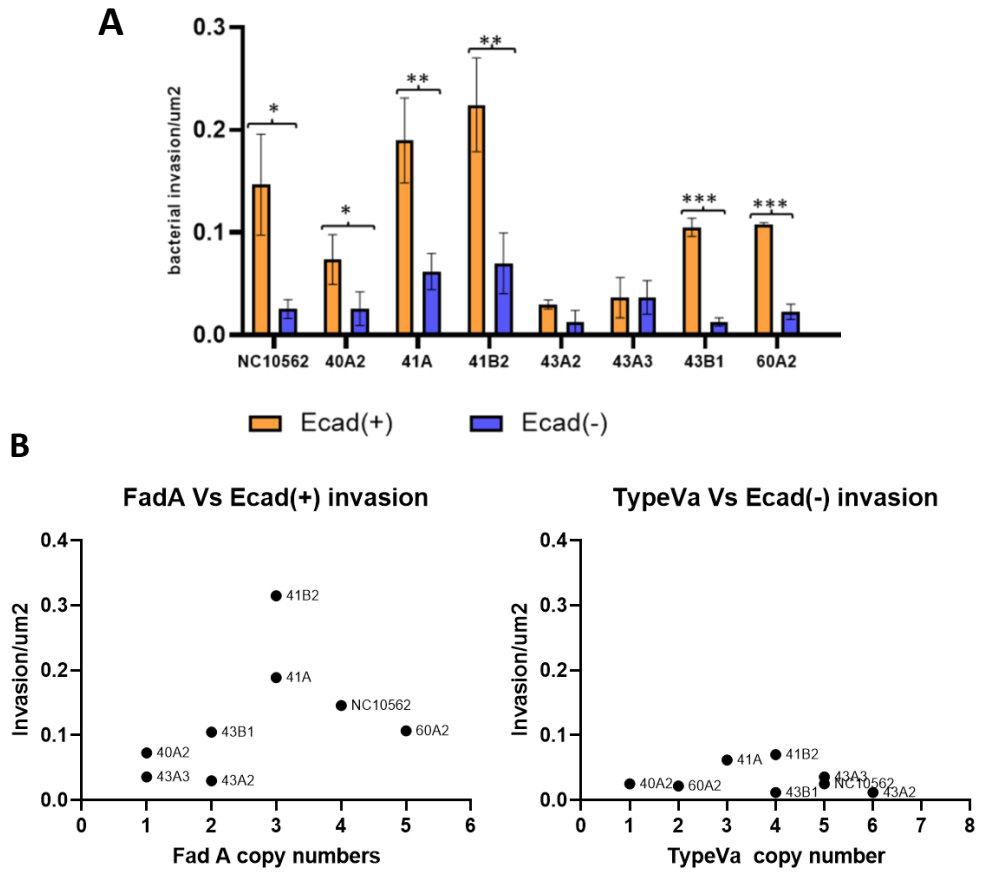

Figure 3.13. A comparison of invasiveness of E-cadherin positive and E-cadherin negative cell lines with *F. nucleatum* subsp. *polymorphum* strains. Invasion assay was performed in 8-well µ-plates for four hours and images of three fields per well obtained using confocal microscopy and processed using Imaris image analysis software. (A, top) All bacterial strains of *F. nucleatum* subsp. *polymorphum* (n=8) including the type strain ATCC10953/NCTC10562 had significantly higher invasion in E-cadherin positive H357 cell line as compared to E-cadherin negative H376 cell line. The invasiveness of the bacteria is expressed as surface area of the bacteria invading/µm^2 of the epithelial cell (statistical analysis: *indicates t-test p-value < 0.05, ** indicates p-value <0.01, ***indicates p-value <0.001, error bars indicate standard deviations of three experimental replicates). (B, bottom) higher copy numbers of type Va autotransporters did not seem to have any major effect on invasiveness of the phenotypes on E-cadherin negative cell lines. However, higher copy numbers of Fad A adhesin seemed to be correlated to higher invasion of E-cadherin positive cell line in some cases.

Table 3.2. Comparison of invasion of *F. nucleatum* subsp. *polymorphum* type strain ATCC10593/NCTC10562 with the clinical isolates in E-cadherin positive H357 and E-cadherin negative H376 cell lines.

Ecad(+)H357	40A2	41A	41B2	43A2	43A3	43B1	60A2
Mean invasion	0.073	0.189	0.224	0.030	0.036	0.105	0.107
Significantly different from NC10562	No	No	No	**Yes**	**Yes**	No	No
P-value	0.2253	0.4884	0.2482	0.0282	0.0433	0.6861	0.6861

Ecad(-)H376	40A2	41A	41B2	43A2	43A3	43B1	60A2
Mean invasion	0.025	0.025	0.062	0.012	0.036	0.012	0.022
Significantly different from NC10562	No	No	No	No	No	No	No
P-value	0.7724	0.1254	0.0880	0.2245	0.5630	0.2846	0.7504

The type strain showed a statistically significant difference in invasion when compared to the clinical isolates 43A2 and 43A3 in the E-cadherin positive H357 cell line (top). However, there was no statistically significant difference in invasion between the type strain and the clinical isolates in the E-cadherin negative cell line (bottom).

3.3.11 Galactose induced inhibition of adhesion and invasion of E-cadherin positive and negative cell lines

As a number of clinical isolates exhibited increased adhesion to cells that did not possess E-cadherin (E-cadherin negative H376 cell line) we investigated whether the presence of Gal-GalNac was responsible for this adhesion, as these cells exhibited high levels of peanut agglutinin staining (Figure 3.5, E). For this purpose, three *F. nucleatum* subsp. *polymorphum* strains were selected, namely, type strain ATCC10953/NCTC10562, clinical isolate 40A2 and clinical isolate 43A3. The clinical isolates that were selected for the assay were the most actively adhering and invading strain (43A3) and the least adhering and invading strain (40A2) identified from previous assays.

All bacterial samples were pre-treated with galactose at a concentration of 60mM (~1% w/v) for thirty minutes before using for infecting the cell lines. Adhesion and invasion assays were performed as described earlier in the methods section.

After two hours of infection of E-cadherin negative H376 cells with the bacterial strains in the presence of 60mM galactose, we found that the percentage of adhesion was drastically reduced compared to their respective untreated controls (Figure 3.14). All three stains of *F. nucleatum* subsp*. polymorphum* had a statistically significant drop in adhesion compared to untreated controls, with the type strain ATCC10953/NCTC10562 and clinical isolate 43A3 being the most significantly affected by galactose (student t-test p value <0.001 in both cases). There was a significant reduction in adhesion of clinical isolate 40A2 to the cell line as well (student t-test p value <0.01).

For the invasion assay, the bacterial infection of the epithelial cells was carried out for four hours under controlled environment as described in the method section in the presence of 60mM galactose and images acquired using confocal microscopy. The images were then processed using Imaris image processing software. Bacterial invasion of epithelial cells was expressed as surface area of invaded bacteria per μm^2 of the epithelial cell. We found that there was a significant reduction in bacterial invasion of the epithelial cells when 60mM of galactose was used as an inhibitor. All bacterial samples including the type strain ATCC10953/NCTC10562, clinical isolates 40A2 and 43A3 showed a statistically very significant drop in invasion as compared to their respective untreated controls (t-test p value <0.001 for ATCC10953/NCTC10562 and clinical isolate 40A2 and t-test p value <0.01

for clinical isolate 43A3). The results expressed hence are the percentage invasion relative to the untreated controls as shown in the figure 3.14.

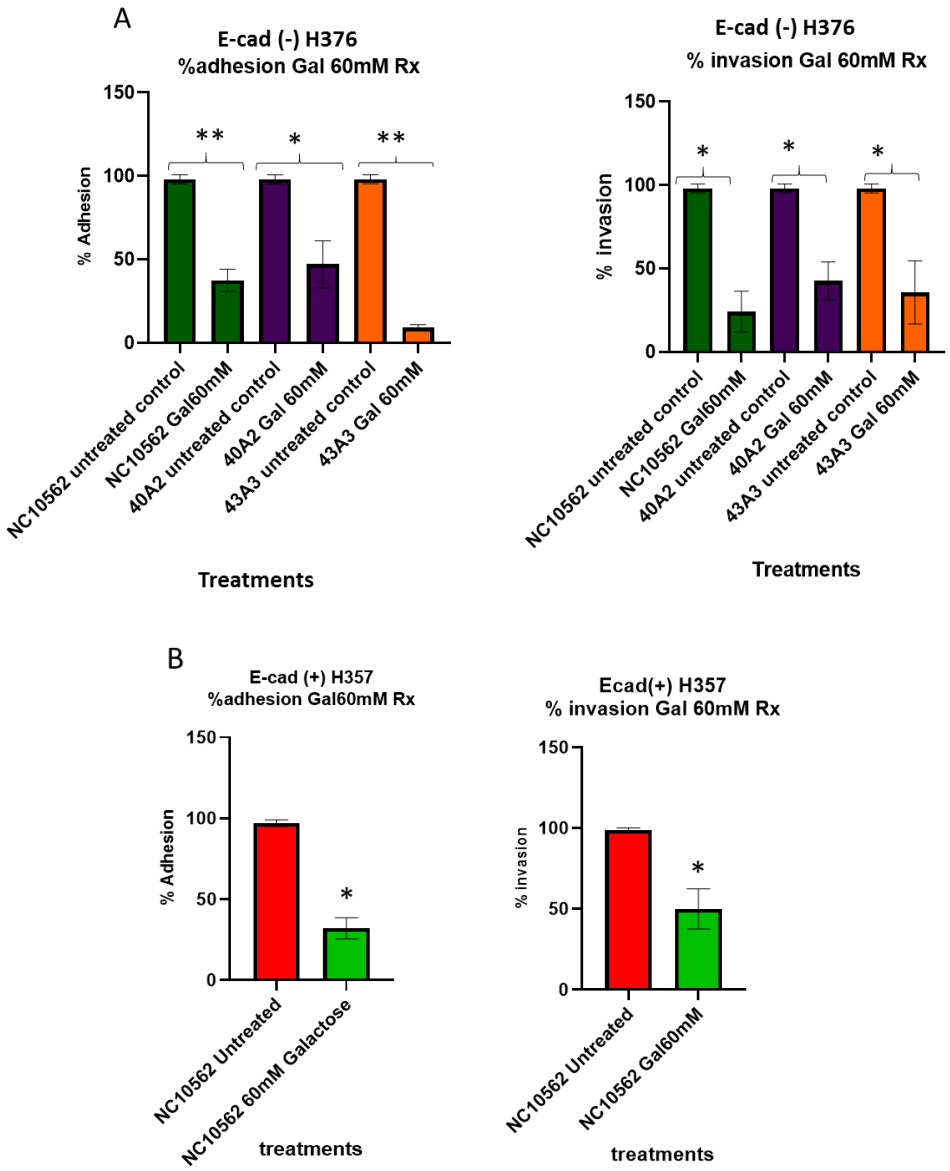

Figure 3.14. Galactose inhibition of adhesion and invasion. All bacterial strains were treated with 60mM galactose for 30 minutes before infecting E-cadherin positive and E-cadherin negative epithelial cells (A). In case of E-cadherin negative cell infection, both adhesion and invasion were significantly reduced as compared to their untreated controls (Top, *indicates t-test p value <0.01, **indicates t-test p value <0.001, error bars indicate standard deviation of three experimental replicates). In case of E-cadherin positive cell, we used *F. nucleatum* subsp. *polymorphum* type strain ATCC10953/NCTC10562 for cellular infections (B). In both cases of adhesion and invasion, the reductions were statistically very significant, perhaps correlating to its high copy numbers of both FadA and typeVa adhesins (bottom, **indicates student t-test p value <0.001, error bars indicate standard deviation of three experimental replicates).

3.3.12 Inhibition of adhesion of *F. nucleatum* subsp*. polymorphum* to E-cadherin positive H357 cell line using a specific peptide targeting FadA adhesin

To inhibit the adhesion of *F. nucleatum* subsp*. polymorphum* to E-cadherin positive cell lines, we had to target the FadA adhesin. For this purpose, a peptide consisting of the region of E-cadherin shown to interact with FadA (ASANWTIQYND) was designed that was expected to competitively engage with the FadA adhesin, therefore inhibiting its adhesion to the E-cadherin receptors of the epithelial cells. To test the hypothesis, we used the type strain of *F.* nucleatum subsp. *polymorphum* ATCC10953/NCTC10562. Along with the E-cadherin positive H357 cell line, we also employed the E-cadherin negative H376 cells to investigate the probability of the presence of alternative receptors for FadA in E-cadherin negative cells.

The overnight bacterial culture of type strain of *F. nucleatum* subsp*. polymorphum* was pre-treated with 0.1mM ASANWTIQYND peptide for thirty minutes as described in the methods section. The epithelial cells were then infected with the peptide treated bacterial culture for two hours and then epithelial cells were washed to remove any non-adherent bacteria. The epithelial cells were then lysed to release adherent bacteria and the cell lysate was serially diluted and plated on BHI agar plates supplemented with defibrinated horse blood. The CFUs formed after four to five days of anaerobic incubation were counted and presented as percentage adhesion. As a control, a peptide scramble was also used, which had the same amino acid as the peptide used, but in a mixed, scrambled sequence.

When pre-treating the bacterial culture with the FadA specific peptide inhibitor at a concentration of 0.1mM, we found that the bacterial adhesion to E-cadherin positive H357 cell line was completely abolished. Interestingly, the scrambled peptide used as a control also showed mild reduction in adhesion, although the reduction was statistically non-significant (student t-test p value >0.05) (figure 3.15A).

On the other hand, pre-treating the bacterial culture with the FadA specific peptide inhibitor at a concentration of 0.1mM and using it to infect E-cadherin negative H376 cell line also resulted in a complete abolishment of adhesion of the bacteria to the cell line indicating the presence of other receptors for FadA adhesin as shown in the figure 3.15B.

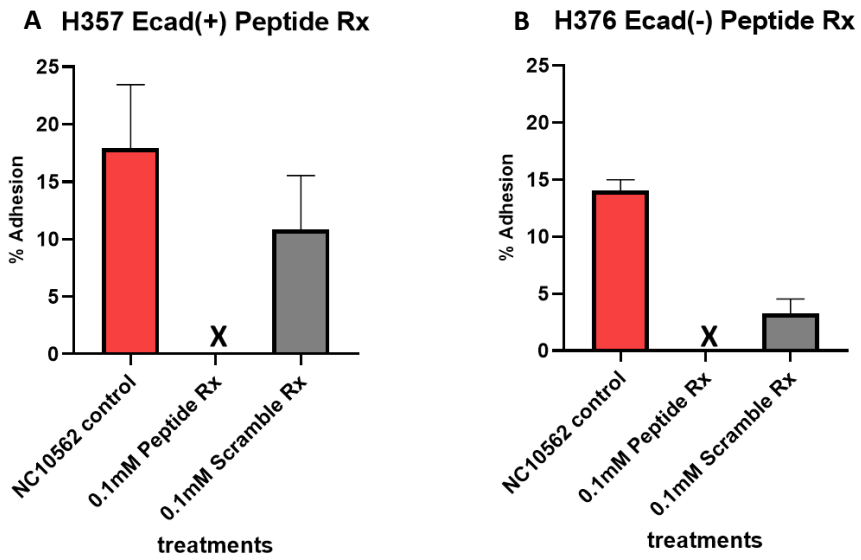

Figure 3.15. **Inhibition of adhesion of *F. nucleatum* subsp. *polymorphum* using FadA specific inhibitor peptide ASANWTIQYND at a concentration of 0.1mM.** Both cell lines were infected with the type strain of F. *nucleatum ssp polymorphum* ATCC10953/NCTC10562 pre-treated with 0.1mM FadA specific peptide inhibitor. There was a complete abolishment in adhesion of the bacteria to the cell lines in both cases (A and B). The inhibition of adhesion in E-cadherin negative H376 cell line is suggestive of the presence of alternative receptors for FadA other than E-cadherins (B).

3.4 Discussion

Oral leukoplakia, erythroplakia, and carcinoma-in-situ lesions have been shown to occur more commonly in patients with a history of tobacco use and alcohol consumption. However, poor oral hygiene has also been indicated as an independent risk factor for the development of OSCC (Hsiao et al., 2018). Previous studies have identified high levels of colonisation with *F. nucleatum* on OSCC and OLK (McIlvanna et al., 2021, Zhang et al., 2019). Due to its association with poor outcomes in CRC, it has been suggested that *F. nucleatum* could play a role in progression of OLK to OSCC. In this study, *Fusobacterium* species were isolated from pathologic and contralateral normal mucosal sites from patients presenting with OLK lesions. In total, 54 isolates were identified as *F. nucleatum* subsp*. polymorphum*, making this the dominant *Fusobacterium* species on these lesional and normal mucosal sites. Eren *et al.* showed that *F. nucleatum* subsp. *polymorphum* was the most abundant *F. nucleatum* subspecies on normal mucosal surfaces, although in that study *F. periodonticum* was the most abundant *Fusobacterium* species (Eren et al., 2014). We did also recover *F. periodonticum,* but in smaller numbers. This may be due to differences in colonisation patterns or due to the use of a selective medium for *F. nucleatum*, which may not be as suitable for *F. periodonticum* isolation.

To examine the interacton of *F. nucleatum* subsp*. polymorphum* with oral epithelial cells, a total of n=7 isolates of *F. nucleatum* subsp*. polymorphum* recovered from patients with OSCC and/or leukoplakia were examined. All seven isolates were identified as *F. nucleatum* subsp*. polymorphum* based in 16S rRNA sequencing and the type strain of *F. nucleatum* subsp*. polymorphum* (ATCC10953/NCTC10562) was included as a comparator. The overarching goal of this study was to characterize the pathogenicity of the *F. nucleatum* subsp*. polymorphum* isolated from the clinical samples.

It has been established that the epithelial-mesenchymal transition observed in early embryonic phase of human development is assisted by E-cadherin, which is very much similar to the dysplastic transition of epithelium, except that in the latter, the transition is uncontrolled and unregulated, leading to malignant transformation in the oral cavity. As described earlier, this malignant transformation has been reported to be characterized by an early loss of intercellular adhesion due to the loss of E-cadherin, loss of well differentiated epithelial cells, increased cellular atypia and an increased cellular motility

(Pećina-Slaus, 2003). We selected two OSCC cell lines that were reported to have a difference in E-cadherin expression, H357, established from OSCC of the tongue of a seventy-four years old male patient and H376, established from OSCC of the floor of the mouth of a forty-year-old female patient. We confirmed the presence of E-cadherins in H357 cells and the absence of the same in H376 cells by performing immunocytochemistry using E-cadherin specific antibodies as described in the methods section of this chapter. We also showed that these cells differed in the degree of Gal-GalNAc staining by using lectin obtained from specific carbohydrate source, such as peanuts that could be visualised and imaged under a fluorescent microscope.

It has been described in the literature that the adhesion of *F. nucleatum* to dysplastic colonocytes is heavily dependent on the presence of adhesins like FadA and Fap2. The FadA adhesin has great affinity to the E-cadherins expressed on epithelial cells of the gut mucosa, perhaps bringing about the dysplastic changes observed in CRC (Rubinstein et al., 2013). However, studies have shown that the dysplastic events in the oral cavity result in the loss of E-cadherin expression, which may support a greater role for the Fap2 adhesin of *F. nucleatum,* which binds to simple sugar receptors such as galactose and N-acetyl-D-galactosamine receptors (Gal-GalNAc) on the epithelial cell surfaces.

Optimum adhesion appears to occur after 2 hours incubation, after which the number of bacteria recovered starts to decline. This may be due to detachment or a loss in viability. Extended incubation for 24 h resulted in a significant loss of viability which is likely due to the sensitivity of *F. nucleatum* to atmospheric oxygen.

In our study, strains of *F. nucleatum* subsp*. polymorphum* exhibited preferences in terms of adhesion to the E-cadherin positive and negative cells. For example, the clinical isolates of *F. nucleatum* subsp*. polymorphum* 40A2, 41A and 41B2 exhibited similar adhesion to both cell lines, whereas the 43A2, 43A3, 43B1 and 60A2 exhibited significantly greater adhesion to the E-cadherin negative cell line H376. However, interestingly, this effect was reversed when employing the type strain ATCC10953/NCTC10562. When this strain was employed in adhesion assays, there was a reduction in the adhesion from 25% to 11% between E-cad positive H357 and E-cad negative H376 cell lines, respectively. This could perhaps be explained due to the nature of the bacterial samples obtained. Whilst the type strain of *F. nucleatum* subsp*. polymorphum* ATCC10562/NCTC10562 was isolated from

dental plaque of a healthy individual, the clinical isolates were all isolated from pathologic lesion sites and healthy contralateral site in the oral cavity of the same patient. These data show that clinical isolates of *F. nucleatum* subsp*. polymorphum* exhibit strong adherence to E-cadherin negative dysplastic cells. Loss of E-cadherin is an early event in dysplasia. This change and other possible changes in the epithelial cell surface during the development of OLK may select for a specific microbiome, as characterised by Amer et al (2017). Some of the strains recovered here may be specifically adapted to adhere to dysplastic cells and this may explain why higher levels of *F. nucleatum* have been reported on the surface of OLK and OSCC.

The increased adhesion to H376 (E-cadherin negative) cells may be related to expression of Type Va autotransporter adhesins such as Fap2. Analysis of the genomes of our clinical isolates shows that the strains with the highest adhesion to H376 cells have higher copy numbers of putative Type Va proteins. In addition, H376 cells exhibit more intense staining with lectin indicating a high level of Gal-GalNAc on the surface of these cells. Galactose was also shown to strongly inhibit adhesion to E-cadherin negative H376 cells and E-cadherin positive H357 cells. Although the type strain ATCC10562/NCTC10562 possesses a high copy number of Type Va proteins, it was not among the most adherent strains to E-cadherin negative H376 cells. This may be due to the nature of Type Va adhesins expressed on this particular isolate, or due to the presence of other unrelated adhesins in the clinical isolates. Clearly adhesion is multi-factorial and mutagenesis may be needed to determine the roles of individual adhesins.

The type strain ATCC10953/NCTC10562 exhibited the highest level of adhesion to the E-cadherin positive H357 cells. This may be related to the high copy number of FadA like adhesins. Pre-treating the bacteria with a specific FadA inhibiting peptide ASANWTIQYND at a concentration of 0.1mM resulted in a complete abolishment of adhesion of the bacterial strains to H357 cells. We also demonstrated a likely role for type Va adhesins in the interaction with these cells as Gal-GalNac could also inhibit adhesion to these cells.

Unexpectedly, we also showed that the peptide exhibited a strong inhibitory effect on adhesion to the E-cadherin negative H376 cell line. This suggests the involvement of additional FadA receptors in the absence of E-cadherin and this requires further investigation.

There were several methods employed to assess and quantify epithelial cell invasion, however, numerous challenges were encountered. The traditional antibiotic protection assay for invasion utilises combinations of antibiotics such as metronidazole and gentamicin to kill extracellular Gram negative anaerobes (Healy and Moran, 2019). However, in our antibiotic protection assays, it was found that the bactericidal effect of metronidazole and gentamicin on *F.* nucleatum subsp. *polymorphum* was insufficient to kill the extracellular bacteria. This effect has also been observed by other investigators (Daniel Slade, Virginia Polytechnic Institute, Personal Communication). As a result, we developed a novel confocal microscopic method to estimate and quantify the invasion of bacteria into oral epithelial cells. Here, we stained *F. nucleatum* with propidium iodide, a fluorescent agent that stains cells and nucleic acids. The internal area of the epithelial cell was visualised by staining the extracellular medium with fluorescein, to which the epithelial cell is impermeable. The results of the invasion assays were expressed as surface area of bacteria per μm^2 of epithelial cell invaded. It was interesting however, that none of the epithelial cells stained positive for fluorescein, indicating there was no obvious breach of the epithelial cell surface when *F. nucleatum* invaded them. Visualisation of the epithelial cells showed that many fusobacteria extended through the cellular membrane, with part of the bacterium inside and part of the bacterium outside the epithelial cell. The lack of internal fluorescein staining indicates that this invasion process does not breach the integrity of the cellular membrane. The exact method involved in bacterial invasion is yet to be investigated.

In general, it was interesting to see that the relative invasion of E-cadherin positive H357 cells was greater compared to invasion of the E-cadherin negative H376 cells. Invasion of E-cadherin positive cells was greatest in isolates 41A and 41B2 and the type strain ATCC10953/NCTC10562, all of which exhibited 3 or more copies of FadA-like genes. Isolate 60A2 however was a weak invader, despite possessing 3 FadA-like genes (FadA1). The clinical isolates 41A and 41B2 also exhibited greater invasion of the E-cad negative H376 cell line in comparison to the type strain ATCC10953/NCTC10562, indicating that their enhanced invasion may not require E-cadherin and by extension, the FadA surface adhesin.

In conclusion, these data show that adherence and invasion of keratinocytes by clinical strains of *F. nucleatum* subsp*. polymorphum* is highly strain dependent and is influenced

by the expression of different receptors on the epithelial cell. It can be concluded that strains vary greatly in their complement of both type Va adhesins and FadA like genes that may influence these interactions. Additionally, a cell line that does not express E-cadherin was not invaded to the same extent as a cell line expressing E-cadherin. However, it must be noted that these cell lines are not isogenic and that other factors may be at play in this interaction. It is also possible that FadA has additional receptors, as this study shows that FadA blocking peptides may inhibit interactions with cells that do not express E-cadherin.

Further investigation will be required to determine the specific invading mechanism of the bacteria. One possible mechanism of invasion is by manipulation and disruption of epithelial cell cytoskeleton and entry via membrane bound vacuoles (Gursoy et al., 2008). This invasion by active actin formation and internalization of *F. nucleatum* subsp. *polymorphum* by the epithelial cells need further investigation and is a proposed future work.

The next section of this study will investigate the responses of host cells to these bacteria and whether differences in adhesion, invasion and host cell cadherin status influences these responses.

Chapter 4

Cellular responses to *F. nucleatum* subsp*. polymorphum* infection – Cell motility, migration and invasion

4.1 Introduction

Oral malignancies such as OSCC and other neoplasms in general are a result of complex response mechanisms that the human body participates in. Although genetic and environmental factors have been largely attributed to the aetiology of tumour formation, research in the recent past directs towards the involvement of microbiological entities such as bacteria and viruses (Alnuaimi et al., 2015, Bhatlekar et al., 2014, Boehm et al., 2020, Han, 2015). As discussed earlier in the general introduction chapter, the involvement of *F. nucleatum* in the progression of CRC involves multiple, complex intracellular pathways that are favourable for tumour growth and survival. The underlying dominant factor is the creation of a chronic proinflammatory microenvironment that enables the cancerous cell to not only survive and thrive but enabling it to migrate and invade newer territories. This is achieved by stimulating the cancerous cell to secrete cytokines that become chemotactic (known as chemokines) and enable other cancerous cells to migrate and invade underlying unaffected tissues.

Cytokines are intercellular signalling proteins that mediate immune responses by cell growth, proliferation, angiogenesis and tissue repair (Roi and Roi, 2020). Cytokines can either be anti-inflammatory that help the body fight against various forms of assaults, or pro-inflammatory agents, that promote inflammatory conditions. IL-6, IL-8 and TNFβ are such pro-inflammatory cytokines that have strong associations with OSCC (Roi and Roi, 2020). IL-8 is secreted by various immune cells that include monocytes, fibroblasts, lymphocytes, lung macrophages neutrophils and non-immune cells such as endothelial cells, keratinocytes, epithelial cells and hepatocytes (Brew et al., 2000). IL-8 has also been found to be secreted by various tumour tissues, of which, oral cancers are notorious secretors (Watanabe et al., 2002). Chemokines on the other hand are chemotactic cytokines that are essential in promoting cellular migration and invasion between tissues (Chow and Luster, 2014). One such chemokine prominent in the proliferation of oral cancers is chemokine (C-C motif) ligand 5 (CCL5), formerly known as RANTES (regulated upon activation, normal T cell expressed and secreted).

CCL5 was originally thought to be secreted by activated T-cells, but latest research has revealed it to be an inflammatory chemokine associated with chronic inflammatory conditions such as cancers (Chuang et al., 2009). The activation of intercellular pathways

such as NF-κβ in OSCC is suggested to stimulate the secretion of CCL5, whose activity is primarily dependent on binding to CCR5 receptors on host cancer cells. This rather promiscuous chemokine also binds to other receptors such as CCR1 and CCR3 and auxiliary receptors such as CCR4 and CD44 (Aldinucci and Colombatti, 2014). However, its interaction with CCR5 remains central.

CCL5/CCR5 interactions further cancerous tissue proliferation in several ways such as acting as growth factors, modulating the extracellular matrix by increased degradation due to the activity of upregulated MMP-9, supplying additional nutrients to the tumour tissue by stimulating new blood vessel formation (angiogenesis), inducing the recruitment of additional stromal and inflammatory cells, and participating in immune evasion mechanisms (Kershaw et al., 2013, Aldinucci and Colombatti, 2014).

Several authors have described the mechanism involving the CCL5/CCR5 axis in OSCC migration and upregulation of MMP-9 expression. Chuang et al in their recent study explored this CCL5/CCR5 axis and its involvement in OSCC cell migration and MMP-9 expression. The CCL5/CCR5 axis activates Phospholipase C (PLCβ3), which stimulates the phosphokinase C signalling pathway (PKCδ). This in turn induces NF-κβ activation through the activation of p65 heterodimer protein, which leads to MMP-9 expression and increases the migration of human oral cancer cells (Chuang et al., 2009). The CCL5/CCR5 axis is summarised in figure 4.1.

In this chapter, we explored and identified the various cytokines and chemokines secreted by the E-cadherin positive and negative OSCC cell lines when infected with strains of *F. nucleatum* subsp. *polymorphum* recovered from dysplasia. We focussed on the secretion of CCL5/RANTES and the subsequent expression of MMP-9 and the effects on mobilisation of the cancerous cells.

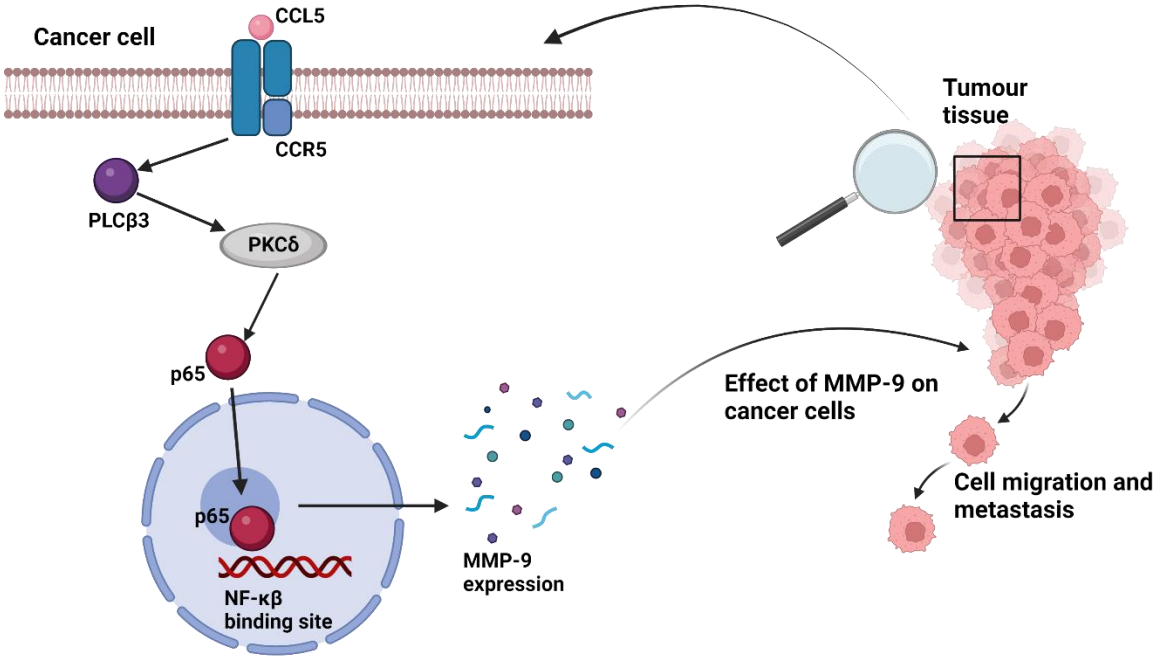

Figure 4.1. CCL5/CCR5 Axis and cell migration in OSCC. The timely binding of CCL5 to its designated receptor on the cancer cell triggers the CCL5/CCR5 axis. Activated CCR5 receptor in-turn activates Phospholipase C (PLCβ3), which stimulates the phosphokinase C signalling pathway (PKCδ). This in turn induces NF-κβ activation through the activation of p65 heterodimer protein, which leads to MMP-9 expression, which is essential for extracellular matrix degradation and OSCC cell migration and invasion (Chuang et al, 2009).

4.2 Materials and methods

4.2.1 Human Matrix Metalloproteinase-9 ELISA

Quantikine ELISA kit for MMP-9 was purchased from R&D systems, USA.

All reagents, working standards and samples for the assay were prepared as directed by the manufacturer's direction. Wash buffer was prepared by adding 20 ml of the wash buffer concentrate to 480 ml of deionized distilled water to prepare a total of 500 ml of wash buffer. Substrate solution was prepared just before use by adding equal amounts of colouring agents A and B supplied in the kit. Human MMP9 standard concentrate was prepared by reconstituting the powder in 5ml of distilled water. The stock solution (20 ng/ml or 20000 pg/ml) was then serially diluted to get the following concentrations of the standard stock solution: 20 ng/ml, 10 ng/ml, 5 ng/ml, 2.5 ng/ml, 1.25 ng/ml, 0.625 ng/ml and 0.313 ng/ml. The calibrator diluent RD5-10 was used as zero standard. Since high concentrations of MMP-9 are found in saliva, a face mask and gloves to protect the assay from contamination were used.

100 µl of assay diluent RD1-34 was added to all wells. 100 µl of standards, samples and controls were added to each well and covered with adhesive strip. The plate was then incubated at room temperature for 2 hours. The wells were then washed three times with 400µl of wash buffer in each well, ensuring not to scratch the base of the wells. 200 µl of Human MMP-9 conjugate was added to each well, covered with adhesive strip and incubated for 1 hour. The wells were then washed with wash buffer three times, ensuring not to scratch the base of the well. 200 µl of substrate solution was added to each well and incubated in darkness for a further 30 minutes at room temperature. The reaction was stopped by adding 50 µl of stop solution to each well. The optical density of each well was determined using a microplate reader set to 540 nm.

4.2.2 Trans-well migration and invasion inhibition

The CCL5/CCR5 inhibitor used for this assay was rhCCL5/met-RANTES purchased from R&D systems, USA. A stock solution of 100 µg/ml using sterile water was prepared for use and stored at -20^{o}C.

The experimental procedure for the trans-well migration and invasion has been described in the general materials and methods section, using 24-wells plates. We used the same protocol for the inhibition of the trans-well migration and invasion along with the employment of the CCL5 inhibitor. Both cell lines (E-cadherin positive and negative) were sub-cultured and counted to 5x10^{5} cells/ml used for seeding the trans-wells. The epithelial cells were treated with 3 ng/ml of rhCCL5/metRANTES for thirty minutes. 400 µl of the CM obtained from infecting both the cell lines with *F. nucleatum* subsp*. polymorphum* strains (type strain ATCC10953/NCTC10562, clinical isolates 40A2, 41A and 43A3) were dispensed into the wells of the plates. The trans-well inserts were carefully placed in the 24-wells containing the CM with/without the inhibitors and 200 µl of epithelial cells were added into the inserts.

The 24-wells plate was incubated at 37^{o}C for 24-hours after which the migrated/invaded cells were stained as described in the general materials and methods section 2.10 and counted.

4.2.3 Trans-well migration and invasion using *F. nucleatum* subsp *nucleatum* mutants

FadA and Fap2 genes deleted mutants of a different sub-species of *F. nucleatum*, namely, *F. nucleatum* subsp. *nucleatum* was kindly provided by Dr. Sarah A Kuehne, School of Dentistry, University of Birmingham, UK. This subspecies of *F. nucleatum* had been altered to lose specific adhesins. In this assay we used the wild type strain of *F. nucleatum* subsp. *nucleatum* FNN23, a mutant with the FadA gene deletion Δ*fadA* and a mutant with the Fap2 gene deletion Δ*fap2*.

Both assays investigating the migration and invasion and the inhibition of the same was performed similarly as described above with *F. nucleatum* subsp*. polymorphum* strains.

4.3 Results

4.3.1 Identifying relevant cytokines and chemokines using a multiplex assay

To better understand the effects of bacterial infection of OSCC cells, particularly *F. nucleatum* subsp*. polymorphum* and the subsequent cellular responses to such treatments, we carried out a multiplex bead array assay performed by Eve Technologies Corporation to identify inflammatory cytokines and chemokines that were most significantly increased. E-cadherin positive H357 cells and negative H376 cells were first infected with *F. nucleatum* subsp. *polymorphum* strains for twenty-four hours as described in the methods section. As a positive control, we used a laboratory strain of *E. coli* DH5α in the assay and DMEM cell culture media without any supplements as a negative control. The supernatants now termed as conditioned media (CM; presumably containing cell inflammatory products) were obtained from each treatment and centrifuged to remove suspended bacteria and used for the assay.

The multiplex assay was carried out to identify seventy-one cytokines and chemokines, however, significant expression of only two cytokines namely, interleukin 6 (IL-6) and interleukin 8 (IL-8) and five chemokines, namely, interferon gamma induced protein 10 (IP-10 or CXCL10), RANTES -Regulated upon Activation, Normal T Cell Expressed and Presumably Secreted (CCL5), monocyte chemoattractant protein 1 (MCP-1/CCL2), vascular endothelial growth factor A (VEGF-A) and macrophage colony stimulating factor (M-CSF) were identified in the supernatants collected from the infections of both cell lines with *F. nucleatum* subsp. *polymorphum* strains and the positive control (figure 4.2).

4.3.1.1 E-cadherin positive H357 cell line infection

When comparing the secretion of individual cytokines secreted by both cell lines when infected with *F. nucleatum* subsp*. polymorphum* strains, we found that with the exception of IL-8, E-cadherin positive H357 cells expressed greater amounts of cytokines (Fig. 4.1). When infecting H357 cells, clinical isolates induced between ~2200 pg/ml (43A3) and ~7200 pg/ml (41A) of IL-8. The type strain of *F. nucleatum* subsp*. polymorphum* ATCC10953/NCTC10562 induced the secretion of a moderate amount of IL-8 of about ~3500 pg/ml. The positive control (DH-5α) induced the secretion of about ~2200 pg/ml. Interestingly, the negative control (DMEM cell culture media, without bacteria or supplements) also induced a baseline secretion of about 220 pg/ml of IL-8 (figure 4.2A).

MCP-1 (CCL2) was the most abundant chemokine to be secreted by the E-cadherin positive H357 cell line when infected with the bacteria (Figure 4.1). The type strain of *F. nucleatum* subsp. *polymorphum* ATCC10953/NCTC10562 induced the highest levels of MCP1 secretion of ~2700 pg/ml. Interestingly, the clinical isolates of *F. nucleatum* subsp*. polymorphum* induced similar range of MCP-1 secretion (41A- ~450 pg/ml, 41B2- ~560 pg/ml and 43A3- ~440 pg/ml), which was similar to *E-coli* DH-5α (~450 pg/ml of MCP-1), but greater than the negative control (~350pg/ml) (figure 4.2A).

IP-10 was the second most abundant chemokine secreted by the E-cadherin positive H357 cell line when infected with bacteria. All bacterial samples induced the secretion of this chemokine, with clinical isolate 41B2 inducing the most (~1850 pg/ml). Clinical isolate 43A3 induced the least amount IP-10 secretion (~500 pg/ml) (figure 4.2A).

All strains of *F. nucleatum* subsp*. polymorphum* induced the secretion of chemokines CCL5 and VEGF-A moderately when infecting the E-cadherin positive H357 cells. Whilst clinical isolates 41A (RANTES- 1054 pg/ml, VEGFA- 919 pg/ml) and 41B2 (RANTES- 1070 pg/ml, VEGFA- 620 pg/ml) induced the most secretion of RANTES and VEGF-A, clinical isolate 43A3 induced the least amounts of RANTES (472 pg/ml) and VEGF-A (405 pg/ml) secretion (figure 4.2A).

MCS-F secretion was the least of all the chemokines secreted by the E-cadherin positive H357 cells when infected with the *F. nucleatum* subsp*. polymorphum* strains (figure 4.2A).

4.3.1.2 E-cadherin negative H376 cell line infection

Like the E-cadherin positive H357 cell line, the E-cadherin negative H376 cell line also secreted high amounts of IL-6 and IL-8. All *F. nucleatum* subsp*. polymorphum* strains induced higher amounts IL-8 secretion compared to E-cadherin positive H357 cell line infections, ranging from ~5600 pg/ml (43A3) to ~8200 pg/ml (41B2). Interestingly, a baseline level of ~3100 pg/ml of IL-8 was identified in the uninfected negative control sample (figure 4.2B).

Amongst the chemokines group, VEGF-A was the most abundantly identified by the multiplex array followed by RANTES. Both the type strain of *F. nucleatum* subsp. *polymorphum* ATCC10953/NCTC10562 and clinical isolate 41B2 induced the most VEGF-A secretion (~500 pg/ml each) and the clinical isolate 43A3 secreted ~300 pg/ml of VEGF-A.

CCL5 was the second most abundantly identified chemokine from the clinical isolate infections, with clinical isolate 41A inducing ~450 pg/ml (highest), followed by clinical isolate 41B2 (~220 pg/ml), the type strain of *F. nucleatum* subsp*. polymorphum* ATCC10953/NCTC10562 (~180 pg/ml) and clinical isolate 43A3 (~120 pg/ml). The positive control DH-5α induced ~600 pg/ml of RANTES when infecting E-cadherin negative H376 cell line (figure 4.2B).

A baseline secretion of all cytokines and chemokines discussed was identified in the uninfected negative control sample when treating the E-cadherin negative H376 cell line. A summary of the data of relevant cytokines and chemokines obtained is shown in the figure 4.2.

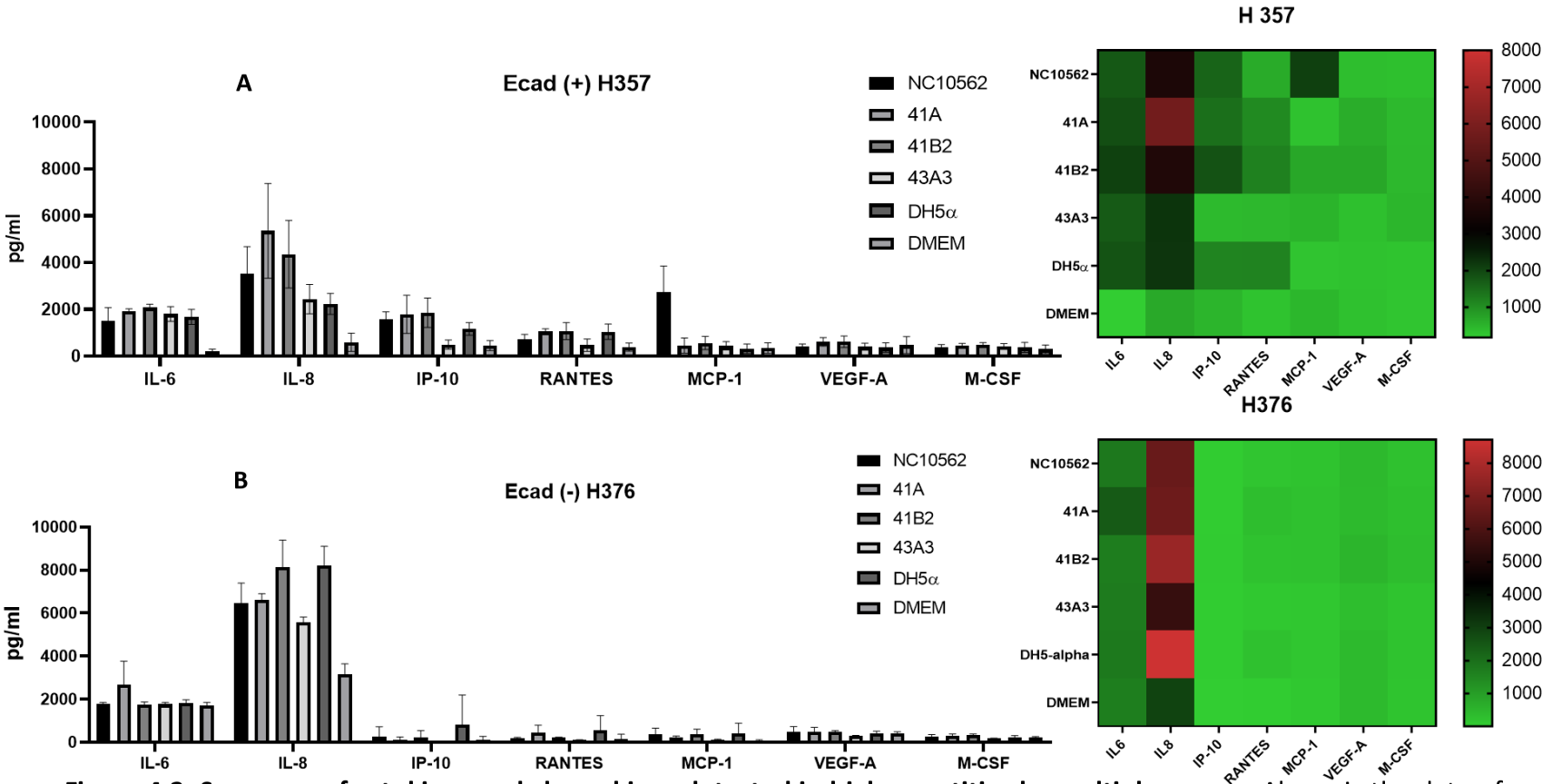

Figure 4.2. Summary of cytokines and chemokines detected in high quantities by multiplex assay. Above is the data of cytokines and chemokines that were significantly high when e-cadherin positive cell line was treated. A total of two cytokines (IL-6 and IL-8) and five chemokines (IP-10, RANTES, MCP-1, VEGF-A and MCS-F) were detected. A positive control (type strain of *E.coli* DH5α) and a negative control (DMEM cell culture media) was used in the assay (A). Similar set up of the experiment was used to infect e-cadherin negative H376 cell lines and the results tabulated (B).

4.3.2 Identifying specific RANTES/CCL5 chemokine secretion by direct ELISA method

The identification of specific cytokines was targeted as a follow up of the multiplex assay to better understand the cellular responses of the cell lines with *F. nucleatum* subsp. *polymorphum* infection. Firstly, we used primary antibody pre-coated ELISA wells for the detection of RANTES/CCL5 in the conditioned media that were collected from infecting the E-cadherin positive H357 and E-cadherin negative H376 cell lines as described in the general materials and methods chapter. The cell lines infection was carried out using three strains of *F. nucleatum* subsp. *polymorphum*, namely, the type strain ATCC10953/NCTC10562 as a control, clinical isolates 40A2 and 43A3. DMEM media without supplements or bacteria was used as a negative control. Along with the bacterial infections, we also used D-galactose solution at a concentration of 60mM to see the effects of Fap2 inhibition on cellular responses such as secretion of RANTES/CCL5.

We found that significant amounts of RANTES/CCL5 were secreted by both cell lines when infected with *F. nucleatum* subsp. *polymorphum* strains and the use of D-Galactose inhibitor significantly reduced the chemokine secretion (figure. 4.3). In the E-cadherin positive H357 cell line, the highest amount of approximately 1000pg/ml of RANTES/CCL5 was secreted when infecting the cell line with clinical isolate 43A3, followed by the type strain ATCC10953/NCTC10562 of approximately 800pg/ml. Infection with clinical isolate 40A2 secreted the least amount of RANTES/CCL5 of approximately 400pg/ml. However, when the bacteria were pre-treated with 60mM of D-Galactose, both the type strain and clinical isolate 40A2 showed a statistically significant reduction in RANTES/CCL5 secretion by the cell line (* indicates student t-test p value <0.05) (figure 4.3A).

Similarly, in the E-cadherin negative H376 cell line, the Clinical isolate 43A3 infection seemed to stimulate the highest RANTES/CCL5 secretion of approximately 1400 pg/ml and the clinical isolate 40A2 infected induced the least RANTES/CCL5 secretion of about 400 pg/ml. The pre-treatment of the bacterial strains with D-Galactose caused a significant reduction in the chemokine secretion in both clinical isolates 40A2 and 43A3 as shown in the figure 4.3B (* indicates t-test p value <0.05, significant).

Interestingly, negative controls in both cell lines seemed to induce a base line secretion of the chemokine as expected and inhibition by D-galactose wasn't statistically significant.

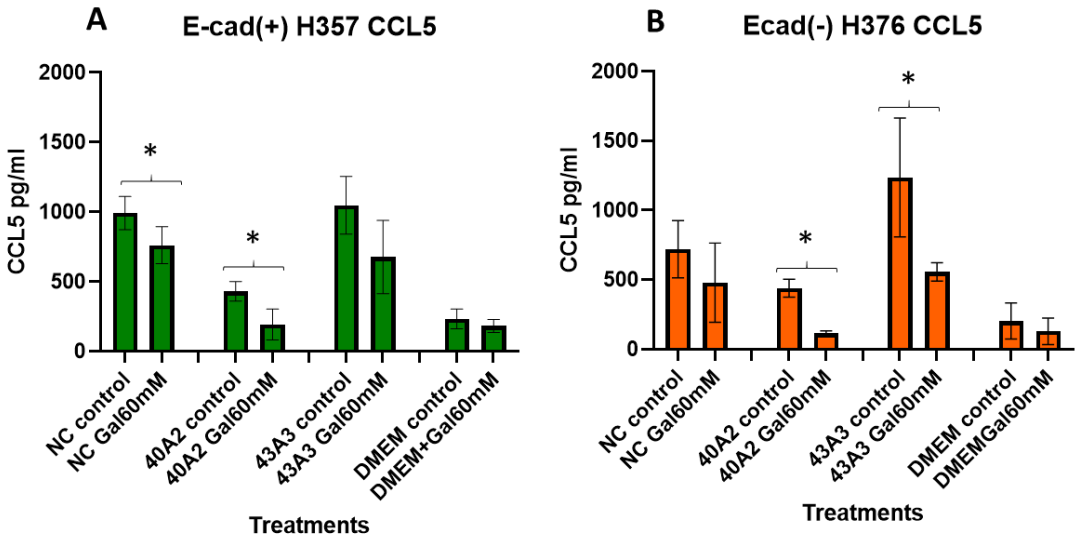

Figure 4.3. RANTES/CCL5 induction by *F. nucleatum* subsp. *polymorphum*. RANTES/CCL5 levels in the conditioned media collected from cell lines infection was estimated using pre-coated ELISA plates. E-cadherin negative H376 cell line secreted the highest amount of RANTES/CCL5 of approximately 1400 pg/ml when infected with the clinical isolate 43A3. Both cell lines secreted similar amounts of the chemokine when infected with the clinical isolate 40A2 (approximately 400pg/ml). A baseline level of RANTES/CCL5 secretion was observed in both cell lines due to their cancerous nature (* indicates t-test p value <0.05, statistically significant, error bars indicate standard deviations of three experimental replicates).

4.3.3 MMP detection by a multiplex assay system

We carried out a multiplex bead array assay to identify matrix metalloproteinases that were secreted by the OSCC cell lines when infected with *F. nucleatum* subsp. *polymorphum* strains for twenty-four hours as described in the methods section. We used the *F. nucleatum* subsp. *polymorphum* type strain ATCC10953/NCTC10562 and the clinical isolate 43A3 for the cell line infections. DMEM cell culture media without any supplements was used as a negative control for the assay. The supernatants collected from the 24-hours infection termed as conditioned media (presumably containing the MMPs of interest) were obtained from each treatment and centrifuged to remove suspended bacteria and used for the assay. The assay was designed to identify nine MMPs, namely, MMP-1, MMP-2, MMP-3, MMP-7, MMP-8, MMP-9, MMP-10, MMP-12 and MMP-13.

The multiplex array could detect and quantify four of these MMPs in our *F. nucleatum* infected samples, namely, MMP-1, MMP-2, MMP-3 and MMP-9. These four MMPs were detected in varying amounts in both cell lines supernatants. In the E-cadherin positive H357 cell line, interestingly, MMP-1 was the most abundant MMP from the control samples (type strain and DMEM) and the clinical isolate 43A3 had the least (the MMP-1 values for both controls were out of range for the assay system, so we designated 800 pg/ml for representation purpose, clinical isolate 43A3 = 650 pg/ml). The second highest MMP to be identified in this cell line was MMP-3, with infected and uninfected samples containing MMP-3 at a range between 350-500 pg/ml. MMP-9, was the third highest MMP to be detected, with infected cells (both the type strain and the clinical isolate 43A3) stimulating the higher levels of secretion than uninfected samples (both samples containing approximately 134 pg/ml MMP-9) (figure 4.4A).

In the E-cadherin negative H376 cell line supernatants, again MMP-1, MMP-3 and MMP-9 were the dominant secreted metalloproteinases. As with the E-cadherin positive cells, MMP-1 was the highest quantified MMP (type strain ~800 pg/ml and 43A3 ~550 pg/ml) with this cell line, followed by MMP-9. Interestingly, the clinical isolate 43A3 supernatant had the highest amounts of MMP-9 (approximately 500 pg/ml) followed by the type strain (approximately 300 pg/ml). The negative control DMEM supernatant contained the least MMP-9 levels (approximately 70 pg/ml) (figure 4.4B). The multiplex assay of all the identifiable MMPs is summarised in the figure 4.4.

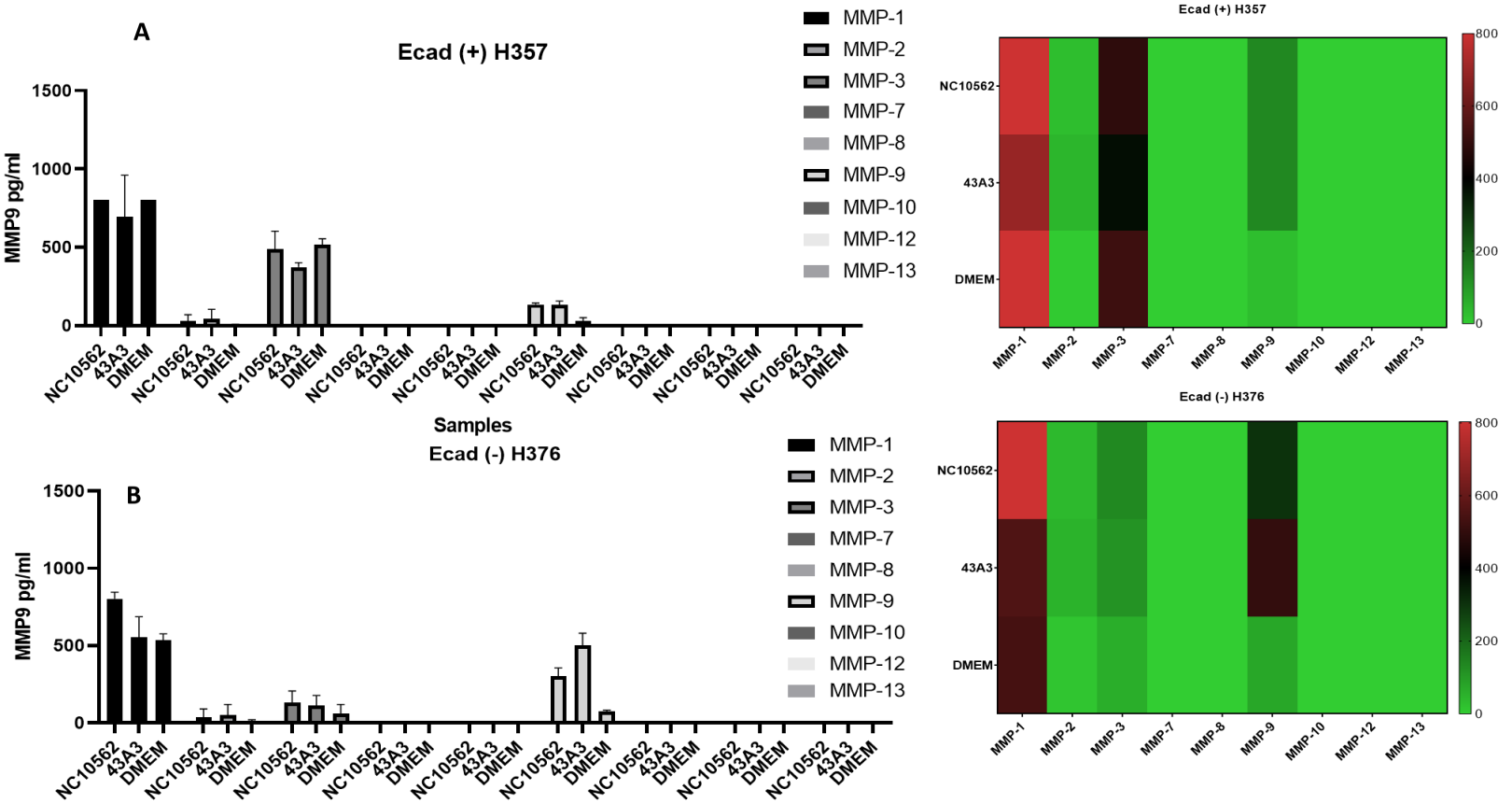

Figure 4.4. MMP multiplex assay. The multiplex assay was designed to identify nine MMPs, however, only four of these molecules were identified in the supernatants that were collected from infecting E-cadherin positive and negative cell lines with strains of *F. nucleatum* subsp. *polymorphum*. Whilst MMP-1 and MMP-3 were the dominant MMPs identified in E-cadherin positive H357 cell line infections (top, A), MMP-1 and MMP-9 were the dominant MMPs identified in E-cadherin negative H376 cell line infections (bottom, B).

4.3.4 Quantification of *F. nucleatum* subsp. *polymorphum* induced MMP9 secretion by direct ELISA method

Matrix Metalloproteinase 9 (MMP9) or gelatinase B is a pro-inflammatory matrix degrading enzyme, suspected to be significant in degrading connective tissue matrix and mobilising tumour cells. To investigate the levels of MMP9 secreted by OSCC cell lines when infected with *F. nucleatum* subsp. *polymorphum*, we performed a direct ELISA assay. E-cadherin positive H357 and E-cadherin negative H376 cells were seeded in 24-well plates and allowed to gain 60-70% confluence as described earlier in the general materials and methods chapter. The cells were then infected with *F. nucleatum* subsp. *polymorphum* type strain ATCC10953/NCTC10562, clinical isolates 40A2 and 43A3 for 24-hours period. DMEM cell culture media without any supplements was used as a negative control. The supernatants were then collected and centrifuged to use in the ELISA kit to estimate the MMP9 levels.

We found that MMP9 was secreted by both cell lines when infected with the bacteria. Although a baseline secretion of MMP-9 was seen with the negative control DMEM treatment, the secretion from type strain and clinical isolate 43A3 infections were significantly higher than the base line in the E-cadherin positive H357 cell line (Kruskal-Wallis test, * indicates p-value <0.05, statistically significant, figure 4.5B). Similarly, A significantly higher MMP-9 secretion was seen with the clinical isolate 43A3 infection of the E-cadherin negative H376 cell line compared to the baseline MMP-9 secretion seen with DMEM treatment (Kruskal-Wallis test, * indicates p-value <0.05, statistically significant, figure 4.5C). However, when direct comparisons of MMP9 levels between the two cell lines were made, we found that the E-cadherin negative H376 cell line secreted higher levels of MMP9. Clinical isolate 43A3 induced the highest quantities of MMP9 of about 500 pg/ml in this cell line, whilst clinical isolate 40A2 induced the secretion of about 240 pg/ml of MMP9, which was the least. The positive control type strain ATCC10953/NCTC10562 induced about 302 pg/ml of MMP9.

The E-cadherin positive H357 cell line infection induced about 130 pg/ml of MMP9 by both clinical isolate 43A3 and the type strain ATCC10953/NCTC10562, followed by about 80 pg/ml by clinical isolate 40A2, which was the least for this cell line. Both cell lines induced

a baseline MMP9 secretion by the negative control as expected (~82 pg/ml for E-cadherin positive and ~ 240 pg/ml for E-cadherin negative cell line).

The MMP9 levels were significantly higher in E-cadherin negative cell line compared to E-cadherin positive cell line when infected with the clinical isolate 40A2 and 43A3 (student t-test p value <0.05). However, the difference in the levels of MMP9 weren't statistically significant when treating the cell lines with the positive control (type strain ATCC10953/NCTC10562) and the negative control as shown in the figure 4.5.

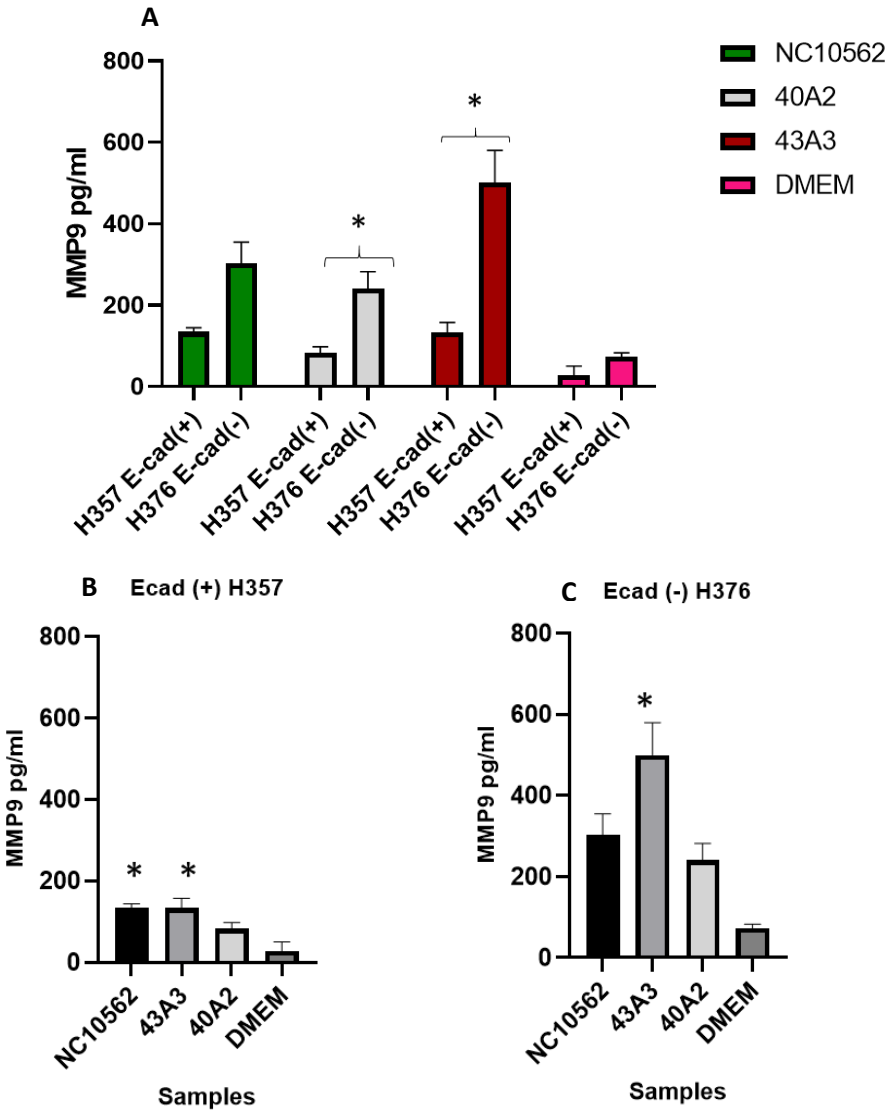

Figure 4.5. **MMP9 induction by *F. nucleatum* subsp. *polymorphum* infection.** MMP9 induction was significantly higher in E-cadherin negative H376 cell line as compared to E-cadherin positive H357 cell line. The difference in MMP9 levels was statistically significant between the two cell lines when infected with the clinical isolates 40A2 and 43A3 (* indicates student t-test p-value <0.05, A). A baseline level of MMP9 secretion was seen with the negative control in both cell lines (containing DMEM cell culture media without any supplements or bacterial suspension), however, the MMP-9 secretions were significantly higher than the baseline secretion when clinical isolate 43A3 strain of *F. nucleatum* subsp. *polymorphum* was used to infect both cell lines (*indicates Kruskal-Wallis test p-value <0.05, statistically significant, B and C, error bars indicate standard deviations of three experimental replicates).

4.3.5 Scratch wound assay to assess OSCC cells motility and migration

CCL5/RANTES is essential for OSCC cell migration and expression of MMP9, which in-turn is crucial for induction and regulation of tumour cell motility and migration. Therefore, to demonstrate the effect of MMP9, and ultimately CCL5 on E-cadherin positive H357 and E-cadherin negative H376 cells, we designed the scratch wound assay. Both cell lines were seeded on 6-wells plates as described earlier in the materials and methods section and allowed to attain a confluence of 100%. An intentional wound (scratch) was produced using a 1000µl pipette tip and the width of the wound recorded. The cells were now treated with the conditioned media (CM) obtained from *F. nucleatum* subsp. *polymorphum* infection as described earlier in the materials and methods section. The treatment was carried out for 24-hours, after which the new-width of the wound was recorded for comparison of the healing (indicative of cell motility and migration).

Five *F. nucleatum* subsp. *polymorphum* strains were used in this assay, namely, the type strain ATCC10953/NCTC10562, clinical isolates 40A2, 41A, 41B2 and 43A3. As a negative control, DMEM cell culture media without any supplements or bacterial suspension was used. After 24-hours treatment of the wound with the CM, we found that both cell lines demonstrated considerable wound healing with *F. nucletum* subsp. *polymorphum* infected supernatants. However, the wound healing that occurred when treating the scratch wound with CM obtained from clinical isolate 43A3 was the most significant (figure 4.6A). The difference in the wound healing between the two cell lines particularly with conditioned media obtained from clinical isolate 43A3 was statistically significant with E-cadherin negative H376 cells producing a wound closure of approximately 80% wound closure and E-cadherin positive H357 cells producing approximately 60% wound (student t-test p value <0.05, statistically significant).CM obtained from most *F. nucleatum* subsp. *polymorphum* strains induced higher cell motility and migration in E-cadherin negative H376 cell line. The motility induced by CM from clinical isolate 43A3 was highly significant compared to the uninfected DMEM control (figure 4.6 B and C, bottom, **indicates Kruskal-Wallis test p-value <0.001, highly significant, *indicates p-value <0.05, significant). Similarly, the motility induced by the same *F. nucleatum* strain in the E-cadherin positive H357 cell line was also very significant when compared to the uninfected DMEM control (figure 4.6, bottom, **indicates Kruskal-wallis test p-value <0.001, very significant).

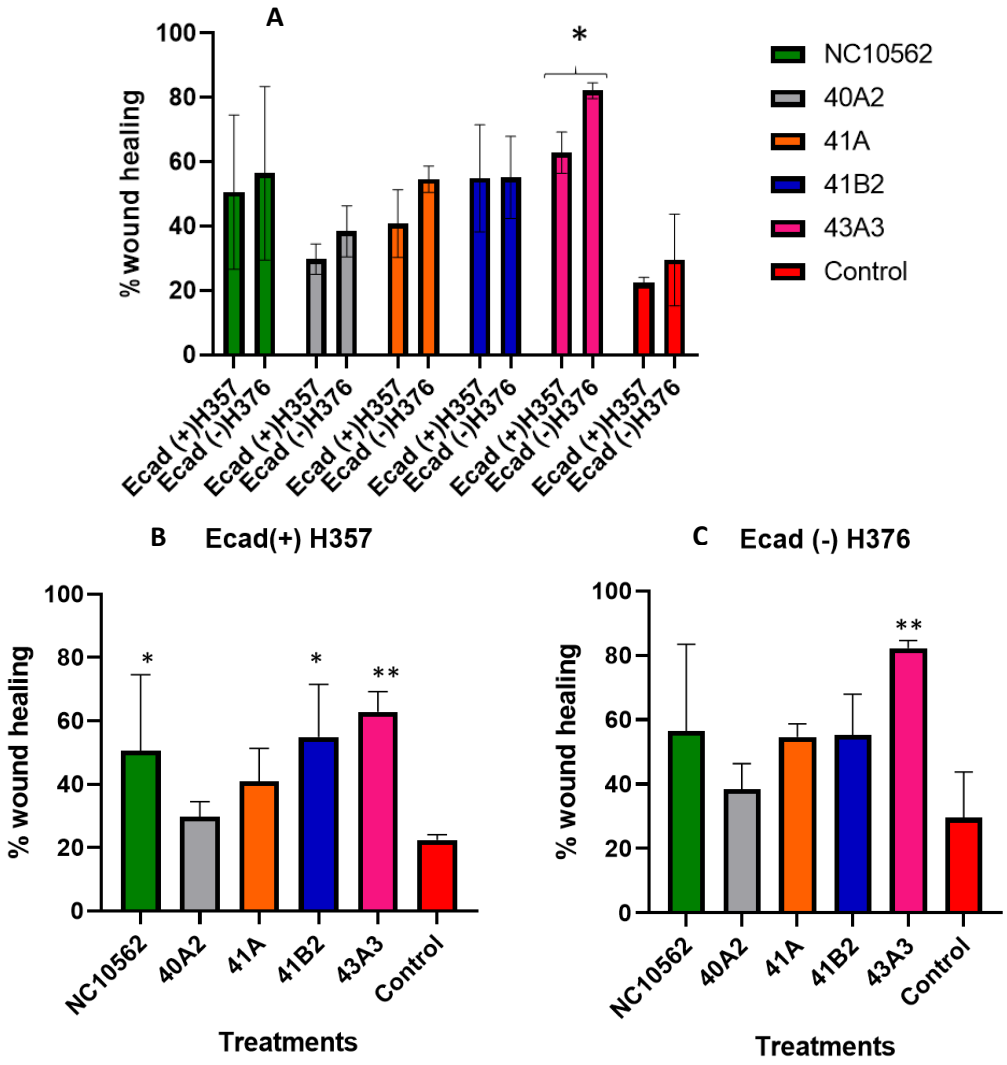

Figure 4.6. **Scratch wound healing induced by CCL5/MMP9.** To demonstrate the effects of CCL5 and MMP9 on cell motility and migration, scratch wound assay was performed. Conditioned media consisting the chemokines was used to treat an intentional wound caused on the two cell lines. The wound closure occurred after 24-hours was the measurement of cell migration and motility. (A) Comparison of the percentage of wound healing between the two cell lines when treated with CM. CM from clinical isolate 43A3 induced significantly greater wound closure with E-cadherin negative H376 cells of approximately 80% wound closure (A, * indicates student t-test p value <0.05, statistically significant). (B) Comparison of wound closure in each cell line treated with CM relative to DMEM alone. A significant difference existed between the cell motility induced with infected cell CM treatment and uninfected DMEM CM treatment in both cell lines (B and C, *indicates Kruskal-Wallis test p-values <0.05, significant, **indicate p-value <0.001, error bars indicate standard deviations of three experimental replicates).

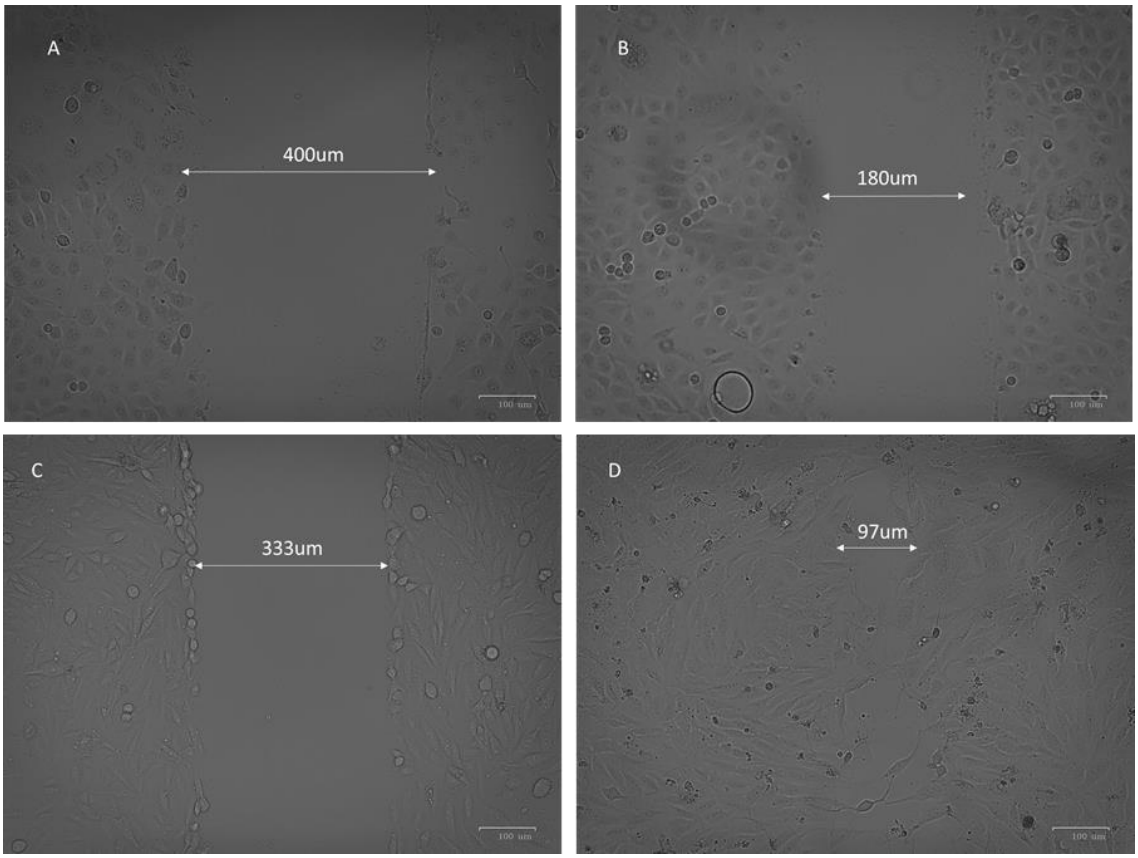

Figure 4.7. Scratch wound assay. Representative images of scratch wounds caused to E-cadherin positive H357 cells (top, A- wound width at 0-H and B- wound width after 24-hours treatment with CM obtained from clinical isolate 43A3) and E-cadherin negative H376 cells (bottom, C: wound width at 0-hours and D: wound width after 24-hours treatment with CM obtained from clinical isolate 43A3). Cell migration was assessed by calculating the amount of wound closure after 24-hours of CM treatment (scale bar=100µm).

4.3.6 Trans-well migration assay to assess OSCC cell invasiveness

As a follow-up of the scratch wound assay that demonstrated cell migration, we performed a trans-well migration assay to assess and compare the migration and invading properties of the E-cadherin positive H357 and E-cadherin negative H376 cell lines when infected with *F. nucleatum* subsp. *polymorphum* strains. We used the type strain ATCC10593/NCTC10562, clinical isolates 40A2, 41A and 43A3 for this assay along with DMEM cell culture media containing neither any supplements nor bacterial suspension as a negative control. The presence of extracellular matrix gel (ECM gel) and the polycarbonate membrane in the trans-well insert offered a physical barrier and the presence of CM beneath the trans-well inserts acted as cellular attractant. Therefore, the cells that successfully penetrated the gel and crossed the polycarbonate membrane barrier were the most migratory and invasive cells influenced to a greater extent by the chemokine attractants (CCL5/MMP-9) in the CM.

As in the scratch wound assay, we found that the E-cadherin negative cells were generally more migratory and invasive in the trans-well assay as well. When the cells were exposed to CM obtained from bacterial infections, we found that the difference in cell migration and invasion between the two cell lines caused by the clinical isolate 43A3 was the highest and statistically significant (figure 4.8; student t-test p value <0.05, statistically significant). The treatment of E-cadherin positive H357 and E-cadherin negative H376 cell lines with respective CM obtained from clinical isolate 43A3 infections caused an average migration and invasion of approximately ~195 and ~700 epithelial cells respectively, through the ECM gel and polycarbonate membrane (Fig. 4.8). On the contrary, treatment with CM obtained from the clinical isolate 40A2 caused the least cell migration and invasion in both cell lines. However, there was a significantly higher migration of cells across the membrane when treating the E-cadherin negative H376 cells with the CM obtained from clinical isolate 40A2 as compared to the E-cadherin positive H357 cells. The average cells migrated and invaded for this treatment were 185 and 100 epithelial cells respectively and the difference in the cell migration and invasion was found to be statistically significant (student t-test p value <0.05, significant).

This trend of higher cell migration and invasion across the polycarbonate membrane of trans-well inserts in E-cadherin negative H376 cells was observed when treatments with

CM obtained from clinical isolate 41A and the type strain ATCC10953/NCTC10562 of *F. nucleatum* subsp. *polymorphum* were performed. An average of 550 E-cadherin negative H376 epithelial cells successfully crossed the ECM/polycarbonate membrane when treated with CM obtained from clinical isolate 41A as compared to an average of 150 E-cadherin positive cells. This difference in the cell migration and invasion was found to be statistically significant (student t-test p value <0.05). Similarly, an average of 500 E-cadherin negative H376 epithelial cells crossed across the ECM/polycarbonate membrane barrier as compared to an average number of 122 E-cadherin positive H357 epithelial cells when exposed to CM obtained from type strain ATCC10593/NCTC10562. The difference in the cell migration and invasion between the two cell lines in the type strain CM was found to be statistically significant as well (student t-test p value <0.05).

Interestingly, a few epithelial cells from both cell lines managed to cross the physical barrier offered by the ECM/polycarbonate membrane of the inserts when exposed to the CM obtained from the negative control (DMEM without supplements or bacterial suspension). There was an average of 100 E-cadherin negative H376 epithelial cells and 50 E-cadherin positive H357 epithelial cells that crossed the barrier. However, the difference in the cell migration and invasion between the two cell lines was not statistically significant as shown in figure 4.8.

When we compared the number of cell migration and invasion between the untreated control (DMEM) and the *F. nucleatum* strains infected samples, we found that there was a statistically significant difference in number of cell migration with some *F. nucleatum* strains infections (figure 4.9). Amongst the E-cadherin positive H357 cell line treatments, the clinical isolates 41A and 43A3 CM treatments caused the most cells to migrate across the ECM/polycarbonate membrane barrier which were statistically significant (153 and 141 cells respectively, Kruskal-Wallis test p-value <0.01, statistically significant). Similarly, the difference in the cell migration between the untreated control (DMEM) and the *F. nucleatum* treated samples (41A and 43A3) were statistically significant in the E-cadherin negative H376 cell lines (figure 4.9). The clinical isolate 41A caused a mean cell migration of 617 cells (Kruskal-Wallis p-value <0.05, statistically significant) and the clinical isolate 43A3 caused a mean cell migration of 756 cells (Kruskal-Wallis p-value <0.001, statistically

very significant) as compared to a mean cell migration of 102 cells with untreated DMEM control (figure 4.9).

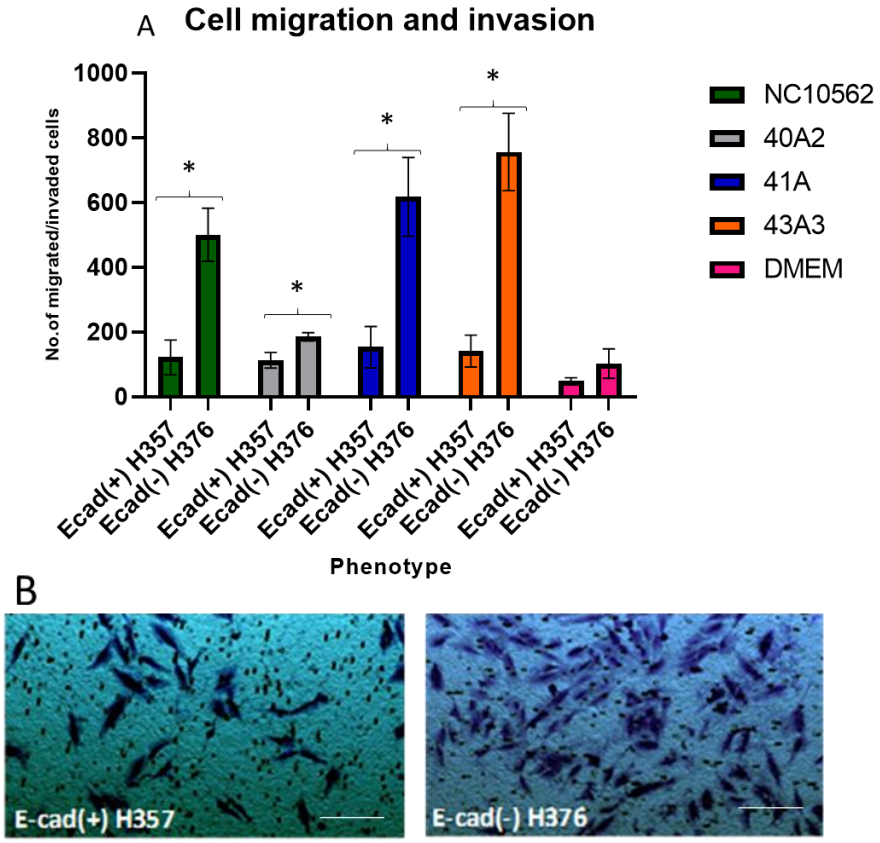

Figure 4.8. Trans-well cell migration and invasion assay. E-cadherin positive and negative cells were exposed to CM obtained from *F. nucleatum* subsp. *polymorphum* type strain ATCC10593/NCTC10562, clinical isolates 40A2, 41A, 43A3 and DMEM cell culture media. The difference in the cell migration and invasion in the two cell lines was statistically significant. The highest and the least migration and invasion were seen when both cells were exposed to CM obtained from clinical isolate 43A3 and 40A2 respectively and the difference in cell migration and invasion between the cell lines was statistically significant (* indicates student t-test p value <0.05, statistically significant; Top, A. Error bars indicate the standard deviations of three experimental replicates). Images of cells stained with crystal violet after 24-hours of migration across ECM and polycarbonate membrane, using CM obtained from clinical isolate 43A3 infection of E-cadherin positive and negative cells (Bottom B) (scale bar= 100µm).

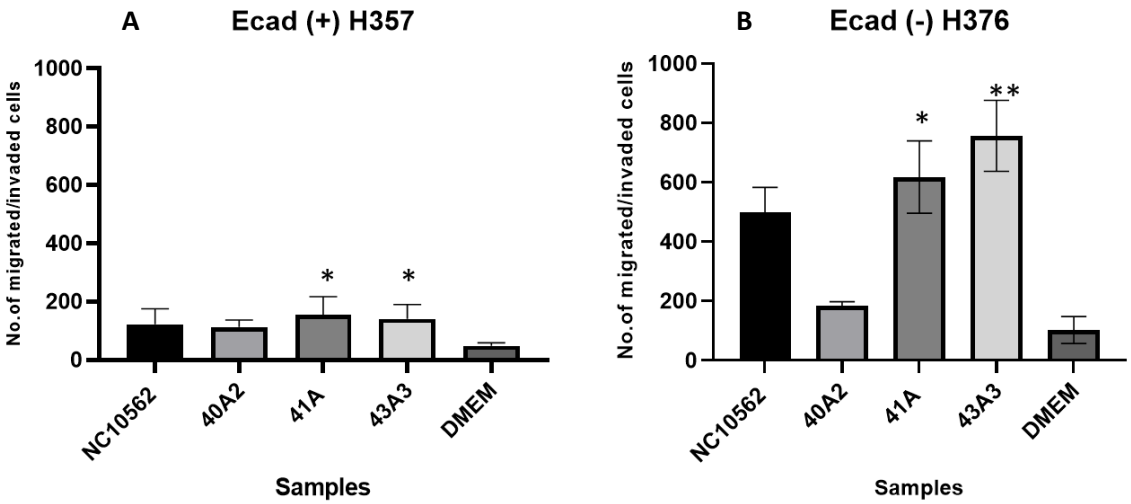

Figure 4.9. Comparison of cell migration between *F. nucleatum* treated samples and untreated control. In case of both E-cadherin positive H357 (A) and negative H376 cell line (B) treatments, CM obtained from the clinical isolates 41A and 43A3 caused the most cell migration compared to the CM obtained from DMEM controls (*indicates Kruskal-Wallis p-value <0.05, statistically significant and **indicates Kruskal-Wallis p-value <0.001, statistically very significant. Error bars indicate standard deviations of three experimental replicates).

4.3.7 Using specific CCL5/RANTES inhibitor rhCCL5/metRANTES to inhibit Trans-well migration and invasion

Cell migration and invasion across the ECM gel and the polycarbonate membrane of the trans-well inserts was inhibited using a specific inhibitor targeting the chemokine CCL5 receptor called CCR5. The inhibitor we used was rhCCL5/metRANTES (metCCL5) used at a final concentration of 3ng/ml to inhibit the action of CCL5/RANTES. The inhibition assay was carried out as described in the materials and methods section of this chapter for 24-hours, after which the under-side of the polycarbonate membrane of the trans-well inserts was stained with crystal violet to stain successfully migrated and invaded OSCC cells. Inhibitor untreated controls for each sample were used side by side. As a positive control, we used DMEM cell culture media containing 3ng/ml of rhCCL5/RANTES to act as a cell attractant.

Both cell lines, namely, E-cadherin positive H357 and E-cadherin negative H376 cells were treated identically. After 24-hours of incubation, we found that both cell lines showed a varied degree of inhibition in migration across the ECM gel/polycarbonate membrane. Amongst the E-cadherin positive H357 cells, the most significant inhibition occurred when the cells were treated with the CM obtained from the clinical isolate 41A (student t-test p value <0.05, statistically significant). An average total of 153.3 cells managed to migrate across the membrane when in contact with the control CM, whilst only 48.3 cells migrated when treated with the inhibitor, producing a 68.5% drop in net migration of cells. This trend in reduced migration of E-cadherin positive H357 cells under the influence of rhCCL5/metRANTES 3 ng/ml treatment was observed with CM obtained from all experimental samples, however, the differences in cell migration between the treated and untreated cells were not statistically significant.

The E-cadherin negative H376 cells showed a similar behaviour to 3 ng/ml rhCCL5/metRANTES treatment as well. Being quite migratory in nature as compared to E-cadherin positive H357 cells as observed in the scratch wound assay and trans-well migration assay, an inhibitor treatment reduced this migratory behaviour in all samples. The most dramatic difference in migration from no treatment to treatment with rhCCL5/metRANTES was seen when the E-cadherin negative H376 cells came in proximity with the CM obtained from clinical isolate 40A2 infection. There was a reduction of cell

migration from 185 cells to 121 cells after inhibitor treatment, accounting for approximately 35% drop in net cell migration and invasion. This reduction in cell migration with treatment with CM obtained from clinical isolate 40A2 consisting the inhibitor was statistically highly significant (Mann-Whitney t-test p value <0.001, statistically very significant). The E-cadherin negative H376 cells behaved in a similar fashion when they were made to contact CM obtained from the clinical isolates 41A and 43A3 infections consisting 3 ng/ml rhCCL5/metRANTES. The reductions in cell migration and invasion were clearly evident and these reductions were also statistically significant. As controls, we used DMEM consisting 3 ng/ml of rhCCL5 as a positive control in the well (not in the trans-well) to stimulate cell migration and CM from cells treated with DMEM without any supplements was used as a negative control. The difference in cell migration between CCL5 treated positive control and untreated negative control in both cell lines were statistically significant as shown in figure 4.10.

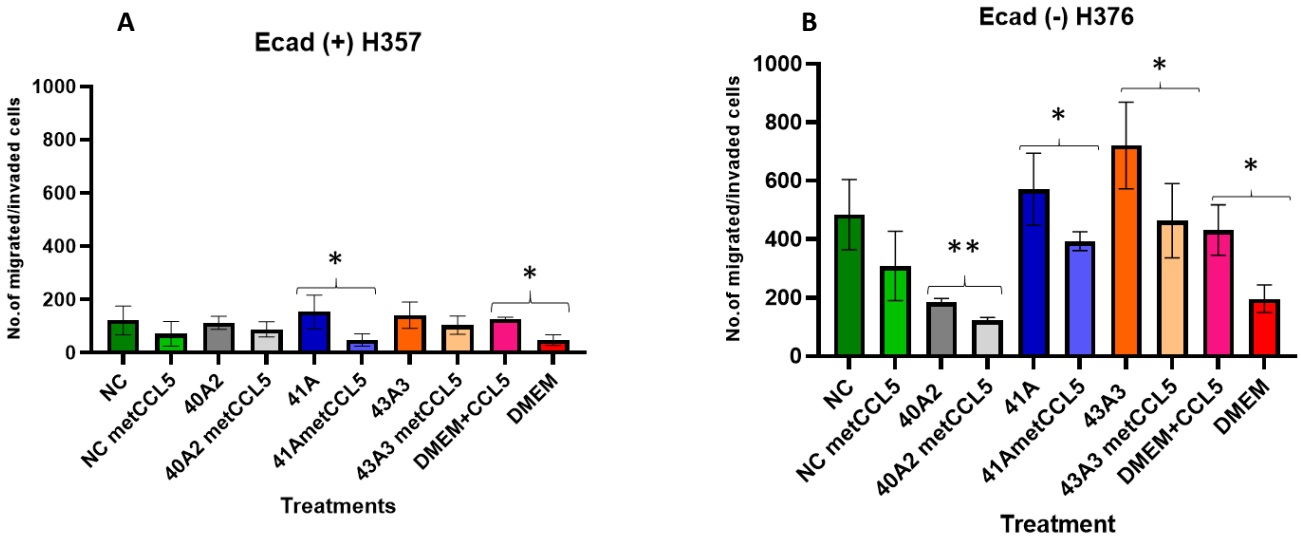

Figure 4.10. Trans-well cell migration and invasion inhibition. A CCL5/RANTES inhibitor, rhCCL5/metRANTES (metCCL5) was used at a concentration of 3 ng/ml. The cells were pre-treated with the inhibitor for thirty minutes and metCCL5 3 ng/ml was also added in the CM in the wells of the 24-wells plate. After 24-hours of incubation, a reduction in cell migration and invasion across the ECM gel/polycarbonate membrane of the trans-well insert was seen. The most statistically significant reduction in cell migration was seen when E-cadherin positive H357 cell contacted the CM obtained from clinical isolate 41A containing the inhibitor (A). On the other hand, there were statistically significant reductions in cell migration the E-cadherin negative H376 cells when the CM from isolates 40A2, 41A and 43A3 were used with rhCCL5/metRANTES pre-treated epithelial cells (B). The difference in cell migration between the positive and the negative controls were also statistically significant between the two cell lines (*indicates Mann-Whitney t-test p value <0.05, statistically significant, **indicates Mann-Whitney t-test p value <0.001, statistically highly significant. Error bars indicate standard deviations of three experimental replicates).

4.3.8 Trans-well migration and invasion using *F. nucleatum* subsp *nucleatum* and its Δ*fadA* and Δ*fap2* knockout mutants

To further investigate the involvement of FadA and Fap2 adhesins of *F. nucleatum* with E-cadherins and their role in stimulating the secretion of chemokines such as CCL5/RANTES, we used a different subspecies of *F. nucleatum*, namely, *F. nucleatum* subsp. *nucleatum.* For the trans-well migration assay, we employed three phenotypes, namely, the type strain of *F. nucleatum* subsp. *nucleatum*, knockout mutants of the type strain with *fadA* gene deletion and *fap2* gene deletion. The trans-well migration and invasion assay was carried out as described in the materials and methods section of this chapter.

After 24-hours of incubation at 37^{o}C to complete the trans-well migration, we found that both E-cadherin positive H357 and E-cadherin negative H376 cells had migrated across the ECM gel/polycarbonate membrane barrier of the inserts. However, the number of cells that had migrated varied with the OSCC cell type and the bacterial phenotype. Most cells that managed to cross the barrier were the E-cadherin negative H376 cells which has been established earlier in the previous chapter. We made direct comparisons of the cell migration between the *F. nucleatum* subsp. *nucleatum* type strain and the respective mutants. In the E-cadherin positive H357 cell line, the most statistically significant cell migration occurred in the CM with Δ*fap2* infection treatment with a mean of 209 cells migrating over 24-hours period. There was relatively less migration in the absence of FadA adhesin (Δ*fadA* mutant) and in the wild type strain with an approximate mean cell migration over 24-hours of 169 cells and 89 cells respectively (figure 4.11A and B, student t-test p value <0.05, statistically significant).

On the other hand, the type strain of *F. nucleatum* subsp. *nucleatum* and its Δ*fadA* and Δ*fap2* mutants induced higher E-cadherin negative cell migration across the barrier as observed previously (an average cell migration of 249 cells, 264 cells and 221 cells respectively).

The cell migration was inhibited with the treatment of a suitable CCL5/RANTES inhibitor. The assay with the inhibitor was carried out as described in the materials and methods section of this chapter. We used 3 ng/ml of rhCCL5/metRANTES to assist in inhibition. In case of both E-cadherin positive H357 and E-cadherin negative H376 cell line, the inhibition was statistically significant with the type strain (difference between the inhibitor treated

and untreated) and the Δ*fadA* mutant (difference between inhibitor treated and untreated) (student t-test p value <0.05, statistically significant). Although there was some inhibition in cell migration and invasion across the ECM gel/polycarbonate barrier when both cell lines were treated with CM obtained from the Δ*fap2* mutant of the type strain, the difference between the migration of inhibitor treated and untreated controls was not statistically significant as shown in figure 4.11C and D. A positive control of DMEM with 3 ng/ml rhCCL5 and a negative control consisting no treatment of DMEM was also used.

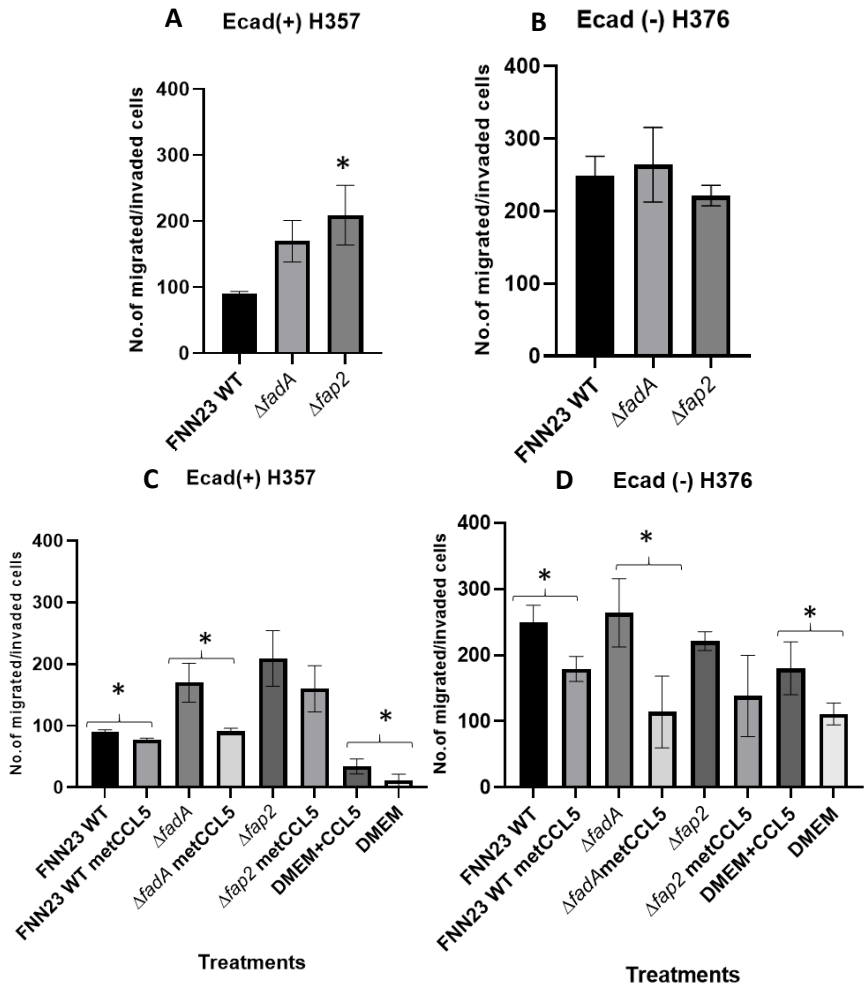

Figure 4.11. Trans-well migration and invasion using *F. nucleatum* subsp. *nucleatum* and its mutants ΔfadA and Δfap2. Direct comparisons of cell migration and invasion between the type strain and respective mutants of both cell lines showed that a statistically significant difference in cell migration existed when exposing the cells to CM obtained from the type strain and the Δ*fad2* mutant in presence of E-cadherin (top A and B, *indicates student t-test p value <0.05, statistically significant). When rhCCL5/metRANTES inhibitor was used at a concentration of 3 ng/ml, a significant inhibition of cell migration occurred between the inhibitor treated and untreated cells (bottom C and D, *indicates student t-test p value <0.05, statistically significant. Error bars indicate standard deviations of three experimental replicates).

4.4. Discussion

Cytokines and chemokines are generally secreted by immune cells as a protective response to physical, chemical or biological assaults on the human body. However, these specialised proteins can also be triggered to be secreted in such inappropriate situations and quantities that they earn the title of being proinflammatory. Proinflammatory cytokines and chemokines create an intra and intercellular environment that can become potentially lethal as in many cancerous conditions. In our work to explore the effects of these proteins on the E-cadherin positive and negative OSCC cell lines, we first carried out infections of both cell lines with *F. nucleatum* subsp. *polymorphum* strains. The infections were set up for 24-hours in a controlled environment of 37^{o}C and 5% CO_2. The supernatants of the infections were precious commodities as they potentally contained all the cytokines and chemokines of interest and we termed it “conditioned media”.

We first carried out a multiplex assay that works on the principle of identifying multiple analytes using beads that are precoated with specific cytokine/chemokine of interest. This method helped us identify and assimilate information about the generally secreted cytokines and chemokines. We used the type strain of *F. nucleatum* subsp. *polymorphum* ATCC10593/NCTC10562, clinical isolates 41A, 41B2 and 43A3 to infect both cell lines. As a positive control, we used *E. coli* DH-5α and we used DMEM cell culture media without any supplements or bacterial suspension as a negative control. The 24-hour infections stimulated the cells to secrete a plethora of cytokines and their chemotactic variants, but the overarching goal here was to identify what strain of *F. nucleatum* subsp. *polymorphum* elicited the most response from the OSCC cell lines. Both cell lines reacted positively to the bacterial infections and secreted various cytokines. The multiplex assay was capable of measuring 71 cytokines and chemokines in total, however, IL-6 and IL-8 were the most prominantly expressd cytokines when infected with clinical isolate 41(A and B). These two cytokines have been reported to be the most secreted in OSCC and other oral cancers in the past (Hwang et al., 2012). We could also show that the cancer cells themselves produced these cytokines without any stimulation by using plain DMEM cell culture media (E-cadherin positive H357 cell line- IL-6 216 pg/ml and IL-8 593 pg/ml; E-cadherin negative H376 cell line- IL-6 1699 pg/ml and IL-8 3146 pg/ml). Interestingly, IL-8 was excessively secreted especially when infecting the E-cadherin negative H376 cells. Both the clinical

isolate 41 and the positive control *E. coli* strain DH-5α were the isolates to elicit the highest cellular response of this cell line to secrete IL-8. Although we showed the correlation between FadA and Fap2 adhesins with adhesion and invasion properties of the *F. nucleatum* strains, it is highly likely these responses maybe associated with Gram negative bacteria, raher than adhesin proteins specific to *Fusobacteria*.

There were a few chemokines that were predominantly secreted when infected with the *F. nucleatum* strains. However, chemokine CCL5/RANTES, MCP-1 and VEGF-A were most intriguing as they have been previosuly shown to be involved in cancer cell migration, invasion and metastasis (Lapteva and Huang, 2010, Yoshimura, 2018). In our assays, we found that these chemokines were secreted in higher quantities in the E-cadherin negative cell line.

Here, we looked specifically at the chemokine CCL5/RANTES and how *F. nucleatum* infection affected the cellular response to its secretion to investigate its effects on mobilising cancerous cells as reported by several authors (Chuang et al., 2009, Aldinucci and Colombatti, 2014). The multiplex assay identified this chemokine in both cell lines and yet again, indicated clinical isolate 41(A and B) to stimulate the highest quantities of the protein, however, this time it was in the E-cadherin positive H357 cell line. Therefore, to make our targets more specific, we performed ELISA to quantify CCL5/RANTES and MMP-9 levels to assist in assessing cell migration and invasion assays. Based on our previous results from the adhesin copy numbers and the consequent adhesion/invasion reslutls, we chose to perform the ELISA using the CM obtained from infecting the cell lines with the *F. nucleatum* subsp. *polymorphum* isolate having the least adhesin copy numbers and adhesion property (40A2) and the isolate with the highest adhesin copy numers and adhesion property (43A3), along with type strain ATCC10953/NCTC10562 (comparitor control) and DMEM (negative control). The levels of CCL5/RANTES and MMP-9 were high in CM collected from infecting E-cadherin negative H376 cells with clinical isolate 43A3. The levels of both proteins were significantly lower in both cell lines when the CM collected from cell line infection with clinical isolate 40A2 were used. Perhaps, clinical isolates such as 41A, 41B and 43A3 that have high copy numbers of Fap2 (3,4 and 5 respectively) seem to be the ones to interact the most with the E-cadherin negative cells in a rather robust manner.

Research work by Chuang et al and others have demonstrated the effect of CCL5/RANTES on OSCC cells, which promote metastasis by enhancing cell motility, migration and invasion of underlying tissues (Aldinucci and Colombatti, 2014, Chuang et al., 2009). These migration effects are triggered by the contact between CCL5 and its receptor CCR5 on the cancer cell. We tested this hypothesis by performing migration assays involving a simple scratch wound and a second method involving a trans-well insert double lined by ECM gel and a polycarbonate membrane. The principle behind both the assays was the involvement of CCL5/RANTES and MMP-9 (from the CM collecetd from infecting both E-cadherin positive H357 and E-cadherin negative H376 cell lines by *F. nucleatum* subsp. *polymorphum* strains) that would ultimately result in the motility of cells.

In the scratch wound assay, the wound closure that occurred after treating the cell lines with CM obtained from pre-infection of the cell lines with *F. nucleatum* subsp. *polymorphum* strains (type strain ATCC10593/NCTC10562, clinical isolate 40A2, 41A, 41B2 and 43A3) for 24-hours corresponded to the cell migration. Cell migration indeed took place in both cell lines and we found that the clinical isolate 43A3 CM brought about the highest cell migration in both cell lines, with E-cadherin negative H376 cell line migrating the most. The cells migrated approximatey 450 µm in 24-hours in the E-cadherin negative H376 cells as compared to approximately 320 µm in the E-cadherin positive H357 cells with CM from clinical isolate 43A3. Notably, the least cell migration occurred when both cell lines were treated with CM from clincal isolate 40A2. The average migration in 24-hours with this *F. nucleatum* strain was approximately 143.3 µm in E-cadherin positive H357 cells and approximately 136.6 µm in E-cadherin negative H376 cells. The difference in both CCL5 and MMP-9 levels in these strains of *F. nucleatum* subsp. *polymorphum* and their direct influence on cell migration could be appreciated in this assay, also, the requirement of E-cadherins for cancerous cells motility and migration seems irrelevant.

Further to investigate the invasiveness of the OSCC cells enhanced by the *F. nucleatum* subsp. *polymorphum* strains, we carried out the trans-well migration assay. To simulate the epithelial basement membrane and the extracellular matrix, the trans-well inserts were coated with an ECM gel and a polycarbonate membrane. This double barrier would truly test the invasive potential of the cell lines and the influence of CCL5 and MMP-9 in the CM obtained from pre-infection of the cell lines with *F. nucleatum* subsp. *polymorphum* strains

(type strain ATCC10593/NCTC10562, clinical isolate 40A2, 41A and 43A3). The assay was carried out for 24-hours to evaluate the effects of the chemoattractant properties of CCL5 and MMP-9. The difference in the invasive nature of the two cell lines was rather distinct and stark. The E-cadherin negative H376 cells were clearly more invasive, especially when infected with *F. nucleatum*, cementing the literature on cancers where the loss of E-cadherins have been associated with aggressiveness, advanced stage and poor prognosis of cancers (Younis et al., 2007). All *F. nucleatum* subsp*. polymorphum* strains brought about increased levels of migration and invasion across the ECMgel/polycarbonate barrier in the E-cadherin negative H376 cells, but the CM obtained from clinical isolate 43A3 infection was the most influential in instigating the migration and invasion. We also used a CCL5 specific inhibitor rhCCL5/metRANTES to further solidify our hypothesis of the involvement CCL5 in OSCC migration and invasion. The employment of rhCCL5/metRANTES 3 ng/ml brought about distinct inhibition of cell migration and invasion across the ECM gel/polycarbonate barrier in both cell lines. The loss of E-cadherins in cancers is quite significant in tumour pathogenesis and metastasis, as described by several authors. Several pathways have been described of the involvement of loss of E-cadherins and metastasis, such as induction of EMT via the modulation of CCL5 secretion promoting metastasis (Long et al., 2015, Onder et al., 2008).

The involvement of *F. nucleatum* adhesins as the main virulence factor for the survival and infection potential of this bacterium has been discussed in vast detail in the literature. Therefore, as a final approach to test the potential involvement of *F. nucleatum* adhesins in chemokine secretion such as CCL5/RANTES in this section of the research, we employed *F. nucleatum* subsp. *nucleatum* and its *ΔfadA* and *Δfap2* mutants. The type strain of *F. nucleatum* subsp. *nucleatum, Fnn* 23726, had its FadA and Fap2 adhesins intact whilst *ΔfadA* mutant had a gene deletion for FadA adhesins and *Δfap2* mutant had a gene deletion for Fap2. The type strain of *F. nucleatum* subsp. *nucleatum Fnn23* and its mutants *ΔfadA* and *Δfap2* were used in the trans-well migration and invasion assay. The most cell migration and invasion occurred in the E-cadherin negative H376 cell line when the CM obtained from *ΔfadA* mutant was used. This is agreeable with the loss of FadA adhesin and the presence of Fap2 adhesin in this mutant which is essential for the interaction with the E-cadherin negative H376 cell line. Similarly, when the CM from *Δfap2* infection was used,

the migration of cells in the E-cadherin negative H376 cells was relatively lower. When the assay was performed on the E-cadherin positve H357 cells , most migration and invasion occurred when the CM from *Δfap2* mutant was used (this mutant has FadA gene intact). However, the migration of cells was still considerably higher when the CM from *ΔfadA* was used compared to the type strain that had all the adhesins intact, which was contradictory to our hypothesis. The use of the rhCCL5/metRANTES inhibitor however, reduced the cell migration and invasion in all circumstances. As described earlier, the use of CCL5 inhibitor is not indicative of the involvement of FadA or Fap2 adhesins, but rather the involvement of CCL5 in cell migration and invasion. However, the cell migration that has been observed here in the absence of FadA adhesin in the E-cadherin positive H357 cell line is perhaps indicative of the involvement of E-cadherin itself and the involvement of perhaps other adhesins such as cmpA, RadD, Aid1 etc in the absence of FadA, which brings about strong responses. This however requires futher investigation to better understand the phenomenon.

In the next chapter, we investigate the influence of chemokine VEGF-A on neo-angeogenesis that is essential in OSCC proliferation, invasion and metastasis.

Chapter 5

Cellular responses to *F. nucleatum* subsp*. polymorphum* infection – Angiogenesis in OSCC

5.1 Introduction

The growth and development of cancers, as discussed in detail in the general introduction chapter, is associated with various factors. However, one very crucial intrinsic factor necessary for its successful survival and metastasis is the availability of nutrition. Hence, developing cancers do so by forming intricate and complex circulatory systems within, that can supply them with all the necessary nutrition, and additionally, remove metabolic wastes. These blood vessels are however abnormal, and studies have shown that they are malformed and highly permeable (Viallard and Larrivée, 2017).

Vascular endothelial growth factor A (VEGF-A) is an important heparin binding growth factor seen upregulated in cancer conditions. They are essential in forming new blood vessels in the rapidly developing tumour. Several types/isoforms of VEGF are known to exist including *VEGF121*, *VEGF165*, *VEGF183* and *VEGF189* that differ from one-another by their heparin binding ability and the ability to bind to the VEGFR1 and VEGFR2 receptors (Patel et al., 2015). The regulation of VEGF-A expression in cancers is controlled by multiple factors such as deleted or mutant tumour suppressor genes, activated oncogenes, hormonal modulators, growth factors, pro-inflammatory cytokines and chemokines such as MCP-1/CCL2, WNT1-inducible signalling pathway protein-1 (WISP-1/CCN-4), and hypoxia (Claffey and Robinson, 1996).

Hypoxia has been implicated as a master trigger factor in regulating VEGF-A expression. Under severe hypoxic conditions, hypoxia-inducible factor-1α (HIF-1α) is activated in cancer cells and HIF-1β is activated in normal cells. The activated HIF-1α/β binds to a hypoxia response element (HRE) upstream of the *VEGFA* gene and activates gene transcription for VEGF-A synthesis as shown in figure 5.1. The expression of HIF-1α/β is however controlled by the activation of focal adhesion kinase (FAK) and phosphoinositide-3 kinase (PI_3) in cancer cells (Kallergi et al., 2009). The expression of VEGF receptor VEGFR2 is upregulated in cancers and plays an important role in VEGF-A expression for angiogenesis (Claesson-Welsh and Welsh, 2013). The activation of the VEGFR2 receptor (also known as kinase insert domain receptor or KDR) takes place when any of the several activating factors bind appropriately to it. The binding of several growth factors, including VEGF, for example, will initiate the tyrosine kinase phosphorylation of the VEGFR2/KDR receptor. Phosphorylated VEGFR2/KDR triggers the synthesis of HIF-1α, essential for the

transcription of VEGF-A via binding to HRE in the nucleus (Spirina et al., 2017) as shown in the figure 5.1.

The involvement of chemokine MCP-1/CCL2 has also been proposed in OSCC by increased expression of VEGF-A and the resultant angiogenesis. Lien et al (2020) described an integrin linked kinase (ILK) and mitogen activated protein kinase (MEK 1/2) signalling pathway involving the chemokine MCP-1/CCL2. The MCP-1/CCL2 receptor CCR2 highly expressed on OSCC cells is activated upon the binding of the chemokine. This binding to the receptor activates ILK, which in-turn phosphorylates MEK1/2. The phosphorylated MEK1/2 directly supresses miRNA-29c, involved with increased suppression of VEGF-A expression. Reduced miR-29c enables the transcription of VEGF-A in sufficient quantities to enable angiogenesis in tumour tissues (Lien et al., 2020). The proposed mechanisms involved in VEGF-A expression and angiogenesis is summarised in figure 5.1.

Resveratrol (3,5,4-trihydroxystilbene) is a naturally occurring stilbenoid belonging to phytoalexin category in plants and many other human foods and has been suggested to have some inhibitory properties in human cancers, perhaps by having a direct effect on the angiogenesis in tumour tissues (Lin et al., 2003). One of the major sources of resveratrol is grapes, blueberries, raspberries, and mulberries. The high content of resveratrol in red wine has been suggested beneficial for human health (Hu et al., 2019). Several intercellular mechanisms have been proposed by authors, some of which may include scavenging of free radicals, inhibition of cell proliferation, suppression of cyclooxygenase (COX) activity, induction of apoptosis and inhibition of enzymes namely ribonucleotide reductase, DNA polymerases and protein kinase C (PKC) (Neves et al., 2012). The proposed mechanism of resveratrol in reducing angiogenesis in tumours involving VEGFR2/KDR receptor is depicted diagrammatically in figure 5.2.

In this chapter, we investigate the effect of *F. nucleatum* subsp. *polymorphum* infection of OSCC cells lines on angiogenesis and the inhibition of angiogenesis using a suitable inhibitor.

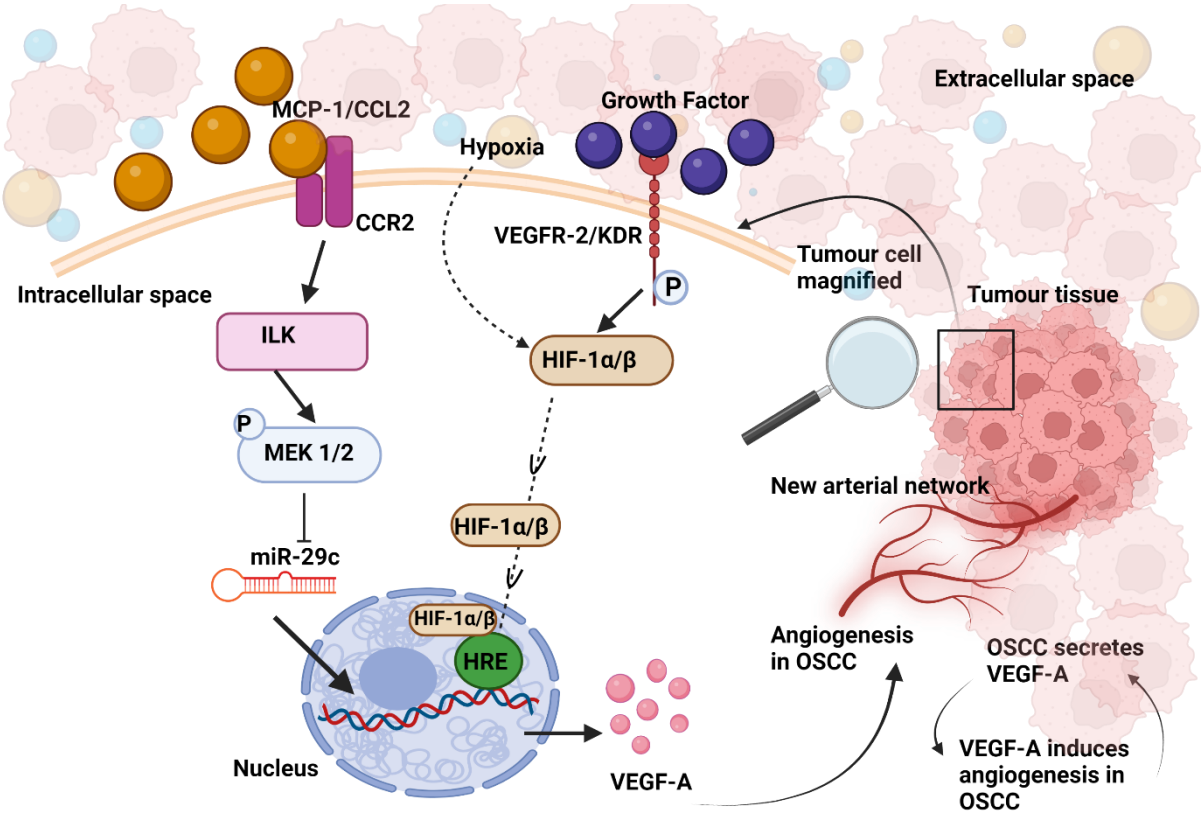

Figure 5.1. Proposed pathways involved in angiogenesis in OSCC. Cellular hypoxia induces the activation of HIF-1α in cancer cells, activating HRE in the nucleus to overexpress VEGF-A. The binding of VEGF to its receptor VEGFR2/KDR also activates the synthesis of HIF-1α/β that ultimately binds to HRE intranuclearly, triggering overexpression of VEGF-A for angiogenesis. Involvement of chemokines such as MCP-1/CCL2 also increase VEGF-A expression in OSCC by binding to CCR2 receptors and activating ILK/MEK1/2 pathway (Claesson-Welsh and Welsh, 2013, Kallergi et al., 2009, Lien et al., 2020).

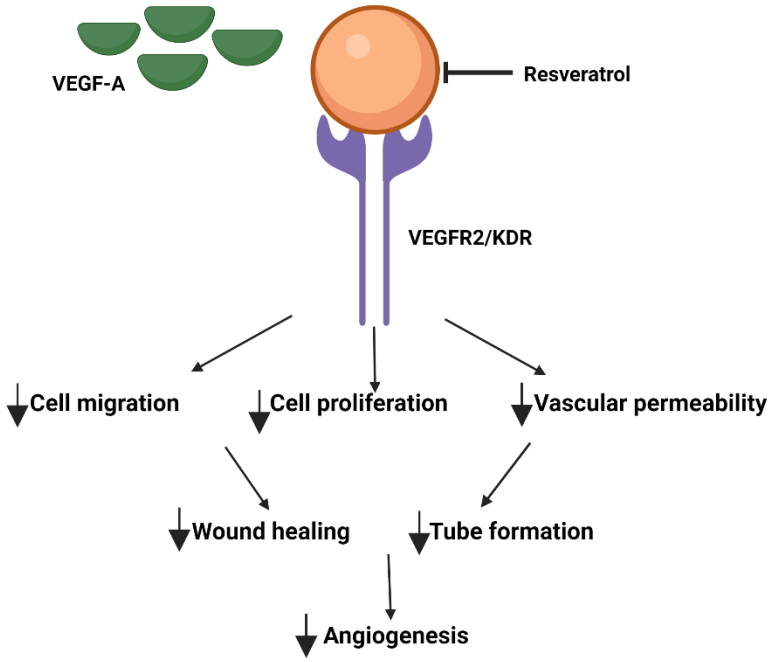

Figure 5.2. Consequences of resveratrol treatment on endothelial cells. Resveratrol is a naturally occurring substance in plants. The mechanisms involved in the anti-carcinogenic properties of resveratrol are plenty, however, one of the mechanisms involved is the competitive inhibition of the VEGFR2/KDR receptor expressed on endothelial cells. The overall inhibition of binding of VEGF-A on VEGFR2/KDR results in reduced cell migration, proliferation and reduced vascular permeability. These cellular activities are essential for new blood vessels formation, which is ultimately affected. The insufficient oxygen and nutrient supply to the growing tumour tissue results in tumour growth arrest.

5.2 Materials and methods

5.2.1 Quantifying VEGF-A chemokine using direct ELISA sandwich Assay

Human VEGF-A ELISA kit was purchased from Sigma-Aldrich, USA.

All reagents, working standards and samples for the assay were prepared as directed by the manufacturer's direction. 20x Wash buffer was prepared by diluting the wash buffer concentrate with deionized distilled water. Assay diluent buffer B was prepared by diluting the concentrate 5-fold with deionized water. Human MMP9 standard concentrate was prepared by reconstituting the powder in 5ml of distilled water. The stock solution (20ng/ml or 20000pg/ml) was then serially diluted in assay diluent buffer B to get the following concentrations of the standard stock solution: 20 ng/ml, 10 ng/ml, 5 ng/ml, 2.5 ng/ml, 1.25 ng/ml, 0.625 ng/ml and 0.313 ng/ml. The calibrator diluent RD5-10 was used as zero standard.

The detection antibody and HRP-streptavidin solution for use in the assay were prepared as per the manufacturer's directions. All the buffers, reagents and samples were brought to room temperature before starting the assay. 100 µl of samples and standard solution were added in appropriate wells. The wells were covered and incubated for 2.5 hours at room temperature. The solutions from the wells were then discarded and washed 4-5 times using the wash buffer that was previously prepared. The washing method consisted of pipetting 300 µl of the wash buffer into the wells and quickly inverting the 96-wells plate to expel the washed solution. This method of washing was repeated 4-5 times. 100 µl of 1x detection antibody was added into each well and incubated for 1 hour with gently shaking at room temperature. The plate was sealed with a plastic cover sheet.

After the end of the incubation period, the solution was discarded and washed with wash buffer as described earlier. 100 µl streptavidin solution that was prepared earlier was added to each well and incubated for an additional 45 minutes with gentle shaking. The solution was discarded from the wells and the wash procedure was repeated using the was buffer. 100 µl of TMB one-step substrate reagent was added to all wells, covered in aluminium foil and incubated for 30-minutes with gentle shaking. 50 µl stop solution was added to all wells at the end of the incubation period and the absorbance was read at 450nm immediately.

5.2.2 HUVEC tube formation assay (angiogenesis)

For the tube formation assay, HUVEC cells were cultured as described in the general materials and methods chapter. CM was collected from respective *F. nucleatum* strains infections of E-cadherin positive and negative cell lines as described in the general materials and methods chapter and stored at -20^{o}C. HUVEC cell culture media was used to prepare bacterial suspensions at MOI 10 for infections of E-cadherin positive and negative cells and subsequent CM collection.

All consumables used directly for the assay such a 96-wells plate and 200 µl pipette tips were frozen for 10-15 minutes in -20^{o}C freezer or chilled overnight in a 4^{o}C refrigerator prior to loading the plate so that Matrigel does not prematurely solidify. The plate and the pipette tips were placed on ice throughout the protocol completion. Matrigel® gel matrix (Corning, USA) was defrosted just before the commencement of the assay and placed on ice immediately and throughout the duration of the assay.

50 µl of Matrigel® was pipetted into each of the experimental wells of the 96-wells plate and incubated at 37^{o}C and 5% CO_2 for thirty minutes to solidify the gel matrix. Once the gel had set, 80,000 HUVEC cells were added in all the wells (80 µl of cell suspension containing 1x10^{6}cells/ml) along with 120 µl of the bacterial treated CM to make up a total of 200 µl solution in each well. For the positive control, we added 50 ng/ml rhVEGF-A (10 µl) into the control well consisting of 80 µl cell suspension and 110 µl HUVEC cell culture media. The experimental set up was now incubated at 37^{o}C and 5% CO_2 for twelve hours for the tube formation to take place.

Quantification of the tube formation was done manually by counting the number of capillary-like branches at 20x magnification of a light microscope. Capillary counts from three fields per well were considered and an average tube formation of the three fields were finally considered.

5.2.3 Inhibition of tube formation using Resveratrol

For the tube formation inhibition assay, HUVEC cells were cultured as described in the general materials and methods chapter. CM was collected from respective *F. nucleatum* strains infections of E-cadherin positive and negative cell lines as described in the general materials and methods chapter and stored at -20^{o}C. HUVEC cell culture media was used to prepare bacterial suspensions at MOI 10 for infections of E-cadherin positive and negative cells and subsequent CM collection.

All consumables used directly for the assay such a 96-wells plate and 200 µl pipette tips were frozen for 10-15 minutes in a -20^{o}C freezer or chilled overnight in a 4^{o}C refrigerator prior to loading the plate so that Matrigel does not prematurely solidify. The plate and the pipette tips were placed on ice throughout the protocol completion. Matrigel® gel matrix (Corning, USA) was defrosted just before the commencement of the assay and placed on ice immediately and throughout the duration of the assay.

50 µl of Matrigel® was pipetted into each of the experimental wells of the 96-wells plate and incubated at 37^{o}C and 5% CO_2 for thirty minutes to solidify the gel matrix. Resveratrol was purchased from Sigma Aldrich, USA and stock solutions of 20mg/ml (88 mM) for the experiment were freshly prepared on the day of use by adding 250 µl DMSO to 5 mg Resveratrol. HUVEC cells were pre-treated for thirty minutes with 1 µM and 1.5 µM concentrations of Resveratrol for the experimental use.

Once the Matrigel® matrix gel had set, 80,000 HUVEC cells (Resveratrol pre-treated) were added in all the wells (80 µl of cell suspension containing 1x10^{6}cells/ml) along with 120 µl of the bacterial treated CM to make up a total of 200 µl solution in each well. For the positive control, we added 50 ng/ml rhVEGF-A (10 µl) into the control well consisting of 80 µl cell suspension and 110 µl HUVEC cell culture media. The experimental set up was now incubated at 37^{o}C and 5% CO_2 for twelve hours for the tube formation to take place.

Quantification of the tube formation was done manually by counting the number of capillary-like branches at 20x magnification of a light microscope. Capillary counts from three fields per well were considered and an average tube formation of the three fields were finally considered.

5.3 Results

5.3.1 Quantifying MCP-1/CCL2 chemokine secretion by direct ELISA method

CCL2, formerly known as Monocyte chemoattractant protein-1 (MCP-1) was detected in sufficient quantities when a multiplex assay was performed that was discussed in the previous chapter. To further target MCP-1/CCL2 specifically, we performed an ELISA with pre-coated wells with a primary antibody for MCP-1/CCL2. CM from a 24-hour infection of both E-cadherin positive H357 cells and E-cadherin negative H376 cells with *F. nucleatum* subsp. *polymorphum* strains were used for the assay. As a positive control, we used 50 ng/ml of rhCCL2 and for the negative control, we used plain DMEM cell culture media with no supplements or bacterial suspension.

Our results showed that both cell lines secreted this chemokine. The clinical isolate 43A3 stimulated the most secretion of MCP-1/CCL2 from the E-cadherin positive H357 cells of approximately 875 pg/ml (figure 5.3A). Both clinical isolate 40A2 and the type strain ATCC10953/NCTC062 stimulated the secretion of approximately 660 pg/ml each. As expected, the cells secreted a base line amount of MCP-1/CCL2 when treated with DMEM of approximately 153 pg/ml. When we performed a Kruskal-Wallis statistical test of the samples to investigate the statistical significance between each sample, setting DMEM as the normal comparator, we found there wasn't any statistically significant difference between the samples and the negative control DMEM (figure 5.3A, p values > 0.05, statistically not significant).

When the CM obtained from infecting the E-cadherin negative H376 cell lines with the type strain and clinical isolates were used in the direct ELISA method for quantifying MCP-1/CCL2, we found that the clinical isolate 43A3 elicited the most chemokine secretion amongst the other isolates. The clinical isolate 43A3 induced the secretion of approximately 930 pg/ml of MCP-1/CCL2. Both clinical isolate 40A2 and type strain ATCC10953/NCTC10562 elicited the secretion of approximately 550 pg/ml each. Plain DMEM used as the negative control stimulated about 200 pg/ml of MCP-1/CCL2 secretion. The difference in MCP-1/CCL2 secretion between clinical isolate 43A3 and the negative control DMEM was statistically significant (figure 5.3B, Kruskal-Wallis test, p value <0.05, statistically significant). The MCP-1/CCL2 secretion between the two cell lines is summarised in figure 5.3C.

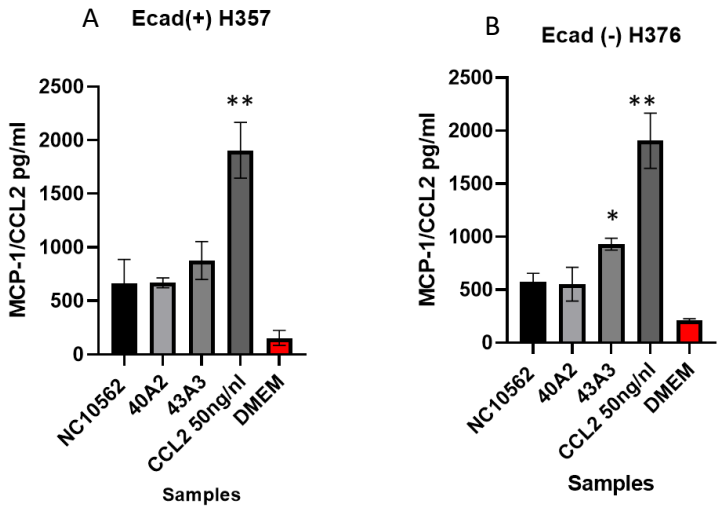

C

Ecad(+)H357	NC10562	40A2	43A3	Positive control
Mean MCP-1/CCL2	660.3	668.15	875.5	1905
Significantly different to DMEM neg control	No	No	No	Yes
P-value	0.247	0.321	0.06	0.008

Ecad(-)H376	NC10562	40A2	43A3	Positive control
Mean MCP-1/CCL2	578	551	930	1905
Significantly different to DMEM neg control	No	No	Yes	Yes
P-value	0.327	0.321	0.04	0.008

Figure 5.3. MCP-1/CCL2 quantification by direct ELISA. Clinical isolates 40A2 and 43A3, and type strain ATCC10953/NCTC10562 (as a comparator) were used for the ELISA. A negative control of DMEM and a positive control of 50 ng/ml rhCCL5 were also used. Clinical isolate 43A3 elicited the most response for MCP-1/CCL2 secretion in both E-cadherin positive H357 and E-cadherin negative H376 cell lines (top A and B). Kruskal-Wallis multiple comparisons test showed significant differences between the isolate 43A3 and the negative control DMEM (below, C).

5.3.2 Quantifying VEGF-A chemokine secretion by direct ELISA method

The chemokine VEGF-A secretion by both E-cadherin positive H357 and negative H376 cell lines was quantified by direct sandwich ELISA method. *F. nucleatum* subsp. *polymorphum* type strain ATCC10953/NCTC10562, clinical isolates 40A2 and 43A3 were used to infect the OSCC cells and stimulate VEGF-A secretion. As a control, we used plain HUVEC media without any additional supplements or bacterial suspension. The treatment of the cells was carried out for 24-hours as described in the materials and methods section of this chapter.

On quantifying the treatment supernatants of the cell lines, we found that all the strains of *F. nucleatum* subsp. *polymorphum* stimulated the cells to secrete VEGF-A. However, there was a baseline secretion of VEGF-A in both E-cadherin positive and negative cell line (approximately 166 pg/ml in E-cadherin positive H357 and 1525 pg/ml in E-cadherin negative H376 cell line) when we used the HUVEC cell culture media as a control as well. Therefore, we compared this baseline VEGF-A level to the levels of VEGF-A secreted by the bacterial stimulation. In the E-cadherin positive H357 cells treatment, the clinical isolate 43A3 secreted the most levels of VEGF-A (approximately 461 pg/ml) compared to the baseline secretion by this cell line (Kruskal-Wallis test, p-value < 0.05, statistically significant) as indicated in the figure 5.4A . The type strain and the clinical isolate 40A2 also stimulated the cells for VEGF-A secretion (approximately 424 pg/ml and 396 pg/ml). The E-cadherin negative H376 cells also secreted considerable amount of VEGF-A when infected with *F. nucleatum* strains. The clinical isolate 43A3 stimulated the most statistically significant amount of VEGF-A (approximately 2142 pg/ml) as compared to the baseline secretion by the cells when treated with plain HUVEC media (Kruskal-Wallis test, p-value < 0.05, statistically significant). Although the type strain and clinical isolate 40A2 also stimulated considerable amounts of VEGF-A secretion by the cell line (2020 pg/ml and 1738 pg/ml respectively), they weren't significant when compared to the baseline secretion by the cell line (figure 5.4B).

We also made a direct comparison of the chemokine secretion between the two cell lines. All treatments with E-cadherin positive H357 cells were statistically significant and different from the treatments with E-cadherin negative H376 cell line (Student t-test p-value <0.05, statistically significant, p-value <0.001, statistically very significant) as shown in the figure 5.4C.

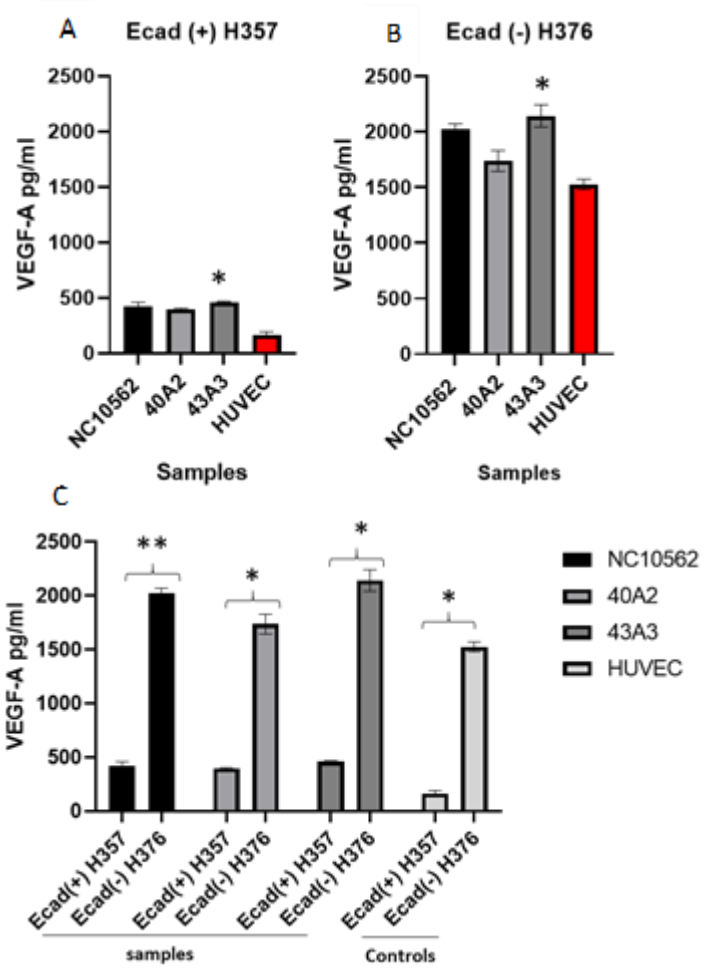

Figure 5.4. VEGF-A secretion by E-cadherin positive and negative cell lines. Comparison of VEGF-A secretion by bacterial treatments to untreated HUVEC control in both cell lines showed a statistically significant secretion in clinical isolate 43A3 treatment (A and B, *indicates Kruskal-Wallis test p-value <0.05, and Mann-Whitney one-tailed test p-value <0.05, statistically significant). Direct comparisons of the two cell lines and the respective VEGF-A secretion showed E-cadherin negative phenotype stimulated a higher level of VEGF-A secretion (C , *indicates student t-test p-value <0.05, statistically significant and **indicates student t-test p-value <0.001, statistically very significant. Error bars indicate standard deviations of three experimental replicates).

5.3.3 Investigating the effect of VEGF-A chemokine on OSCC cells- tube formation assay

Tube formation assay to investigate the effect of VEGF-A on HUVEC cell line was performed as described in the materials and methods section of this chapter. We used CM from infecting E-cadherin positive H357 and E-cadherin negative H376 cell lines for 24-hours with *F. nucleatum* subsp*. polymorphum* type strain ATCC10953/NCTC10562, clinical isolate 40A2 and 43A3 for carrying out the assay. As controls, we used HUVEC cell culture media containing 50 ng/ml of rhVEGF-A as a positive control and CM consisting of plain HUVEC media as negative control. The tube formation assay was performed for 12-hour period.

The tubes formed from the respective CM treatments and the positive control was compared to the negative control treatment. There were observable differences between the number of capillary-like tubes formed between the samples from the same cell line and between the two cell lines. When employing the CM from the E-cadherin positive H357 cell line treatment on HUVEC cells, we found that the highest number of tubes were formed when the CM from clinical isolate 43A3 was used in the assay. There were approximately 27.3 tubes formed with this treatment compared to the HUVEC media (negative control, approximately 10.3 tubes), the difference between which was statistically significant (Kruskal-Wallis test, p-value <0.05, statistically significant) as shown in the figure 5.5A. Treatments with CM obtained from the type strain and clinical isolate 40A2 infection of the E-cadherin positive cells formed about 19 tubes and 16 tubes respectively.

Similar comparisons were made with the treatments of the HUVEC cell line with CM obtained from 24-hour bacterial infection of the E-cadherin negative H376 cell line. We found that significant capillaries like tubes were formed with CM treatments obtained from type strain ATCC10953/NCTC10562 and clinical isolate 43A3 compared to the negative control. There were approximately 31 tubes formed with the CM from type strain and 36 tubes formed from CM from clinical isolate 43A3 as compared to 20 tube formed from the negative control treatment. These differences between the type strain and clinical isolate 43A3 from the negative control were statistically significant as shown in the figure 5.5A (Kruskal-Wallis test, p-value <0.05, statistically significant).

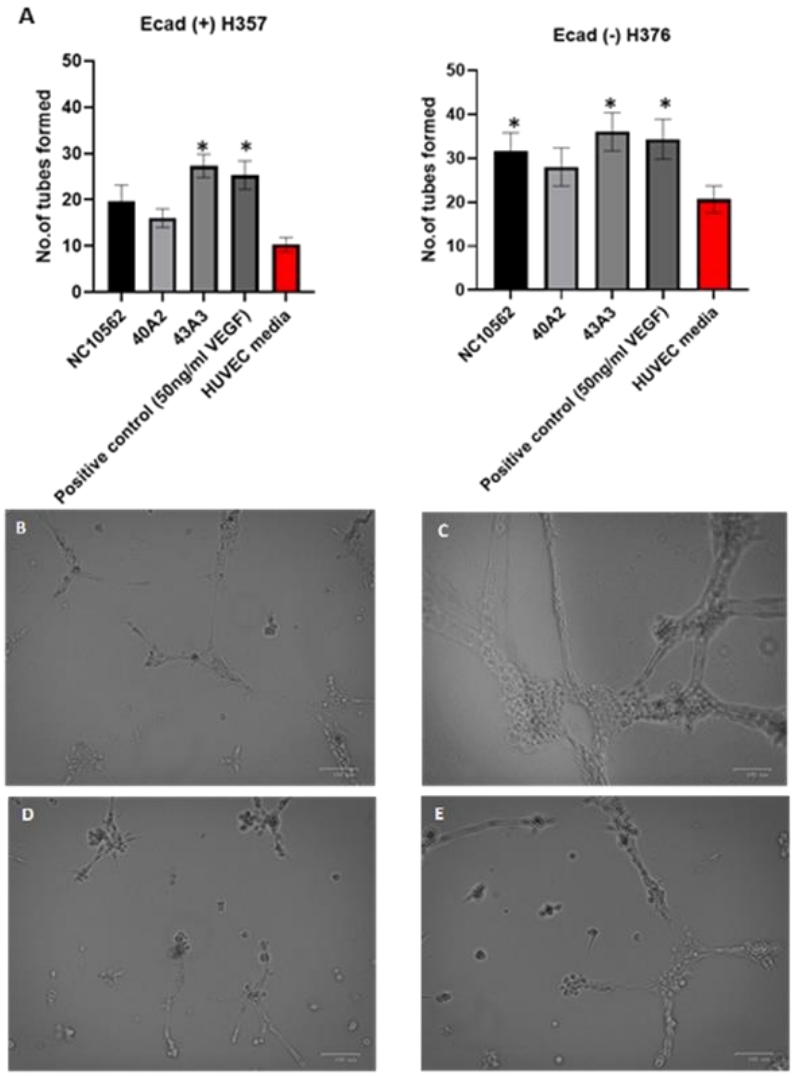

Figure 5.5. Tube formation assay. HUVEC cells were used to assess tube formation using CM obtained from E-cadherin positive and negative cell lines treatments. *F. nucleatum* subsp. *polymorphum* type strain ATCC10953/NCTC10562, clinical isolate 40A2 and 43A3 were used for the stimulation of the tube formation. Top, Significant tubes were formed when the clinical isolate 43A3 E-cadherin positive CM was used compared to the negative control and significantly high number of tubes were formed when the type strain and clinical isolate 43A3 E-cadherin negative CM were used compared to the negative control (A, *indicates Kruskal-Wallis test p-value <0.05, statistically significant). Bottom, Difference between the tube formation after 12-hours incubation at 37ºC and 5% CO_2. Representative pictures of HUVEC cell treatments with CM obtained from negative control and clinical isolate 43A3 of E-cadherin negative H376 cell line (B and C respectively), and HUVEC treatments with negative control and clinical isolate 43A3 of E-cadherin positive H357 cell line (D and E respectively). The white lines represent scale bar=100 µm

5.3.4 Tube formation inhibition assay

To evaluate the effect of a suitable inhibitor on the tube formation ability of HUVEC cells, we used resveratrol at a concentration of 1 µM and 1.5 µM. We used CM obtained from prior 24-hour infections of both E-cadherin positive and negative cell lines with *F. nucleatum* subsp. *polymorphum* type strain ATCC10953/NCTC10562, clinical isolate 40A2 and 43A3. As controls, we used 50 ng/ml rhVEGF-A as a positive control and CM from plain HUVEC cell culture media of the E-cadherin positive and negative cell lines as a normal comparator. The detailed description of the inhibition assay procedure is described in the materials and methods section of this chapter.

Resveratrol 1 µM and 1.5 µM was used concomitantly with their respective untreated controls. The inhibitor treatment was carried out for 12-hours, after which we found that there was a reduction in HUVEC tube formation in both cases of E-cadherin phenotype CM. The use of 1 µM resveratrol reduced the tube formation, albeit the use of 1.5 µM resveratrol significantly reduced the number of HUVEC tubes formed in all cases, including *F. nucleatum* subsp. *polymorphum* infections and the plain HUVEC comparator when compared to their respective inhibitor untreated controls (Kruskal-Wallis test p-value <0.05, statistically significant) as shown in the figure 5.6A and B.

The treatment of HUVEC cell lines with the CM obtained from infections of E-cadherin negative H376 cell line with *F. nucleatum* strains produced the most tube formation with an average of 37 tubes at this instance, and the use of resveratrol at 1.5 µM reduced this number to 17 tubes, a total reduction of 55%. On the other hand, the use of 1 µM resveratrol produced an overall reduction of 30% of tube formation (26 tubes). A similar trend of halving the number of tubes formed with the use of resveratrol 1.5 µM as opposed to resveratrol 1 µM was observed with the other E-cadherin negative H376 CM *F. nucleatum* strains treatments, including the plain HUVEC comparator treatment as well as shown in the figure 5.6B.

The overall HUVEC tube formation was relatively lower when CM from E-cadherin positive H357 cells was used. The highest number of tubes were formed when CM from clinical isolate 43A3 was used in this assay (average of 27 tubes) and the tube formation dropped to 17 tubes and 15 tubes with the use of 1 µM and 1.5 µM resveratrol respectively (38% and 45% reduction in tube formation respectively). Treatments with CM obtained from

type strain and clinical isolate 40A2 showed a somewhat similar response in tube formation and inhibition when resveratrol was used (type strain had a total average of 21 tubes formed, and the use of 1 µM resveratrol formed 18 tubes, resulting in a 15% reduction and 1.5 µM resveratrol formed 13 tubes, resulting in a 39% reduction ; clinical isolate 40A2 had a total average of 19 tubes formed, and the use of 1 µM resveratrol formed 18 tubes, resulting in a 6% reduction and 1.5 µM resveratrol formed 11 tubes, resulting in a 43% reduction) as shown in the figure 5.6A .

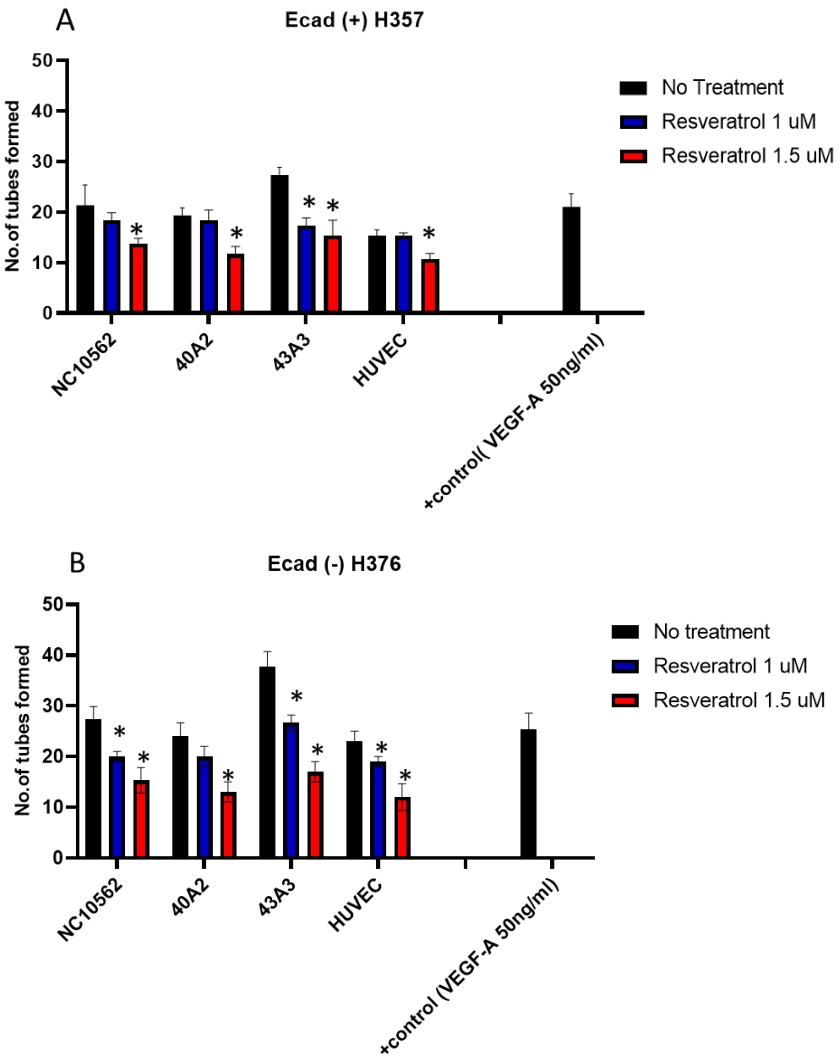

Figure 5.6. Inhibition of HUVEC tube formation by resveratrol. We employed resveratrol at concentrations of 1 µM and 1.5 µM to see its inhibitory effects on HUVEC tube formation. The use of 1 and 1.5 µM resveratrol caused a significant reduction in tube formation in all samples compared to their respective untreated controls (*indicates Mann-Whitney one-tailed test p-value <0.05, statistically significant. Error bars indicate standard deviation of three experimental replicates).

5.4 Discussion

Neo-angiogenesis is a very significant pathophysiologic process in cancer biology that enables the formation of new capillary networks to maintain a constant and steady flow of oxygen rich blood, supplying all the essential nutrients for the growing tissue (Li et al., 2019). This abnormal growth of blood vessels in the tumour is essential for the removal of metabolic wates and toxic substances, however, the capillary network is described as disorganised, immature and permeable by some authors (Viallard and Larrivée, 2017). The chemokine VEGF-A which is known for its angiogenetic function in general physiology and in pathologic conditions such as cancers was assessed using HUVEC cell line, the endothelial cell line that has the innate ability to form blood vessel like tubes *in vitro*. We used the supernatants (CM) that were obtained from infecting E-cadherin positive H357 and negative H376 cell lines with *F. nucleatum* subsp. *polymorphum* type strain ATCC10953/NCTC10562, clinical isolates 40A2 and 43A3 for all the assays investigating VEGF-A and its effects on the HUVEC cell line for tube formation.

MCP-1/CCL2, a well-known proinflammatory chemokine, has been implicated in the instigation of angiogenesis in tumour cells by increased nuclear expression of VEGF-A (Lien et al., 2020). We investigated the MCP-1/CCL2 levels in the CM obtained from the *F. nucelatum* subsp. *polymorphum* strains infections of the E-cadherin positive and negative cell lines by direct ELISA method. Both cell lines, irrespective of their E-cadherin status, showed to secrete significant levels of MCP-1/CCL2 when infected with the bacteria compared to the untreated control. Although the levels of MCP-1/CCL2 in both cell phenotypes remained somewhat similar, the clinical isolate 43A3 infection showed to stimulate the chemokine secretion that was statistically significant when compared to the untreated control in E-cadherin negative H376 phenotype (approximately 930 pg/ml, Kruskal-Wallis test p-value <0.05, statistically significant). This difference is perhaps relevant to our study, as the E-cadherin negative cells show an EMT phenotype with the loss of E-cadherins, suggesting an affinity of the *F. nucleatum* strain towards such pathologic transformations of epithelial cells. This suggestive affinity of *F. nucleatum* subsp. *polymorphum* towards EMT phenotypes epithelial cells would require further detailed exploration in the future.

The Levels of VEGF-A in the CM as mentioned earlier were quantified using a direct sandwich ELISA method. VEGF-A secretion is regulated by multiple factors *in vivo*, including activated oncogenes, deleted or mutant tumour suppressor genes, pro-inflammatory cytokines and chemokines such as MCP-1/CCL2, WNT1-inducible signalling pathway protein-1 (WISP-1/CCN-4), hormonal modulators and hypoxia (Claffey and Robinson, 1996). Contrary to the MCP-1/CCL2 levels in both OSCC cell phenotypes, there was a clear distinction in the levels of VEGF-A. The E-cadherin negative H376 cell line secreted high levels of VEGF-A with and without *F. nucleatum* infection. This could be attributed to the metastatic phenotype of the cell line and the absence of E-cadherin. The VEGF-A levels were higher when the cell line was infected with *F. nucleatum*, especially when infected with clinical isolate 43A3, which produced a statistically significant amount of VEGF-A, compared to the uninfected control (approximately 2100 pg/ml, Kruskal-Wallis test p-value <0.05, statistically significant). The difference in VEGF-A expression when stimulated by *F. nucleatum* infection between the two cell lines was statistically significant when direct comparisons using student t-test was made. The similar MCP-1/CCL2 expression seen in both cell lines and higher VEGF-A expression seen in E-cadherin negative H376 cell line is perhaps indicative of an MCP-1/CCL2 independent pathway involved in VEGF-A expression in this situation. The increased expression of VEGF-A by the E-cadherin negative H376 phenotype once again reinforces the selective affinity of *F. nucleatum* subsp. *polymorphym* to an OSCC cell phenotype that has lost its adhesive properties to one-another due to the lack of E-cadherins and also the partial transition from epithelial to mesenchymal phenotype.

The expression of VEGF-A and the consequent tube formation by HUVEC cells was also assessed *in vitro* in 96-well plates, the bottom of each well coated with a gel matrix Matrigel® to simulate the basement membrane. The number of tubes formed over 12-hours incubation period was indicative of the levels of VEGF-A present in the CM sample being used. Also, higher VEGF-A levels produced stronger, better formed tubes/capillary-like networks compared to immature tube-like structures with lower VEGF-A levels. However, for quantification purposes, any tube-like formation was considered as a tube for counting. For this assay, we used CM obtained from pre-infecting E-cadherin positive and negative cell lines with the *F. nucleatum* subsp. *polymorphum* type strain

ATCC10953/NCTC10562, clinical isolates 40A2 and 43A3 for 24-hours. When using the CM from E-cadherin positive H357 cell line infection, we found that over-all tube-like structures were formed by the HUVEC cells. However, the tubes thus formed were quite immature and obvious network formation was lacking. The CM obtained from clinical isolate 43A3 produced the greatest number of tubes (approximate average of 27.33 tubes, statistically significant compared to untreated control which produced an average of 10.3 tubes, Kruskal-Wallis test p value <0.05, significant). On the other hand, in the E-cadherin negative H376 CM treatment, clinical isolate 43A3 produced an average of 36 tubes, the highest tube formation with this group, followed by the type strain ATCC10953/NCTC10562 which produced an average of 31 tubes. Both strains resulted in a statistically significant tube formation compared to the untreated control (Kruskal-Wallis test p-value <0.05, significant). The CM from this E-cadherin negative cell-type resulted in well-formed tubes with complex intermeshing, fully formed capillary-like networks.

We further pre-treated the HUVEC cells with a VEGF-A antagonist, called Resveratrol, to see the effects of VEGF-A inhibition. Resveratrol is a polyphenol compound found in plants and possesses excellent anti-inflammatory and anti-carcinogenic properties through NF-κβ dependent pathways (Rauf et al., 2018). However, in angiogenesis, resveratrol interrupts the vascular-endothelial junction (V-E junction) by abolishing the anchoring molecules (such as *β*-catenin) and disrupting cell signalling via the VEGF receptor VEGFR-2 for tyrosine phosphorylation required for forming V-E junction and cell migration (Lin et al., 2003). The treatment with Resveratrol was dose dependent and we used 1µM and 1.5µM concentrations of the inhibitor. The effect of the inhibitor was profound on all bacterial treatments in both cell lines. The inhibitory effect of Resveratrol was dose dependent with increased concentration producing increased inhibition of tube formation. The use of 1.5µM Resveratrol almost halved the tube formation in most treatments in CM from both E-cadherin positive and negative cell line. The use of higher concentrations of Resveratrol could perhaps bring a total abolishment of tube formation, which needs to be yet explored.

In conclusion, our experiments show that although chemokines like VEGF-A are secreted by active tumour cells, concurrent infections with bacteria, specifically, *F. nucleatum* subsp. *polymorphum* are highly beneficial to the tumour cells. This results in secretion of high levels of VEGF-A, enabling the endothelial cells within the tumour to produce increased

blood vessels. Use of resveratrol in cancers could be of immense benefit in anti-carcinogenic treatments.

Chapter 6

General Discussion

6.1 General discussion

The symbiosis between the microbiome and human health has been well studied in the past decades and emerging data are continuously emphasising the importance of this symbiotic relationship in maintaining general health. Any disturbance in this symbiosis, either in the composition or in the diversity of the microbiota has been linked to a plethora of pathologies, including cancers (Sadrekarimi et al., 2022). In our study, we focused on the relationship of *F. nucleatum* subsp. *polymorphum* with altered oral epithelia, based on the data we obtained from the recovery of the most dominant *Fusobacterium* species in the dysplastic oral epithelium. The overarching goal was to characterize the pathogenicity of *F. nucleatum* subsp. *polymorphum* isolates recovered by swabbing of dysplastic oral epithelium from patients with malignant and premalignant conditions. The clinical isolates (n=7) were compared to the type strain of *F. nucleatum* subsp. *polymorphum* ATCC10953/NCTC10562. The interaction of these strains of *F. nucleatum* subsp. *polymorphum* with oral keratinocytes was analysed using OSCC immortalised cell lines that differed in their levels of E-cadherin expression. We confirmed the presence and absence of E-cadherins on the cell lines by using immunocytochemistry. Epithelial cadherin (E-cadherin) is an important biomolecule required for the maintenance of a healthy, tight, cell-cell adhesion in normal epithelium (van Roy and Berx, 2008). Alterations in cell-cell adhesion are generally a pre-requisite for normal embryonic growth and development in the human embryo, but this can also cause significant defects in tissue architecture and may lead to cancer development and tumour cell metastasis in established mature epithelium (Abdalla et al., 2017a). Epithelial to mesenchymal transition (EMT) is another important event in embryogenesis, but in cancerous conditions EMT is uncontrolled and this also contributes to the progression and metastasis of OSCC, and an early biomarker of this event is the loss of E-cadherins and an over expression of Vimentin (Chaw et al., 2012). This loss of cell-cell adhesion due to downregulation of E-cadherin is also an early event noted in oral dysplasia, and hence, we used an E-cadherin negative H376 cell line along with E-cadherin positive H357 OSCC cell line in all our experiments.

Extensive research emerging on the pattern of *F. nucleatum* adhesion to dysplastic colonocytes suggests heavy dependency on the presence of adhesins like FadA and Fap2 in the bacteria. The FadA adhesin has great affinity to the E-cadherins expressed on epithelial cells of the gut mucosa, perhaps bringing about the dysplastic changes observed

in CRC (Rubinstein et al., 2013). However, studies have shown that the dysplastic events in the oral cavity result in an early loss of E-cadherin expression, which may support a greater role for the Fap2 adhesin of *F. nucleatum,* which binds to simple sugar receptors such as galactose and N-acetyl-D-galactosamine receptors (Gal-GalNAc) on the epithelial cell surfaces. We could successfully demonstrate the over-expression of Gal-GalNaAc receptors on E-cadherin negative H376 cells in our study by using specific lectins that could be visualised and imaged in a fluorescent microscope.

The adhesion pattern of the clinical isolates was quite similar in both cell lines, except for clinical isolates obtained from patient numbers 43 and 60. The isolates 43A2, 43A3, 43B1 and 60A2 showed a preference to adhere better to E-cadherin negative H376 cells compared to other clinical isolates (40A2, 41A and 41B2). This data suggests the loss of E-cadherins and other possible changes in dysplastic epithelial cell surface during the development of OLK and other oral dysplasia may select for a specific microbiome, as characterised by Amer et al (Amer et al., 2017). A better understanding of this phenomenon was obtained when the normal comparator type strain ATCC10953/NCTC10562 was subjected to adhesion assay. There was a reduction in the adhesion from 25% to 11% between E-cad positive H357 and E-cad negative H376 cell lines, respectively, suggesting the involvement of the nature of the bacterial samples obtained. Whilst the type strain of *F. nucleatum ss. polymorphum* ATCC10562/NCTC10562 was isolated from dental plaque of a healthy individual, the clinical isolates were all isolated from dysplastic pathologic sites and normal contralateral site (of the corresponding patient). Some of the strains recovered for this study may be specifically adapted to adhere to dysplastic cells and this may explain why higher levels of *F. nucleatum* have been reported on the surface of OLK and OSCC lesions. We also demonstrated a direct correlation between adhesin copy numbers in the isolates and their ability to adhere to epithelial cells. The clinical isolates that adhered better to E-cadherin negative H376 cell lines had four or more type Va autotransporters (encoding Fap2-like proteins) compared to the isolates that showed lower adhesion. However, the type strain ATCC10562/NCTC10562 was not among the most adherent strains to E-cadherin negative H376 cells although it had a high copy number of Type Va proteins. This may be due to the nature of the Type Va adhesins expressed on this particular isolate, or due to the presence of other unrelated adhesins in the clinical isolates. The type strain however showed high

levels of adhesion with the E-cadherin positive H357 cell line, which could be correlated to the high copy numbers of FadA adhesins. The use of several inhibitors such as galactose for E-cadherin negative cell line (targeting Fap2) and FadA inhibiting peptide ASANWTIQYND for the use with E-cadherin positive H357 cells helped in understanding the role of these inhibitors in targeting specific adhesins necessary for adhesion, but it also highlights the involvement of several other adhesins that could perhaps participate in aiding adhesion of *F. nucleatum* subsp. *polymorphum* in the absence of FadA or Fap2 like adhesins.

The novel confocal microscopic method developed in our study was a great aid to assess and quantify the invasion of epithelial cells by *F. nucleatum* subsp. *polymorphum*. Conventional invasion assays that employed antibiotic treatments (200 µg/ml metronidazole and 300µg/ml gentamycin) did not seem to completely eradicate the external non-adhered/invaded bacteria, which led to misleading results. Therefore, the use of confocal microscope as an aid in quantifying *F. nucleatum* subsp. *polymorphum* invasion of epithelial cells gave more accurate results allowed us to visualise invading bacteria. We showed that the relative invasion of E-cadherin positive H357 cells was greater compared to invasion of the E-cadherin negative H376 cells. Most clinical isolates that showed greater invasion in E-cadherin positive H357 cells had a higher copy numbers of FadA-like genes. For example, clinical isolates 41A and 41B2 and the type strain ATCC10953/NCTC10562, all of which exhibited 3 or more copies of FadA-like genes showed higher invasion levels in the E-cadherin positive H357 cell line. The isolate 60A2 in this instance however was a weak invader, despite possessing 3 FadA-like genes (FadA1). On the other hand, clinical isolates 41A and 41B2 exhibited greater invasion of the E-cad negative H376 cell line as well in comparison to the type strain ATCC10953/NCTC10562, indicating that their enhanced invasion may not require E-cadherin and by extension, the FadA surface adhesin. Our data show that adherence and invasion of keratinocytes by clinical strains of *F. nucleatum* subsp. *polymorphum* is highly strain dependent and is influenced by the expression of different receptors on the epithelial cells. Also, strains seem to vary greatly in their complement of both type Va adhesins and FadA like genes that may influence these interactions. Additionally, a cell line that does not express E-cadherin was not invaded to the same extent as a cell line expressing E-cadherin. This result questions the importance of intracellular invasion during tumour progression, as loss of E-cadherin is a general feature

of malignant cells. It should also be noted that these cell lines are not isogenic and that other factors may be at play in this interaction.

The use of a multiplex assay system to identify the potential proinflammatory cytokines and chemokines (n=71) expressed by the keratinocytes provided a basis for experimental design for further investigating the interactions of *F. nucleatum* subsp*. polymorphum* with the OSCC cell lines. Although cytokines are generally secreted by the active immune system to keep pathogens and foreign bodies in check, chronic conditions such as cancers can evade the body's defence mechanisms and lead to an unhealthy release of these proteins that are favourable for further growth and development of tumours (Vilgelm and Richmond, 2019). As expected in any chronic inflammatory condition, IL-6 and IL-8 were among first and the most secreted cytokines by the E-cadherin positive H357 and E-cadherin negative H376 cell lines when infected with the *F. nucleatum* subsp*. polymorphum* strains. Clinical isolates 41A and 41B2 and the type strain of *F. nucleatum* subsp*. polymorphum* were the strains to induce the most cytokine secretion in both cell lines*.* These cytokines were also detected in the uninfected negative control, which reflected the constitutively inflamed state of the cell lines themselves. Incidentally, the positive control used for this multiplex assay (*E. coli* type strain DH-5α) also induced the secretion of a significantly high IL-8 (approximately 8000 pg/ml) cytokine, indicating that these responses may be a general response to Gram-negative infection induced by LPS exposure. *F. nucleatum* infection also induced high levels of chemokines CCL5/RANTES, CCL2/MCP-1 and VEGF-A and also the extracellular matrix metalloproteinase MMP-9. These protein molecules are quite significant in cancer biology as they have been established to influence the cancer cells in mobilising, migrating and metastatic transformation of benign tumours (Aldinucci and Colombatti, 2014, Claffey and Robinson, 1996, Swann and Smyth, 2007). Therefore, it was crucial to further investigate the effects of these chemokines on the epithelial cell lines. The inclusion of *E. coli* as a control in this multiplex assay and the high levels of IL-6 and IL-8 thus secreted suggests that these cytokines are perhaps secreted because of Gram-negative bacterial infections, rather than the involvement of E-cadherin status of the affected cell lines.

Although the overall levels of the chemokines were high in the medium obtained from infecting E-cadherin positive H357 cells with the *F. nucleatum* strains, dramatic effects on

cell migration and invasion in the E-cadherin negative H376 cell lines were observed. Having obtained an overall landscape of chemokines that were secreted by the two cell lines when infected with the *F. nucelatum* subsp. *polymorphum* strains, we proceeded to independently verify these chemokines with antibody specific ELISA kits. The *F. nucleatum* subsp. *polymorphum* strains selected for all the ELISA assays was based on our previous results from the adhesin copy numbers and the consequent adhesion/invasion reslults, which showed the *F. nucleatum* subsp. *polymorphum* isolates having the least adhesin copy numbers and adhesion property (40A2) and the isolate with the highest adhesin copy numers and adhesion property (43A3). We also used the type strain ATCC10953/NCTC10562 as a comparitor. By doing so, we could show that when the cell lines were infected with certain *F. nucleatum* subsp. *polymorphum* strains such as the clinical isolate 43A3 with high adhesin copy numbers, the E-cadherin negative H376 cell lines responded dramatically, secreting high levels of the chemokine RANTES/CCL5, MMP9 and VEGF-A. The levels of these proteins were significantly lower in both cell lines when the medium collected from cell line infection with clinical isolate 40A2 were used. This could perhaps be due to low FadA and Fap2 gene copies in this clinical isolate that contributes to an overall low interaction with cell lines.

We demonstrated the cell motility and migration by performing a scratch wound asssay and a trans-well invasion assay that also showed the invasive potential of the cell lines. The ability of the epithelial cells to close the scratch wound over twenty-four hours period of conditioned medium (CM) treatment with respective *F. nucleatum* subsp. *polymorphum* strain infection was an indication of the cell motility induced by the chemokine CCL5/RANTES and MMP-9. The clinical isolate 43A3 CM brought about the most cell migration in both cell lines, with E-cadherin negative H376 cells being the most migratory. The cells migrated approximatey 450 µm in 24-hours in the E-cadherin negative H376 cells as compared to approximately 320 µm in the E-cadherin positive H357 cells with CM from clinical isolate 43A3. However, when the CM from the clinical isolate 40A2 was used, the least cell migration occurred in both cell lines.

The difference in both CCL5 and MMP-9 levels in these strains of *F. nucleatum* subsp. *polymorphum* and their direct influence on cell migration could be appreciated in this assay. Also, the absence of E-cadherins in canerous cells seems to promote cell motility and migration. The use of transwells to investigate the invasiveness of the OSCC cell lines

using the CM collected from previous infections with *F. nucleatum* subsp. *polymorphum* strains proved to be very informative. The E-cadherin negative H376 cells were clearly more invasive, especially when infected with *F. nucleatum*, correlating with the literature on cancers where the loss of E-cadherins have been associated with aggressiveness, advanced stage and poor prognosis of cancers (Younis et al., 2007). All *F. nucleatum* subsp. *polymorphum* strains led to increased levels of migration and invasion across the ECM gel/polycarbonate barrier in the E-cadherin negative H376 cells, but the CM obtained from clinical isolate 43A3 infection was the most influential in instigating the increased migration and invasion. We also used rhCCL5/metRANTES as an inhibitor to see the effects on the cell motility, migration and invasion. The use of 3ng/ml of rhCCL5/metRANTES proved effective in reducing the cell motility, migration and invasion effectively in both cell lines. rhCCL5/metRANTES is a competitor inhibitor for CCR5 receptors, that ultimately inhibits or reduces MMP-9 expression drastically by interfering the PLCβ/NF-κβ pathway involved in the CCL5/CCR5 axis for MMP-9 expression (Chuang et al., 2009) as shown in the figure 6.1.

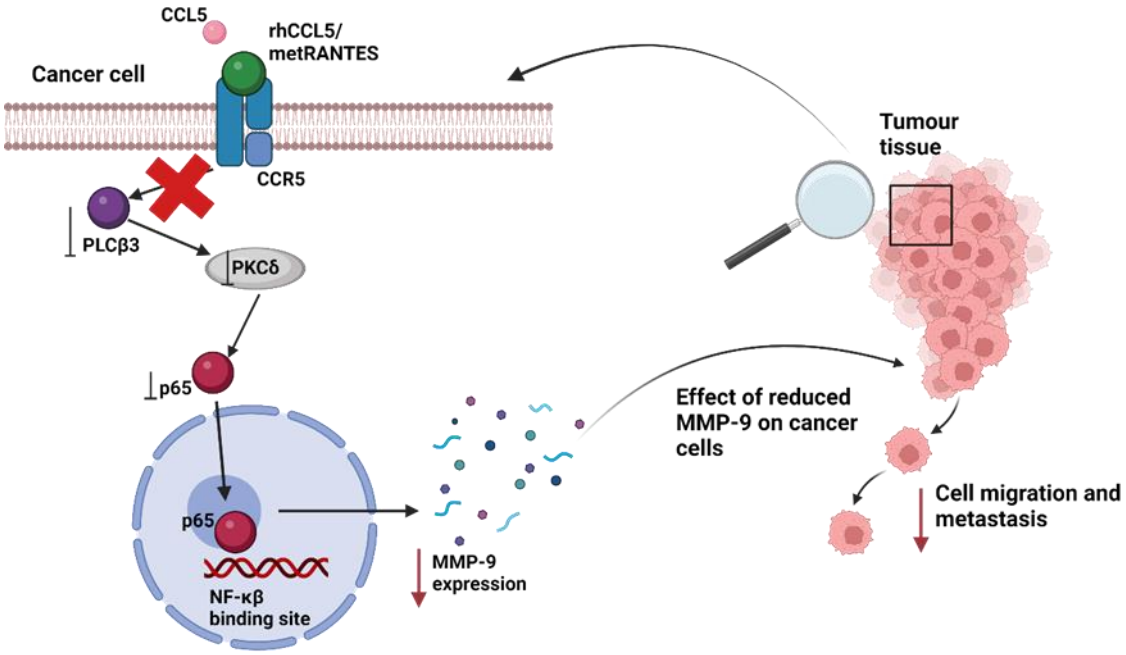

Figure 6.1. CCL5/CCR5 axis inhibition. Competitive inhibition of CCL5/RANTES by rhCCL5/metRANTES by competitively occupying the CCR5 receptors. This blocking of the CCR5 receptor inhibits the initiation of the PLCβ/PKCδ/NF-κβ pathway that is essential in nuclear expression of MMP-9. The overall effect is either complete inhibition of MMP-9 expression or reduced MMP-9 secretion, ultimately reducing OSCC cell migration.

Unsuccessful attempts were made to generate *F. nucleatum* subsp. *polymorphum* mutants in which the *fadA* and *fap2* genes were deleted to further investigate the role of these adhesin genes of the bacteria on adhesion and invasion of oral keratinocytes. The challenges of generating such mutants were beyond the scope of this study and therefore we obtained *F. nucleatum* subsp. *nucleatum* type strain FNN23726 and its respective FadA and Fap2 mutants *ΔfadA* and *Δfap2.* The employment of these strains in trans-well migration and invasion assay showed relatively lower cell migration in E-cadherin negative H376 cells when CM from *Δfap2* infection was used and unexpectedly there was higher cell migration in E-cadherin positive H357 cells when the *ΔfadA* mutant was used. This behaviour indicates the involvement of other accessory adhesins such as LPS, RadD and Aid1 in the absence of FadA adhesin to assist in cell migration. This certainly needs further investigation in the future, and strategies to do so are a work in progress.

To investigate the influence of VEGF-A on OSCC development, we used endothelial cells which are essential in blood vessels formation *in vivo*. The *in vitro* set up in our experiment consisted of HUVEC cells that were subjected to treatment with CM obtained from *F. nucleatum* subsp. *polymorphum* strains infection. Again, we chose the clinical isolate 43A3 and 40A2 based on the adhesin copy numbers (43A3 has high FadA and Fap2 copy numbers and 40A2 has low FadA and Fap2 copy numbers). VEGF-A secretion in the human body is regulated by multiple factors, including activated oncogenes, deleted or mutant tumour suppressor genes, pro-inflammatory cytokines and chemokines such as MCP-1/CCL2, WNT1-inducible signalling pathway protein-1 (WISP-1/CCN-4), hormonal modulators and hypoxia (Claffey and Robinson, 1996). Hypoxia has been described as the master controller of VEGF-A secretion *in vivo*. Under severe hypoxic conditions, hypoxia-inducible factor-1α (HIF-1α) is activated in cancer cells and HIF-1β is activated in normal cells, that ultimately result in overexpression of VEGF-A, essential for the formation of new blood vessels to meet the increased oxygen demand in the hypoxic tissue (Kallergi et al., 2009). The levels of VEGF-A in the conditioned media were quantified using a direct sandwich ELISA method. The E-cadherin negative H376 cell line secreted high levels of VEGF-A with and without *F. nucleatum* infection. This could be attributed to the EMT metastatic phenotype of the cell line and the absence of E-cadherin. The VEGF-A levels were higher when the cell line was infected with *F. nucleatum* strains, especially when infected with clinical isolate 43A3, which produced a significant amount of VEGF-A, compared to the uninfected control

(approximately 2100 pg/ml). The high levels of VEGF-A secretion induced by the clinical isolate 43A3 in the E-cadherin negative H376 cell line consequently reflected on its ability to form tubes in the tube formation assay. The tubes formed by the treatment of HUVEC cells with this phenotype resulted in large number of well-formed "capillary-like" tubes over twelve-hour period. The tube formations were reduced when an increasing concentration of Resveratrol®, a selective VEGFR inhibitor was used. We used concentrations of 1 µM and 1.5 µM to inhibit the tube formations, and we could show that there was reduction in tube formations with increasing the concentrations of the inhibitor. However, it would be interesting to see what concentration of Resveratrol® is optimum for inhibition, after which, there could be either no effect or there could be a complete destruction of the HUVEC cells themselves. This increased expression of VEGF-A by the E-cadherin negative H376 phenotype and the resultant tube formation once again reinforces the selective affinity of *F. nucleatum* subsp. *polymorphym* to an OSCC cell phenotype that has lost its adhesive properties to one-another due to the lack of E-cadherins and also the partial transition from epithelial to mesenchymal phenotype.

In conclusion, our study has discovered that although *F. nucleatum* is a normal commensal of the oral cavity, *F. nucleatum* subsp. *polymorphum* is the most abundantly isolated strain from oral epithelium that have undergone dysplastic changes. Some of these strains of *F. nucelatum* recovered in this study may be specifically adapted to adhere to dysplastic cells, as seen with higher levels of *F. nucelatum* subsp. *polymorphum* isolated from OLK and OSCC. We also showed this phenomenon of preference to adhesion to dysplastic cells by specific *F. nucelatum* strains in our adhesion and invasion assays. As explained in the chapter 1, dysplasia is an abnormality in the stratification and maturation of the epithelial cells, characterised by the early loss of cell-cell adhesion because of downregulation of E-cadherin expression. This loss of E-cadherins and the concurrent EMT of the epithelial cells during the development of OLK and OSCC may select for a specific microbiome. Interestingly, invasion of cells that have lost E-cadherin was significantly lower than in E-cadherin positive cells, suggesting that intracellular invasion may not be significant requirement for induction of pro-malignant phenotypes. The greatest proinflammatory and pro-metastatic responses were observed in E-cadherin negative cells infected with the highly adherent strain 43A3, which was only weakly invasive in E-cadherin negative cells. Our data also indicate that the bacterial adhesins such as FadA and Fap2 play a vital role in

the bacterial adhesion and invasion of the dysplastic phenotypes of the oral keratinocytes and in the absence of these adhesins, accessory adhesins such as LPS, RadD and Aid1 could play a surrogating role in aiding adhesion and invasion. The use of inhibitors such as galactose and FadA specific inhibitor ASANWTIQYND in inhibiting adhesion of *F. nucleatum* subsp. *polymorphum* reinforces the role of FadA and Fap2 like adhesins in adhesion events and the possible involvement of other adhesins in the absence of FadA or Fap2 adhesin. Our data also shows that adherence and invasion by *F. nucleatum* subsp. *polymorphum* is highly strain dependent and influenced by the receptors on the epithelial cells. It also emphasises on the great variability in the complement of type Va (Fap2) and FadA like adhesin genes that influence these interactions. The specific roles of other adhesins of *F. nucleatum* subsp. *polymorphum* such as RadD, Aid1 is quite unknown and ongoing research by Claire Crowlely in our group suggests that the copy number of these genes varies greatly between strains and is influenced by horizontal gene transfer and intergenic recombination creating hybrid genes.

The discovery of the correlation of adhesin copy numbers in *F. nucleatum* subsp. *polymorphum* and its influence in adhesion, invasion, cell motility and migration were significant. Being a Gram-negative bacterium, *F. nucleatum* subsp. *polymorphum* seems to trigger the secretion of high levels of proinflammatory cytokines and chemokines that are essential for the metastasis of OSCC. We could also show that the absence of E-cadherin in OSCC cells favoured cell motility, migration and invasion and these phenomena were enhanced in the presence of *F. nucleatum* subsp. *polymorphum* infection. The employment of inhibitors such as rhCCL5/metRANTES reduced cell motility and invasion significantly *in vitro*, and the *in vivo* effects of such inhibitors in OSCC could be a future study. Also, infecting the OSCC cells with *F. nucleatum* subsp. *polymorphum* significantly enhanced the secretion of chemokine VEGF-A required for tube-like vessel formation *in vitro*. The over-expression of this chemokine in E-cadherin negative cells reflects the stronger impact of *F. nucleatum* subsp. *polymorphum* infection on E-cadherin negative cells expressing an EMT cell phenotype. Although not investigated here, it would be interesting to determine if long-term infection of E-cadherin positive cells by *F. nucleatum* could result in down-regulation of E-cadherin expression. This has been suggested by other and may indicate that *F. nucleatum* may also drive EMT (Shao et al., 2021). The summary of the major findings of this study is depicted in the figure 6.2.

Finally, the effects of chemokines such as IP-10 and M-CSF on the OSCC cells used here are yet to be investigated. The use of *F. nucleatum* subsp. *nucleatum* and its FadA and Fap2 mutants in the trans-well invasion assay reinforces the involvement of accessory adhesins in the absence of FadA or Fap2 adhesins. Our attempts to generate *F. nucleatum* subsp. *polymorphum* FadA and Fap2 mutants that have the respective genes deleted is a prospective project in the future.

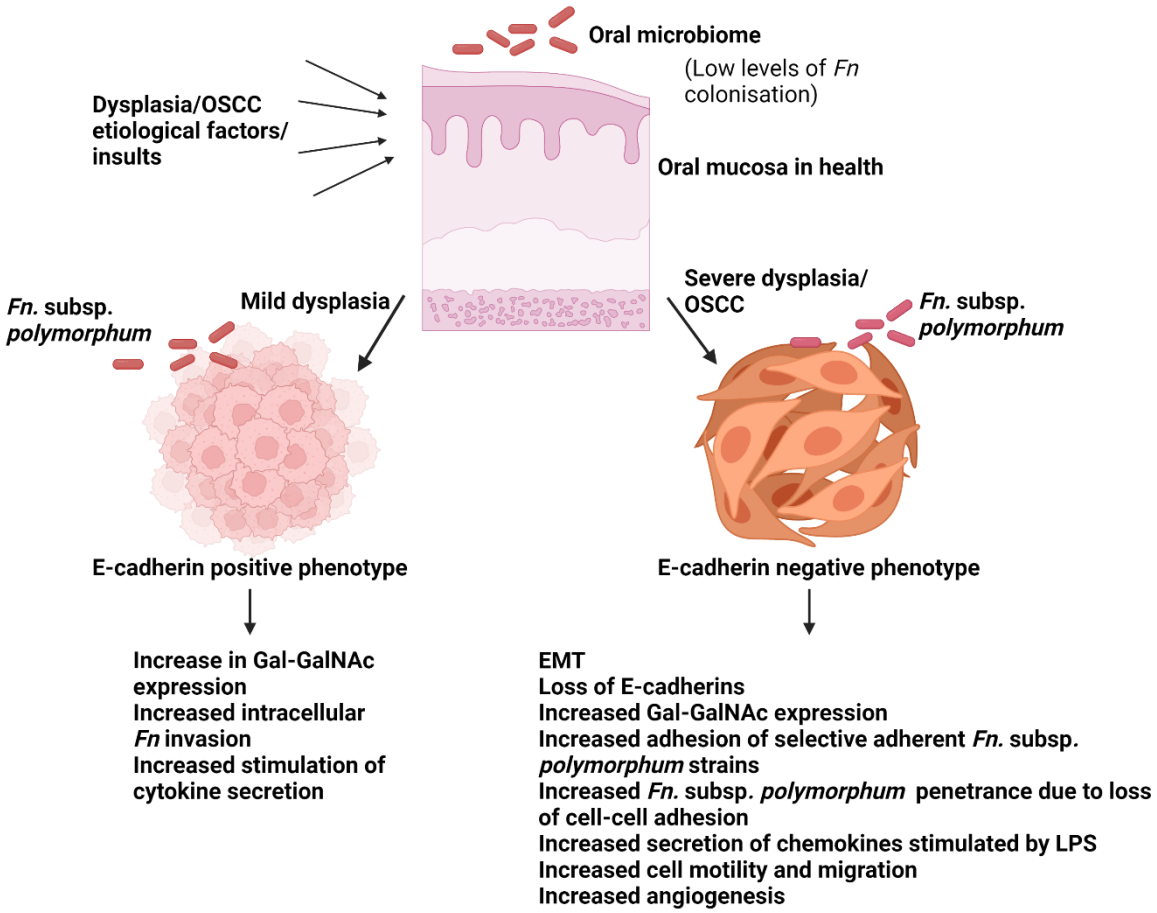

Figure 6.2. Summary of *F. nucleatum* subsp. *polymorphum* infection on dysplastic oral epithelium. Normal epithelium is colonised at low level by *F. nucleatum*. Colonisation may be kept in balance by the normal microbiome and low-level invasion of the upper epithelial layers may occur. The development of dysplasia differs from patient to patient and may progress from mild to severe or appear *de novo* as severe. Mild forms may be E-cadherin positive and have changes in surface receptors (e.g. Gal-GalNac) that could promote *F. nucleatum* colonisation. The presence of E-cadherin may protect the tissue from the proinflammatory effects of *F. nucleatum* colonisation while allowing intracellular invasion. Progression to severe dysplasia/OSCC may increase Gal-GalNac expression and result in loss of E-cadherin. Loss of E-cadherin and tissue structure may allow penetration of *F. nucleatum* within the tumour (as has been reported) and allow the pro-inflammatory effects of infection to mediate their effects on cell motility, migration and invasion required for cancer progression and metastasis.

References

1985. Tobacco habits other than smoking; betel-quid and areca-nut chewing; and some related nitrosamines. IARC Working Group. Lyon, 23-30 October 1984. *IARC Monogr Eval Carcinog Risk Chem Hum,* 37**,** 1-268.

2004. Betel-quid and areca-nut chewing and some areca-nut derived nitrosamines. *IARC Monogr Eval Carcinog Risks Hum,* 85**,** 1-334.

ABDALLA, Z., WALSH, T., THAKKER, N. & WARD, C. M. 2017a. Loss of epithelial markers is an early event in oral dysplasia and is observed within the safety margin of dysplastic and T1 OSCC biopsies. 12**,** e0187449.

ABDALLA, Z., WALSH, T., THAKKER, N. & WARD, C. M. 2017b. Loss of epithelial markers is an early event in oral dysplasia and is observed within the safety margin of dysplastic and T1 OSCC biopsies. *PLoS One,* 12**,** e0187449.

ABED, J., EMGÅRD, J. E., ZAMIR, G., FAROJA, M., ALMOGY, G., GRENOV, A., SOL, A., NAOR, R., PIKARSKY, E., ATLAN, K. A., MELLUL, A., CHAUSHU, S., MANSON, A. L., EARL, A. M., OU, N., BRENNAN, C. A., GARRETT, W. S. & BACHRACH, G. 2016. Fap2 Mediates Fusobacterium nucleatum Colorectal Adenocarcinoma Enrichment by Binding to Tumor-Expressed Gal-GalNAc. *Cell Host Microbe,* 20**,** 215-25.

ABSHIRE, D. & LANG, M. K. 2018. The Evolution of Radiation Therapy in Treating Cancer. *Semin Oncol Nurs,* 34**,** 151-157.

ALDINUCCI, D. & COLOMBATTI, A. 2014. The inflammatory chemokine CCL5 and cancer progression. *Mediators Inflamm,* 2014**,** 292376.

ALNUAIMI, A. D., WIESENFELD, D., O'BRIEN-SIMPSON, N. M., REYNOLDS, E. C. & MCCULLOUGH, M. J. 2015. Oral Candida colonization in oral cancer patients and its relationship with traditional risk factors of oral cancer: a matched case-control study. *Oral Oncol,* 51**,** 139-45.

AMER, A., GALVIN, S., HEALY, C. M. & MORAN, G. P. 2017. The Microbiome of Potentially Malignant Oral Leukoplakia Exhibits Enrichment for Fusobacterium, Leptotrichia, Campylobacter, and Rothia Species. *Front Microbiol,* 8**,** 2391.

BACHRACH, G., ROSEN, G., BELLALOU, M., NAOR, R. & SELA, M. N. 2004. Identification of a Fusobacterium nucleatum 65 kDa serine protease. *Oral Microbiol Immunol,* 19**,** 155-9.

BARTH, A. I., NATHKE, I. S. & NELSON, W. J. 1997. Cadherins, catenins and APC protein: interplay between cytoskeletal complexes and signaling pathways. *Curr Opin Cell Biol,* 9**,** 683-90.

BHATLEKAR, S., FIELDS, J. Z. & BOMAN, B. M. 2014. HOX genes and their role in the development of human cancers. *J Mol Med (Berl),* 92**,** 811-23.

BINDER GALLIMIDI, A., FISCHMAN, S., REVACH, B., BULVIK, R., MALIUTINA, A., RUBINSTEIN, A. M., NUSSBAUM, G. & ELKIN, M. 2015. Periodontal pathogens Porphyromonas gingivalis and Fusobacterium nucleatum promote tumor progression in an oral-specific chemical carcinogenesis model. *Oncotarget,* 6**,** 22613-23.

BITU, C. C., CARRERA, M., LOPES, M. A., KOWALSKI, L. P., SOARES, F. A. & COLETTA, R. D. 2012. HOXB7 expression is a prognostic factor for oral squamous cell carcinoma. *Histopathology,* 60**,** 662-5.

BOCCIA, S., CADONI, G., SAYED-TABATABAEI, F. A., VOLANTE, M., ARZANI, D., DE LAURETIS, A., CATTEL, C., ALMADORI, G., VAN DUIJN, C. M., PALUDETTI, G. & RICCIARDI, G. 2008. CYP1A1, CYP2E1, GSTM1, GSTT1, EPHX1 exons 3 and 4, and NAT2 polymorphisms, smoking, consumption of alcohol and fruit and vegetables and risk of head and neck cancer. *J Cancer Res Clin Oncol,* 134**,** 93-100.

BOEHM, E. T., THON, C., KUPCINSKAS, J., STEPONAITIENE, R., SKIECEVICIENE, J., CANBAY, A., MALFERTHEINER, P. & LINK, A. 2020. Fusobacterium nucleatum is associated with worse prognosis in Lauren's diffuse type gastric cancer patients. *Sci Rep,* 10**,** 16240.

BOLSTAD, A. I., JENSEN, H. B. & BAKKEN, V. 1996. Taxonomy, biology, and periodontal aspects of Fusobacterium nucleatum. *Clin Microbiol Rev,* 9**,** 55-71.

BRENNAN, C. A. & GARRETT, W. S. 2019. Fusobacterium nucleatum - symbiont, opportunist and oncobacterium. *Nat Rev Microbiol,* 17**,** 156-166.

BREW, R., ERIKSON, J. S., WEST, D. C., KINSELLA, A. R., SLAVIN, J. & CHRISTMAS, S. E. 2000. Interleukin-8 as an autocrine growth factor for human colon carcinoma cells in vitro. *Cytokine,* 12**,** 78-85.

BROOK, I. & WALKER, R. I. 1986. The relationship between Fusobacterium species and other flora in mixed infection. *J Med Microbiol,* 21**,** 93-100.

BROUNS, E. R., BAART, J. A., BLOEMENA, E., KARAGOZOGLU, H. & VAN DER WAAL, I. 2013. The relevance of uniform reporting in oral leukoplakia: definition, certainty factor

and staging based on experience with 275 patients. *Med Oral Patol Oral Cir Bucal,* 18**,** e19-26.

BULLMAN, S., PEDAMALLU, C. S., SICINSKA, E., CLANCY, T. E., ZHANG, X., CAI, D., NEUBERG, D., HUANG, K., GUEVARA, F., NELSON, T., CHIPASHVILI, O., HAGAN, T., WALKER, M., RAMACHANDRAN, A., DIOSDADO, B., SERNA, G., MULET, N., LANDOLFI, S., RAMON, Y. C. S., FASANI, R., AGUIRRE, A. J., NG, K., ELEZ, E., OGINO, S., TABERNERO, J., FUCHS, C. S., HAHN, W. C., NUCIFORO, P. & MEYERSON, M. 2017. Analysis of Fusobacterium persistence and antibiotic response in colorectal cancer. *Science,* 358**,** 1443-1448.

CALMELS, S., OHSHIMA, H., HENRY, Y. & BARTSCH, H. 1996. Characterization of bacterial cytochrome cd(1)-nitrite reductase as one enzyme responsible for catalysis of nitrosation of secondary amines. *Carcinogenesis,* 17**,** 533-6.

CASASANTA, M. A. & YOO, C. C. 2020. Fusobacterium nucleatum host-cell binding and invasion induces IL-8 and CXCL1 secretion that drives colorectal cancer cell migration. 13.

CASTELLARIN, M., WARREN, R. L., FREEMAN, J. D., DREOLINI, L., KRZYWINSKI, M., STRAUSS, J., BARNES, R., WATSON, P., ALLEN-VERCOE, E., MOORE, R. A. & HOLT, R. A. 2012. Fusobacterium nucleatum infection is prevalent in human colorectal carcinoma. *Genome Res,* 22**,** 299-306.

CHAW, S. Y., ABDUL MAJEED, A., DALLEY, A. J., CHAN, A., STEIN, S. & FARAH, C. S. 2012. Epithelial to mesenchymal transition (EMT) biomarkers--E-cadherin, beta-catenin, APC and Vimentin--in oral squamous cell carcinogenesis and transformation. *Oral Oncol,* 48**,** 997-1006.

CHEN, S., SU, T., ZHANG, Y. & LEE, A. 2020. Fusobacterium nucleatum promotes colorectal cancer metastasis by modulating KRT7-AS/KRT7. 11**,** 511-525.

CHENICHERI, S., R, U., RAMACHANDRAN, R., THOMAS, V. & WOOD, A. 2017. Insight into Oral Biofilm: Primary, Secondary and Residual Caries and Phyto-Challenged Solutions. *Open Dent J,* 11**,** 312-333.

CHO, Y., GORINA, S., JEFFREY, P. D. & PAVLETICH, N. P. 1994. Crystal structure of a p53 tumor suppressor-DNA complex: understanding tumorigenic mutations. *Science,* 265**,** 346-55.

CHOCOLATEWALA, N. M. & CHATURVEDI, P. 2009. Role of human papilloma virus in the oral carcinogenesis: an Indian perspective. *J Cancer Res Ther,* 5**,** 71-7.

CHOW, M. T. & LUSTER, A. D. 2014. Chemokines in cancer. *Cancer Immunol Res,* 2**,** 1125-31.

CHUANG, J. Y., YANG, W. H., CHEN, H. T., HUANG, C. Y., TAN, T. W., LIN, Y. T., HSU, C. J., FONG, Y. C. & TANG, C. H. 2009. CCL5/CCR5 axis promotes the motility of human oral cancer cells. *J Cell Physiol,* 220**,** 418-26.

CLAESSON-WELSH, L. & WELSH, M. 2013. VEGFA and tumour angiogenesis. *J Intern Med,* 273**,** 114-27.

CLAFFEY, K. P. & ROBINSON, G. S. 1996. Regulation of VEGF/VPF expression in tumor cells: consequences for tumor growth and metastasis. *Cancer Metastasis Rev,* 15**,** 165-76.

COPPENHAGEN-GLAZER, S., SOL, A., ABED, J., NAOR, R., ZHANG, X., HAN, Y. W. & BACHRACH, G. 2015. Fap2 of Fusobacterium nucleatum is a galactose-inhibitable adhesin involved in coaggregation, cell adhesion, and preterm birth. *Infect Immun,* 83**,** 1104-13.

CRITCHLOW, S. B., MORGAN, C. & LEUNG, T. 2014. The oral health status of pre-treatment head and neck cancer patients. *Br Dent J,* 216**,** E1.

DE SOUZA SETUBAL DESTRO, M. F., BITU, C. C., ZECCHIN, K. G., GRANER, E., LOPES, M. A., KOWALSKI, L. P. & COLETTA, R. D. 2010. Overexpression of HOXB7 homeobox gene in oral cancer induces cellular proliferation and is associated with poor prognosis. *Int J Oncol,* 36**,** 141-9.

DORON, L., COPPENHAGEN-GLAZER, S., IBRAHIM, Y., EINI, A., NAOR, R., ROSEN, G. & BACHRACH, G. 2014. Identification and characterization of fusolisin, the Fusobacterium nucleatum autotransporter serine protease. *PLoS One,* 9**,** e111329.

EDWARDS, A. M., GROSSMAN, T. J. & RUDNEY, J. D. 2006. Fusobacterium nucleatum transports noninvasive Streptococcus cristatus into human epithelial cells. *Infect Immun,* 74**,** 654-62.

EPSTEIN, J. B., CABAY, R. J. & GLICK, M. 2005. Oral malignancies in HIV disease: changes in disease presentation, increasing understanding of molecular pathogenesis, and current management. *Oral Surg Oral Med Oral Pathol Oral Radiol Endod,* 100**,** 571-8.

EREN, A. M., BORISY, G. G., HUSE, S. M. & MARK WELCH, J. L. 2014. Oligotyping analysis of the human oral microbiome. *Proc Natl Acad Sci U S A,* 111**,** E2875-84.

EREN, A. M., MAIGNIEN, L., SUL, W. J., MURPHY, L. G., GRIM, S. L., MORRISON, H. G. & SOGIN, M. L. 2013. Oligotyping: Differentiating between closely related microbial taxa using 16S rRNA gene data. *Methods Ecol Evol,* 4.

FARDINI, Y., WANG, X., TEMOIN, S., NITHIANANTHAM, S., LEE, D., SHOHAM, M. & HAN, Y. W. 2011. Fusobacterium nucleatum adhesin FadA binds vascular endothelial cadherin and alters endothelial integrity. *Mol Microbiol,* 82**,** 1468-80.

FOSTER, J. S. & KOLENBRANDER, P. E. 2004. Development of a multispecies oral bacterial community in a saliva-conditioned flow cell. *Appl Environ Microbiol,* 70**,** 4340-8.

GANESAN, K., GUO, S., FAYYAZ, S., ZHANG, G. & XU, B. 2019. Targeting Programmed Fusobacterium nucleatum Fap2 for Colorectal Cancer Therapy. *Cancers (Basel),* 11.

GEETHA, K. M., LEEKY, M., NARAYAN, T. V., SADHANA, S. & SALEHA, J. 2015. Grading of oral epithelial dysplasia: Points to ponder. *J Oral Maxillofac Pathol,* 19**,** 198-204.

GMUR, R., MUNSON, M. A. & WADE, W. G. 2006. Genotypic and phenotypic characterization of fusobacteria from Chinese and European patients with inflammatory periodontal diseases. *Syst Appl Microbiol,* 29**,** 120-30.

GOODE, E. L., ULRICH, C. M. & POTTER, J. D. 2002. Polymorphisms in DNA repair genes and associations with cancer risk. *Cancer Epidemiol Biomarkers Prev,* 11**,** 1513-30.

GRIJPSTRA, J., ARENAS, J., RUTTEN, L. & TOMMASSEN, J. 2013. Autotransporter secretion: varying on a theme. *Res Microbiol,* 164**,** 562-82.

GUHA, N., BOFFETTA, P., WÜNSCH FILHO, V., ELUF NETO, J., SHANGINA, O., ZARIDZE, D., CURADO, M. P., KOIFMAN, S., MATOS, E., MENEZES, A., SZESZENIA-DABROWSKA, N., FERNANDEZ, L., MATES, D., DAUDT, A. W., LISSOWSKA, J., DIKSHIT, R. & BRENNAN, P. 2007. Oral health and risk of squamous cell carcinoma of the head and neck and esophagus: results of two multicentric case-control studies. *Am J Epidemiol,* 166**,** 1159-73.

GUHA, N., WARNAKULASURIYA, S., VLAANDEREN, J. & STRAIF, K. 2014. Betel quid chewing and the risk of oral and oropharyngeal cancers: a meta-analysis with implications for cancer control. *Int J Cancer,* 135**,** 1433-43.

GUPTA, R. S. & SETHI, M. 2014. Phylogeny and molecular signatures for the phylum Fusobacteria and its distinct subclades. *Anaerobe,* 28**,** 182-98.

GUR, C., MAALOUF, N., SHHADEH, A., BERHANI, O. & SINGER, B. B. 2019a. Fusobacterium nucleatum supresses anti-tumor immunity by activating CEACAM1. 8**,** e1581531.

GUR, C., MAALOUF, N., SHHADEH, A., BERHANI, O., SINGER, B. B., BACHRACH, G. & MANDELBOIM, O. 2019b. Fusobacterium nucleatum supresses anti-tumor immunity by activating CEACAM1. *Oncoimmunology,* 8**,** e1581531.

GURSOY, U. K., KÖNÖNEN, E. & UITTO, V. J. 2008. Intracellular replication of fusobacteria requires new actin filament formation of epithelial cells. *Apmis,* 116**,** 1063-70.

HALBLEIB, J. M. & NELSON, W. J. 2006. Cadherins in development: cell adhesion, sorting, and tissue morphogenesis. *Genes Dev,* 20**,** 3199-214.

HAN, Y. W. 2015. Fusobacterium nucleatum: a commensal-turned pathogen. *Curr Opin Microbiol,* 23**,** 141-7.

HAN, Y. W., SHI, W., HUANG, G. T., KINDER HAAKE, S., PARK, N. H., KURAMITSU, H. & GENCO, R. J. 2000. Interactions between periodontal bacteria and human oral epithelial cells: Fusobacterium nucleatum adheres to and invades epithelial cells. *Infect Immun,* 68**,** 3140-6.

HEALY, C. M. & MORAN, G. P. 2019. The microbiome and oral cancer: More questions than answers. *Oral Oncol,* 89**,** 30-33.

HECHT, S. S. 2003. Tobacco carcinogens, their biomarkers and tobacco-induced cancer. *Nat Rev Cancer,* 3**,** 733-44.

HENDERSON, I. R., NAVARRO-GARCIA, F., DESVAUX, M., FERNANDEZ, R. C. & ALA'ALDEEN, D. 2004. Type V protein secretion pathway: the autotransporter story. *Microbiol Mol Biol Rev,* 68**,** 692-744.

HENNE, K., SCHILLING, H., STONEKING, M., CONRADS, G. & HORZ, H. P. 2018. Sex-specific differences in the occurrence of Fusobacterium nucleatum subspecies and Fusobacterium periodonticum in the oral cavity. *Oncotarget,* 9**,** 20631-20639.

HERRERO, R., CASTELLSAGUÉ, X., PAWLITA, M., LISSOWSKA, J., KEE, F., BALARAM, P., RAJKUMAR, T., SRIDHAR, H., ROSE, B., PINTOS, J., FERNÁNDEZ, L., IDRIS, A., SÁNCHEZ, M. J., NIETO, A., TALAMINI, R., TAVANI, A., BOSCH, F. X., REIDEL, U., SNIJDERS, P. J., MEIJER, C. J., VISCIDI, R., MUÑOZ, N. & FRANCESCHI, S. 2003. Human papillomavirus and oral cancer: the International Agency for Research on Cancer multicenter study. *J Natl Cancer Inst,* 95**,** 1772-83.

HIRAI, M., KITAHARA, H., KOBAYASHI, Y., KATO, K., BOU-GHARIOS, G., NAKAMURA, H. & KAWASHIRI, S. 2017. Regulation of PD-L1 expression in a high-grade invasive human oral squamous cell carcinoma microenvironment. *Int J Oncol,* 50**,** 41-48.

HO, T. J., CHIANG, C. P., HONG, C. Y., KOK, S. H., KUO, Y. S. & YEN-PING KUO, M. 2000. Induction of the c-jun protooncogene expression by areca nut extract and arecoline on oral mucosal fibroblasts. *Oral Oncol,* 36**,** 432-6.

HOMANN, N., JOUSIMIES-SOMER, H., JOKELAINEN, K., HEINE, R. & SALASPURO, M. 1997. High acetaldehyde levels in saliva after ethanol consumption: methodological aspects and pathogenetic implications. *Carcinogenesis,* 18**,** 1739-43.

HSIAO, J. R., CHANG, C. C., LEE, W. T., HUANG, C. C., OU, C. Y., TSAI, S. T., CHEN, K. C., HUANG, J. S., WONG, T. Y., LAI, Y. H., WU, Y. H., HSUEH, W. T., WU, S. Y., YEN, C. J., CHANG, J. Y., LIN, C. L., WENG, Y. L., YANG, H. C., CHEN, Y. S. & CHANG, J. S. 2018. The interplay between oral microbiome, lifestyle factors and genetic polymorphisms in the risk of oral squamous cell carcinoma. *Carcinogenesis,* 39**,** 778-787.

HSIEH, Y. Y., TUNG, S. Y., PAN, H. Y., CHANG, T. S., WEI, K. L., CHEN, W. M., DENG, Y. F., LU, C. K., LAI, Y. H., WU, C. S. & LI, C. 2021. Fusobacterium nucleatum colonization is associated with decreased survival of helicobacter pylori-positive gastric cancer patients. *World J Gastroenterol,* 27**,** 7311-7323.

HU, W. H., DUAN, R., XIA, Y. T., XIONG, Q. P., WANG, H. Y., CHAN, G. K., LIU, S. Y., DONG, T. T., QIN, Q. W. & TSIM, K. W. 2019. Binding of Resveratrol to Vascular Endothelial Growth Factor Suppresses Angiogenesis by Inhibiting the Receptor Signaling. 67**,** 1127-1137.

HUANG, Z., XIE, N., LIU, H., WAN, Y., ZHU, Y., ZHANG, M., TAO, Y., ZHOU, H., LIU, X., HOU, J. & WANG, C. 2019. The prognostic role of tumour-infiltrating lymphocytes in oral squamous cell carcinoma: A meta-analysis. 48**,** 788-798.

HWANG, Y. S., LEE, S. K., PARK, K. K. & CHUNG, W. Y. 2012. Secretion of IL-6 and IL-8 from lysophosphatidic acid-stimulated oral squamous cell carcinoma promotes osteoclastogenesis and bone resorption. *Oral Oncol,* 48**,** 40-8.

IKEGAMI, A., CHUNG, P. & HAN, Y. W. 2009. Complementation of the fadA mutation in Fusobacterium nucleatum demonstrates that the surface-exposed adhesin promotes cellular invasion and placental colonization. *Infect Immun,* 77**,** 3075-9.

INABA, H., SUGITA, H., KUBONIWA, M., IWAI, S., HAMADA, M., NODA, T., MORISAKI, I., LAMONT, R. J. & AMANO, A. 2014. Porphyromonas gingivalis promotes invasion of oral squamous cell carcinoma through induction of proMMP9 and its activation. *Cell Microbiol,* 16**,** 131-45.

JIANG, S. & DONG, Y. 2017. Human papillomavirus and oral squamous cell carcinoma: A review of HPV-positive oral squamous cell carcinoma and possible strategies for future. *Curr Probl Cancer,* 41**,** 323-327.

JONES, S. J. 1972. A special relationship between spherical and filamentous microorganisms in mature human dental plaque. *Arch Oral Biol,* 17**,** 613-6.

JUNG, D. W., CHE, Z. M., KIM, J., KIM, K., KIM, K. Y., WILLIAMS, D. & KIM, J. 2010. Tumor-stromal crosstalk in invasion of oral squamous cell carcinoma: a pivotal role of CCL7. *Int J Cancer,* 127**,** 332-44.

KALLERGI, G., MARKOMANOLAKI, H., GIANNOUKARAKI, V., PAPADAKI, M. A., STRATI, A., LIANIDOU, E. S., GEORGOULIAS, V., MAVROUDIS, D. & AGELAKI, S. 2009. Hypoxia-inducible factor-1alpha and vascular endothelial growth factor expression in circulating tumor cells of breast cancer patients. *Breast Cancer Res,* 11**,** R84.

KAPLAN, A., KAPLAN, C. W., HE, X., MCHARDY, I., SHI, W. & LUX, R. 2014. Characterization of aid1, a novel gene involved in Fusobacterium nucleatum interspecies interactions. *Microb Ecol,* 68**,** 379-87.

KAPLAN, C. W., LUX, R., HAAKE, S. K. & SHI, W. 2009. The Fusobacterium nucleatum outer membrane protein RadD is an arginine-inhibitable adhesin required for inter-species adherence and the structured architecture of multispecies biofilm. *Mol Microbiol,* 71**,** 35-47.

KAPLAN, C. W., MA, X., PARANJPE, A., JEWETT, A., LUX, R., KINDER-HAAKE, S. & SHI, W. 2010. Fusobacterium nucleatum outer membrane proteins Fap2 and RadD induce cell death in human lymphocytes. *Infect Immun,* 78**,** 4773-8.

KARPOZILOS, A. & PAVLIDIS, N. 2004. The treatment of cancer in Greek antiquity. *Eur J Cancer,* 40**,** 2033-40.

KERSHAW, M. H., WESTWOOD, J. A. & DARCY, P. K. 2013. Gene-engineered T cells for cancer therapy. *Nat Rev Cancer,* 13**,** 525-41.

KIM, H. S., LEE, D. S., CHANG, Y. H., KIM, M. J., KOH, S., KIM, J., SEONG, J. H., SONG, S. K., SHIN, H. S., SON, J. B., JUNG, M. Y., PARK, S. N., YOO, S. Y., CHO, K. W., KIM, D. K.,

MOON, S., KIM, D., CHOI, Y., KIM, B. O., JANG, H. S., KIM, C. S., KIM, C., CHOE, S. J. & KOOK, J. K. 2010. Application of rpoB and zinc protease gene for use in molecular discrimination of Fusobacterium nucleatum subspecies. *J Clin Microbiol,* 48**,** 545-53.

KIM, S. M. 2016. Human papilloma virus in oral cancer. *J Korean Assoc Oral Maxillofac Surg,* 42**,** 327-336.

KOSTIC, A. D., CHUN, E., ROBERTSON, L., GLICKMAN, J. N., GALLINI, C. A., MICHAUD, M., CLANCY, T. E., CHUNG, D. C., LOCHHEAD, P., HOLD, G. L., EL-OMAR, E. M., BRENNER, D., FUCHS, C. S., MEYERSON, M. & GARRETT, W. S. 2013. Fusobacterium nucleatum potentiates intestinal tumorigenesis and modulates the tumor-immune microenvironment. *Cell Host Microbe,* 14**,** 207-15.

KOSTIC, A. D., GEVERS, D., PEDAMALLU, C. S., MICHAUD, M., DUKE, F., EARL, A. M., OJESINA, A. I., JUNG, J., BASS, A. J., TABERNERO, J., BASELGA, J., LIU, C., SHIVDASANI, R. A., OGINO, S., BIRREN, B. W., HUTTENHOWER, C., GARRETT, W. S. & MEYERSON, M. 2012. Genomic analysis identifies association of Fusobacterium with colorectal carcinoma. *Genome Res,* 22**,** 292-8.

LANCY, P., JR., DIRIENZO, J. M., APPELBAUM, B., ROSAN, B. & HOLT, S. C. 1983. Corncob formation between Fusobacterium nucleatum and Streptococcus sanguis. *Infect Immun,* 40**,** 303-9.

LAPTEVA, N. & HUANG, X. F. 2010. CCL5 as an adjuvant for cancer immunotherapy. *Expert Opin Biol Ther,* 10**,** 725-33.

LI, A., THOMAS, R. Z., VAN DER SLUIS, L., TJAKKES, G. H. & SLOT, D. E. 2020. Definitions used for a healthy periodontium-A systematic review. *Int J Dent Hyg,* 18**,** 327-343.

LI, S., XU, H. X., WU, C. T., WANG, W. Q., JIN, W., GAO, H. L., LI, H., ZHANG, S. R., XU, J. Z., QI, Z. H., NI, Q. X., YU, X. J. & LIU, L. 2019. Angiogenesis in pancreatic cancer: current research status and clinical implications. *Angiogenesis,* 22**,** 15-36.

LIAO, W. T., JIANG, D., YUAN, J., CUI, Y. M., SHI, X. W., CHEN, C. M., BIAN, X. W., DENG, Y. J. & DING, Y. Q. 2011. HOXB7 as a prognostic factor and mediator of colorectal cancer progression. *Clin Cancer Res,* 17**,** 3569-78.

LIEN, M. Y., CHANG, A. C., TSAI, H. C., TSAI, M. H., HUA, C. H., CHENG, S. P., WANG, S. W. & TANG, C. H. 2020. Monocyte Chemoattractant Protein 1 Promotes VEGF-A

Expression in OSCC by Activating ILK and MEK1/2 Signaling and Downregulating miR-29c. *Front Oncol,* 10**,** 592415.

LIN, M. T., YEN, M. L., LIN, C. Y. & KUO, M. L. 2003. Inhibition of vascular endothelial growth factor-induced angiogenesis by resveratrol through interruption of Src-dependent vascular endothelial cadherin tyrosine phosphorylation. *Mol Pharmacol,* 64**,** 1029-36.

LISTGARTEN, M. A., MAYO, H. & AMSTERDAM, M. 1973. Ultrastructure of the attachment device between coccal and filamentous microorganisms in "corn cob" formations of dental plaque. *Arch Oral Biol,* 18**,** 651-6.

LIU, Y., ELF, S. E., ASAI, T., MIYATA, Y., LIU, Y., SASHIDA, G., HUANG, G., DI GIANDOMENICO, S., KOFF, A. & NIMER, S. D. 2009. The p53 tumor suppressor protein is a critical regulator of hematopoietic stem cell behavior. *Cell Cycle,* 8**,** 3120-4.

LONG, H., XIANG, T., QI, W., HUANG, J., CHEN, J., HE, L., LIANG, Z., GUO, B., LI, Y., XIE, R. & ZHU, B. 2015. CD133+ ovarian cancer stem-like cells promote non-stem cancer cell metastasis via CCL5 induced epithelial-mesenchymal transition. *Oncotarget,* 6**,** 5846-59.

LOPES, C. F., DE ANGELIS, B. B., PRUDENTE, H. M., DE SOUZA, B. V., CARDOSO, S. V. & DE AZAMBUJA RIBEIRO, R. I. 2012. Concomitant consumption of marijuana, alcohol and tobacco in oral squamous cell carcinoma development and progression: recent advances and challenges. *Arch Oral Biol,* 57**,** 1026-33.

MANTOVANI, F. & COLLAVIN, L. 2019. Mutant p53 as a guardian of the cancer cell. 26**,** 199-212.

MARKOPOULOS, A. K. 2012. Current aspects on oral squamous cell carcinoma. *Open Dent J,* 6**,** 126-30.

MARSH, P. D. 2006. Dental plaque as a biofilm and a microbial community - implications for health and disease. *BMC Oral Health,* 6 Suppl 1**,** S14.

MATHUR, R., SINGHAVI, H. R., MALIK, A., NAIR, S. & CHATURVEDI, P. 2019. Role of Poor Oral Hygiene in Causation of Oral Cancer-a Review of Literature. *Indian J Surg Oncol,* 10**,** 184-195.

MCILVANNA, E., LINDEN, G. J., CRAIG, S. G., LUNDY, F. T. & JAMES, J. A. 2021. Fusobacterium nucleatum and oral cancer: a critical review. 21**,** 1212.

MEUSKENS, I., SARAGLIADIS, A., LEO, J. C. & LINKE, D. 2019. Type V Secretion Systems: An Overview of Passenger Domain Functions. *Front Microbiol,* 10**,** 1163.

MIMA, K., NISHIHARA, R., QIAN, Z. R., CAO, Y., SUKAWA, Y., NOWAK, J. A., YANG, J., DOU, R., MASUGI, Y., SONG, M., KOSTIC, A. D., GIANNAKIS, M., BULLMAN, S., MILNER, D. A., BABA, H., GIOVANNUCCI, E. L., GARRAWAY, L. A., FREEMAN, G. J., DRANOFF, G., GARRETT, W. S., HUTTENHOWER, C., MEYERSON, M., MEYERHARDT, J. A., CHAN, A. T., FUCHS, C. S. & OGINO, S. 2016. Fusobacterium nucleatum in colorectal carcinoma tissue and patient prognosis. *Gut,* 65**,** 1973-1980.

MIRZA, S. S., SHAFIQUE, K., VART, P. & ARAIN, M. I. 2011. Areca nut chewing and dependency syndrome: is the dependence comparable to smoking? a cross sectional study. *Subst Abuse Treat Prev Policy,* 6**,** 23.

MOORE, W. E. & MOORE, L. V. 1994. The bacteria of periodontal diseases. *Periodontol 2000,* 5**,** 66-77.

MORRISON, W. B. 2010. Cancer chemotherapy: an annotated history. *J Vet Intern Med,* 24**,** 1249-62.

MUGHEES, M. & SENGUPTA, A. 2021. Mechanism of tumour microenvironment in the progression and development of oral cancer. 48**,** 1773-1786.

NEVES, A. R., LUCIO, M., LIMA, J. L. & REIS, S. 2012. Resveratrol in medicinal chemistry: a critical review of its pharmacokinetics, drug-delivery, and membrane interactions. *Curr Med Chem,* 19**,** 1663-81.

NEVILLE, B. W. & DAY, T. A. 2002. Oral cancer and precancerous lesions. *CA Cancer J Clin,* 52**,** 195-215.

NOMOTO, D., BABA, Y., LIU, Y., TSUTSUKI, H., OKADOME, K., HARADA, K., ISHIMOTO, T., IWATSUKI, M., IWAGAMI, S., MIYAMOTO, Y., YOSHIDA, N., WATANABE, M., MOROISHI, T., KOMOHARA, Y., SAWA, T. & BABA, H. 2022. Fusobacterium nucleatum promotes esophageal squamous cell carcinoma progression via the NOD1/RIPK2/NF-κB pathway. *Cancer Lett,* 530**,** 59-67.

ONDER, T. T., GUPTA, P. B., MANI, S. A., YANG, J., LANDER, E. S. & WEINBERG, R. A. 2008. Loss of E-cadherin promotes metastasis via multiple downstream transcriptional pathways. *Cancer Res,* 68**,** 3645-54.

PARHI, L. & ALON-MAIMON, T. 2020. Breast cancer colonization by Fusobacterium nucleatum accelerates tumor growth and metastatic progression. 11**,** 3259.

PATEL, K. R., VAJARIA, B. N., BEGUM, R., PATEL, J. B., SHAH, F. D., JOSHI, G. M. & PATEL, P. S. 2015. VEGFA isoforms play a vital role in oral cancer progression. *Tumour Biol,* 36**,** 6321-32.

PEĆINA-SLAUS, N. 2003. Tumor suppressor gene E-cadherin and its role in normal and malignant cells. *Cancer Cell Int,* 3**,** 17.

PEÑA-OYARZÚN, D., REYES, M., HERNÁNDEZ-CÁCERES, M. P., KRETSCHMAR, C., MORSELLI, E., RAMIREZ-SARMIENTO, C. A., LAVANDERO, S., TORRES, V. A. & CRIOLLO, A. 2020. Role of Autophagy in the Microenvironment of Oral Squamous Cell Carcinoma. *Front Oncol,* 10**,** 602661.

PERERA, I., IPE, D., ULETT, G. C., SPEICHER, D. J., CHEN, T. & JOHNSON, N. W. *J Dent Res*.

PERERA, M. & AL-HEBSHI, N. N. 2018. Inflammatory Bacteriome and Oral Squamous Cell Carcinoma. 97**,** 725-732.

PIKKARAINEN, P. H., BARAONA, E., JAUHONEN, P., SEITZ, H. K. & LIEBER, C. S. 1981. Contribution of oropharynx microflora and of lung microsomes to acetaldehyde in expired air after alcohol ingestion. *J Lab Clin Med,* 97**,** 631-6.

POHLNER, J., LANGENBERG, U., WÖLK, U., BECK, S. C. & MEYER, T. F. 1995. Uptake and nuclear transport of Neisseria IgA1 protease-associated alpha-proteins in human cells. *Mol Microbiol,* 17**,** 1073-83.

PÖSCHL, G. & SEITZ, H. K. 2004. Alcohol and cancer. *Alcohol Alcohol,* 39**,** 155-65.

PROCINO, A. & CILLO, C. 2013. The HOX genes network in metabolic diseases. *Cell Biol Int,* 37**,** 1145-8.

RANGANATHAN, K. & KAVITHA, L. 2019. Oral epithelial dysplasia: Classifications and clinical relevance in risk assessment of oral potentially malignant disorders. *J Oral Maxillofac Pathol,* 23**,** 19-27.

RAUF, A., IMRAN, M., BUTT, M. S., NADEEM, M., PETERS, D. G. & MUBARAK, M. S. 2018. Resveratrol as an anti-cancer agent: A review. *Crit Rev Food Sci Nutr,* 58**,** 1428-1447.

RAVEN, R. W. 1985. Surgical oncology--theory and practice. *J Surg Oncol,* 30**,** 145-8.

REIDY, J., MCHUGH, E. & STASSEN, L. F. 2011. A review of the relationship between alcohol and oral cancer. *Surgeon,* 9**,** 278-83.

RIVERA, C. & VENEGAS, B. 2014. Histological and molecular aspects of oral squamous cell carcinoma (Review). *Oncol Lett,* 8**,** 7-11.

RIVLIN, N., BROSH, R., OREN, M. & ROTTER, V. 2011. Mutations in the p53 Tumor Suppressor Gene: Important Milestones at the Various Steps of Tumorigenesis. *Genes Cancer,* 2**,** 466-74.

ROI, A. & ROI, C. I. 2020. The Challenges of OSCC Diagnosis: Salivary Cytokines as Potential Biomarkers. 9.

RUBINSTEIN, M. R., WANG, X., LIU, W., HAO, Y., CAI, G. & HAN, Y. W. 2013. Fusobacterium nucleatum promotes colorectal carcinogenesis by modulating E-cadherin/beta-catenin signaling via its FadA adhesin. *Cell Host Microbe,* 14**,** 195-206.

SADREKARIMI, H., GARDANOVA, Z. R., BAKHSHESH, M., EBRAHIMZADEH, F., YASERI, A. F., THANGAVELU, L., HASANPOOR, Z., ZADEH, F. A. & KAHRIZI, M. S. 2022. Emerging role of human microbiome in cancer development and response to therapy: special focus on intestinal microflora. *J Transl Med,* 20**,** 301.

SAID, I. T., SHAMSUDDIN, A. M., SHERIEF, M. A., TALEB, S. G., AREF, W. F. & KUMAR, D. 1999. Comparison of different techniques for detection of Gal-GalNAc, an early marker of colonic neoplasia. *Histol Histopathol,* 14**,** 351-7.

SCHMIDT, B. L., KUCZYNSKI, J., BHATTACHARYA, A., HUEY, B., CORBY, P. M., QUEIROZ, E. L., NIGHTINGALE, K., KERR, A. R., DELACURE, M. D., VEERAMACHANENI, R., OLSHEN, A. B. & ALBERTSON, D. G. 2014. Changes in abundance of oral microbiota associated with oral cancer. *PLoS One,* 9**,** e98741.

SCHOELCH, M. L., REGEZI, J. A., DEKKER, N. P., NG, I. O., MCMILLAN, A., ZIOBER, B. L., LE, Q. T., SILVERMAN, S. & FU, K. K. 1999. Cell cycle proteins and the development of oral squamous cell carcinoma. *Oral Oncol,* 35**,** 333-42.

SCULLY, C. & BAGAN, J. 2009. Oral squamous cell carcinoma: overview of current understanding of aetiopathogenesis and clinical implications. *Oral Dis,* 15**,** 388-99.

SHANG, F. M. & LIU, H. L. 2018. Fusobacterium nucleatum and colorectal cancer: A review. *World J Gastrointest Oncol,* 10**,** 71-81.

SHAO, W., FUJIWARA, N., MOURI, Y., KISODA, S., YOSHIDA, K., YOSHIDA, K., YUMOTO, H., OZAKI, K., ISHIMARU, N. & KUDO, Y. 2021. Conversion from epithelial to partial-EMT phenotype by Fusobacterium nucleatum infection promotes invasion of oral cancer cells. *Sci Rep,* 11**,** 14943.

SIGNAT, B., ROQUES, C., POULET, P. & DUFFAUT, D. 2011. Fusobacterium nucleatum in periodontal health and disease. *Curr Issues Mol Biol,* 13**,** 25-36.

SKUSE, A. 2015. Wellcome Trust–Funded Monographs and Book Chapters. *Constructions of Cancer in Early Modern England: Ravenous Natures.* London (UK): Palgrave Macmillan

SOUTO, G. R., CALIARI, M. V., LINS, C. E., DE AGUIAR, M. C., DE ABREU, M. H. & MESQUITA, R. A. 2010. Tobacco use increase the number of aneuploid nuclei in the clinically healthy oral epithelium. *J Oral Pathol Med,* 39**,** 605-10.

SPIRINA, L. V., USYNIN, Y. A., YURMAZOV, Z. A., SLONIMSKAYA, E. M., KOLEGOVA, E. S. & KONDAKOVA, I. V. 2017. [Transcription factors NF-kB, HIF-1, HIF-2, growth factor VEGF, VEGFR2 and carboanhydrase IX mRNA and protein level in the development of kidney cancer metastasis]. *Mol Biol (Mosk),* 51**,** 372-377.

STRAUSS, J., WHITE, A., AMBROSE, C., MCDONALD, J. & ALLEN-VERCOE, E. 2008. Phenotypic and genotypic analyses of clinical Fusobacterium nucleatum and Fusobacterium periodonticum isolates from the human gut. *Anaerobe,* 14**,** 301-9.

SUCIU, M., MORARIU, S. H., ORMENISAN, A., GRIGORAS, R. I., BOSTAN, R. H., MOCANU, S., VARTOLOMEI, M. D. & COTOI, O. S. 2014. Oral squamous cell carcinoma of the maxilla, a second malignancy after a right ethmoido-maxillary chondrosarcoma. *Rom J Morphol Embryol,* 55**,** 1247-51.

SWANN, J. B. & SMYTH, M. J. 2007. Immune surveillance of tumors. *J Clin Invest,* 117**,** 1137-46.

TALAMINI, R., VACCARELLA, S., BARBONE, F., TAVANI, A., LA VECCHIA, C., HERRERO, R., MUÑOZ, N. & FRANCESCHI, S. 2000. Oral hygiene, dentition, sexual habits and risk of oral cancer. *Br J Cancer,* 83**,** 1238-42.

TEZAL, M., SULLIVAN, M. A., REID, M. E., MARSHALL, J. R., HYLAND, A., LOREE, T., LILLIS, C., HAUCK, L., WACTAWSKI-WENDE, J. & SCANNAPIECO, F. A. 2007. Chronic periodontitis and the risk of tongue cancer. *Arch Otolaryngol Head Neck Surg,* 133**,** 450-4.

TSAI, S. T., WONG, T. Y., OU, C. Y., FANG, S. Y., CHEN, K. C., HSIAO, J. R., HUANG, C. C., LEE, W. T., LO, H. I., HUANG, J. S., WU, J. L., YEN, C. J., HSUEH, W. T., WU, Y. H., YANG, M. W., LIN, F. C., CHANG, J. Y., CHANG, K. Y., WU, S. Y., LIAO, H. C., LIN, C. L., WANG, Y. H., WENG, Y. L., YANG, H. C. & CHANG, J. S. 2014. The interplay between alcohol

consumption, oral hygiene, ALDH2 and ADH1B in the risk of head and neck cancer. *Int J Cancer,* 135**,** 2424-36.

UITTO, V. J., BAILLIE, D., WU, Q., GENDRON, R., GRENIER, D., PUTNINS, E. E., KANERVO, A. & FIRTH, J. D. 2005. Fusobacterium nucleatum increases collagenase 3 production and migration of epithelial cells. *Infect Immun,* 73**,** 1171-9.

VAN DER MERWE, M., VAN NIEKERK, G., BOTHA, A. & ENGELBRECHT, A. M. 2021. The onco-immunological implications of Fusobacterium nucleatum in breast cancer. *Immunol Lett,* 232**,** 60-66.

VAN ROY, F. & BERX, G. 2008. The cell-cell adhesion molecule E-cadherin. *Cell Mol Life Sci,* 65**,** 3756-88.

VIALLARD, C. & LARRIVÉE, B. 2017. Tumor angiogenesis and vascular normalization: alternative therapeutic targets. *Angiogenesis,* 20**,** 409-426.

VILGELM, A. E. & RICHMOND, A. 2019. Chemokines Modulate Immune Surveillance in Tumorigenesis, Metastasis, and Response to Immunotherapy. *Front Immunol,* 10**,** 333.

VOUSDEN, K. H. 2002. Activation of the p53 tumor suppressor protein. *Biochim Biophys Acta,* 1602**,** 47-59.

WANG, M., XIAO, C., NI, P., YU, J. J., WANG, X. W. & SUN, H. 2018. Correlation of Betel Quid with Oral Cancer from 1998 to 2017: A Study Based on Bibliometric Analysis. *Chin Med J (Engl),* 131**,** 1975-1982.

WARNAKULASURIYA, S., REIBEL, J., BOUQUOT, J. & DABELSTEEN, E. 2008. Oral epithelial dysplasia classification systems: predictive value, utility, weaknesses and scope for improvement. *J Oral Pathol Med,* 37**,** 127-33.

WARNAKULASURIYA, S., TRIVEDY, C. & PETERS, T. J. 2002. Areca nut use: an independent risk factor for oral cancer. *Bmj,* 324**,** 799-800.

WATANABE, H., IWASE, M., OHASHI, M. & NAGUMO, M. 2002. Role of interleukin-8 secreted from human oral squamous cell carcinoma cell lines. *Oral Oncol,* 38**,** 670-9.

WU, F., SHI, X., ZHANG, R., TIAN, Y., WANG, X., WEI, C., LI, D., LI, X., KONG, X., LIU, Y., GUO, W., GUO, Y. & ZHOU, H. 2018. Regulation of proliferation and cell cycle by protein regulator of cytokinesis 1 in oral squamous cell carcinoma. *Cell Death Dis,* 9**,** 564.

WU, X., LI, J., YAN, T., KE, X., LI, X., ZHU, Y., YANG, J. & LI, Z. 2021. HOXB7 acts as an oncogenic biomarker in head and neck squamous cell carcinoma. 21**,** 393.

XU, M., YAMADA, M., LI, M., LIU, H., CHEN, S. G. & HAN, Y. W. 2007. FadA from Fusobacterium nucleatum utilizes both secreted and nonsecreted forms for functional oligomerization for attachment and invasion of host cells. *J Biol Chem,* 282**,** 25000-9.

YANG, G. Y. & SHAMSUDDIN, A. M. 1996. Gal-GalNAc: a biomarker of colon carcinogenesis. *Histol Histopathol,* 11**,** 801-6.

YE, X., WANG, R., BHATTACHARYA, R., BOULBES, D. R., FAN, F., XIA, L., ADONI, H., AJAMI, N. J., WONG, M. C., SMITH, D. P., PETROSINO, J. F., VENABLE, S., QIAO, W., BALADANDAYUTHAPANI, V., MARU, D. & ELLIS, L. M. 2017. Fusobacterium Nucleatum Subspecies Animalis Influences Proinflammatory Cytokine Expression and Monocyte Activation in Human Colorectal Tumors. *Cancer Prev Res (Phila),* 10**,** 398-409.

YOSHIMURA, T. 2018. The chemokine MCP-1 (CCL2) in the host interaction with cancer: a foe or ally? *Cell Mol Immunol,* 15**,** 335-345.

YOUNIS, L. K., EL SAKKA, H. & HAQUE, I. 2007. The Prognostic Value of E-cadherin Expression in Breast Cancer. *Int J Health Sci (Qassim),* 1**,** 43-51.

ZHANG, L., LIU, Y., ZHENG, H. J. & ZHANG, C. P. 2019. The Oral Microbiota May Have Influence on Oral Cancer. *Front Cell Infect Microbiol,* 9**,** 476.

ZHANG, S., CAI, S. & MA, Y. 2018. Association between Fusobacterium nucleatum and colorectal cancer: Progress and future directions. *J Cancer,* 9**,** 1652-1659.

ZHANG, S., LI, C., LIU, J., GENG, F., SHI, X., LI, Q., LU, Z. & PAN, Y. 2020. Fusobacterium nucleatum promotes epithelial-mesenchymal transiton through regulation of the lncRNA MIR4435-2HG/miR-296-5p/Akt2/SNAI1 signaling pathway. *Febs j,* 287**,** 4032-4047.

ZULFIQAR, M., YAMAGUCHI, T., SATO, S. & OHO, T. 2013. Oral Fusobacterium nucleatum subsp. polymorphum binds to human salivary alpha-amylase. *Mol Oral Microbiol,* 28**,** 425-34.

ZYGOGIANNI, A. G., KYRGIAS, G., KARAKITSOS, P., PSYRRI, A., KOUVARIS, J., KELEKIS, N. & KOULOULIAS, V. 2011. Oral squamous cell cancer: early detection and the role of alcohol and smoking. *Head Neck Oncol,* 3**,** 2.